

Review

Manifestation on the choice of a suitable combination of MIS for proficient Schottky diodes for optoelectronic applications: A comprehensive review

G. Alan Sibu^a, P. Gayathri^a, T. Akila^a, R. Marnadu^b, V. Balasubramani^{a,*}^a Department of Physics, Saveetha School of Engineering, Saveetha Institute of Medical and Technical Sciences, Saveetha University, Chennai, Tamil Nadu 602 105, India^b Department of Physics, Government Arts College for Women, Dindigul, Tamil Nadu 624 208, India

ARTICLE INFO

Keywords:
 Schottky Barrier diodes
 Thin films
 MIS diodes
 Photovoltaic devices
 Optoelectronic applications

ABSTRACT

In this review, we explore the last fifty years of Metal-Insulator-Semiconductor (MIS) Schottky barrier diode research, highlighting a surge in interest in tailored filaments for thin films, photovoltaic cells, and advanced electronics. The fundamental principles of MIS functionalization on the intermediate insulator layer within the MIS structure are detailed, followed by a comprehensive discussion of approaches to MIS-based diode fabrication, meticulously addressing specific details of metal, insulator and semiconductor layers. This review delves into bespoke device manufacturing methods, underscoring their significance in the scientific landscape. It examines principal materials used in production, focusing on optical, electrical applications explores the evolution of insulating materials, doping effects, manufacturing technologies and potential device applications. Challenges in MIS diode manufacturing are outlined, exploring various techniques, their advantages and disadvantages. JNSP thin film coating emerges as a preferred technique due to its cost-effectiveness, ease of handling, and non-toxic nature. From our comprehensive review, it is evident that transition metals are preferred materials in previous research. The article concludes by addressing future perspectives, guiding novel advancements and contemplating applications of bespoke filaments in optoelectronic devices and applications. This holistic exploration aims to contribute to the ongoing discourse and evolution of MIS-based devices across diverse fields.

1. Introduction

The evolution of MIS diodes is intricately linked to the progress of semiconductors. MIS configurations surfaced as the semiconductor industry flourished in the mid-20th century and assumed significance in regulating the electron flow within semiconductors. During the 1960s, the MIS structure gained prominence for enhancing the efficacy of transistors FET, pivotal components in integrated circuits that facilitate control over transportation expenses. MIS architectures contributing to heightened performance and dependability. Across the years, ongoing advancements in semiconductor technology have refined the materials utilized in MIS structure configurations, resulting in superior performance and downsizing. This framework has now become an integral

element of microelectronic devices like integrated circuits and sensors, playing a pivotal role in the management of transportation costs.

Semiconductor devices are crucial components in the realm of optical electronics, encompassing a variety of applications, including photodiodes, optoelectronic transistors, photosensors, photodetectors, solar cells and these devices are integral to both nano/microelectronics and optoelectronic applications, offering tuneable properties that have captivated the scientific community's attention. Due to the rapid optical response, ultra-speed, low current leakage, stability and extended lifespan of SDs have spurred intensive research in photonics-oriented devices [1–4]. The ability of SDs to respond to varying light intensities opens up promising avenues for enhancing their performance through adjustable parameters [5]. This capability stems from the generation of

Abbreviations: SDs, Schottky Diodes; SBDs, Schottky Barrier Diodes; JNSP, Jet Nebulizer Spray Pyrolysis; PVD, Physical Vapour Deposition; CVD, Chemical Vapour Deposition; MIS, Metal Insulator Semiconductor; SG, Sol Gel; TAT, Trap Assisted Tunnelling; GD, Gaussian Distribution; FE, Field Emission; CVT, Current Voltage Temperature; ULSI, Ultra-Large-Scale Integration; RP, Richardson Plot; PFE, Poole Frenkel Emission; TE, Thermionic Emission; TFE, Thermionic Field Emission; SCLC, Space Charge Limited Conduction; NS, Nano Structure; MRI, Magnetic Resonance Imaging; DC, Direct Current; RF, Radio Frequency; MS, Magnetron Sputtering; ALD, Atomic Layer Deposition; LPD, Liquid Phase Deposition; EBD, Electron Beam Deposition; CPM, Co- Precipitation Method; EPM, Electrochemical Polymerization Method; SILAR, Successive Ionic Layer Absorption & Reaction; SGSC, Sol Gel Spin Coating; HEMTs, High Electron Mobility Transistors.

* Corresponding author.

E-mail address: balasubramaniv3@gmail.com (V. Balasubramani).

Table 1

A Comprehensive and comparative analysis of MIS Diodes: Exploring Schematic, energy level diagram and Photodiode parameters.

Author Name	Schematic Diagram	Coating Method	Variations	Ideal Parameters	Photodiode Parameters	Energy Level Diagram	Aim and Summary	Ref
Marnadu et.al.,		Jet Nebulizer Spray Pyrolysis (JNSP)	variation of mole concentration WO3 (0.1, 0.15, 0.2, 0.25) M	Ideality factor (n)= 4.35 Barrier height $\Phi_B=0.65$ (eV) Saturation Current $(I_0)=2.06\times10^{-8}$ (A)	Photosensitivity (P_S)= 960.95% Photoresponsivity $R=33.40$ (mA/W) Quantum Efficiency=12.95% Detectivity (D^*) = 2.7×10^8 jones		The author demonstrated a sensitive Cu/WO ₃ -nanoplates/p-Si structured SBDs with varying concentrations of WO ₃ as the insulating layer. XRD revealed a single-phase monoclinic structure with crystallite size of 51.3 nm, exhibited a randomly formed nanoplate array in the FE-SEM. E _g ranged from 3.2 to 3.4 eV in UV-Vis investigation. 0.2 M WO ₃ films displayed improved electrical conductivity and reduced resistivity in I-V parameters. This MIS diode showed a maximum responsivity 33.40 mA W ⁻¹ quantum efficiency 12.95% detectivity (D^*) of 13.35×10^9 jones, indicating its suitability for UV photodetector applications.	[23]
Marnadu et.al.,		JNSP	Temperature variation (350, 400, 450, 500) °C	n=3.76 $\Phi_B=0.67$ (eV)	-		Using JNSP technique, successfully deposited WO ₃ thin films on glass substrates at varying temperatures (350–500°C). XRD revealed a crystal phase transition from monoclinic to orthorhombic. Then the average Crystalline size D _{ave} is 46.5 nm. FE-SEM images displayed an interconnected network of grains with a randomly oriented surface. E _g values ranged from 3.2 to 3.6 eV. Electrical conductivity of the film increased ($16.80 \times 10^{-15} \Omega\text{cm}^{-1}$) and activation energy decreased (0.092 eV) with rising substrate temperature. Compared to other SBDs, the device constructed at 400°C exhibited the Φ_B is increased and lowest n value. This suggests that MIS-structured SBDs with a WO ₃ insulating layer produced at 400°C hold potential for temperature-dependent its increased potential and sufficient feasibility for device applications.	[24]
Marnadu et.al.,		JNSP	Change in Composite Concentration of Sn (0, 4, 8 and 12) wt%	n=2.35 $\Phi_B= 0.63$ (eV) $I_0= 8.94\times10^{-4}$ (A)	$P_S = 960.95-137.63\%$ $R= 5083.5$ (mA W ⁻¹) QE=1971.1% Detectivity= 12.089×10^{10} jones		The author successfully demonstrated a diode Cu/Sn-WO ₃ /p-Si using JNSP method. Structural study exhibited a polycrystalline nature with dual phases (monoclinic and orthorhombic), maximum D _{ave} of 50.8 nm, diverse surface morphologies (nanoplates, nanowires, nano porous). Higher Sn concentrations resulted in a maximum (E _g) of 3.6 eV. The electrical conductivity improved from 10^{15} to $10^{13} \text{ S cm}^{-1}$, with a minimum	[25]

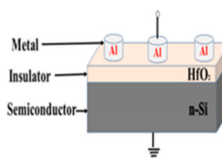
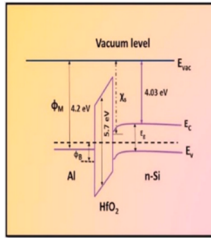
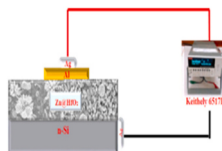
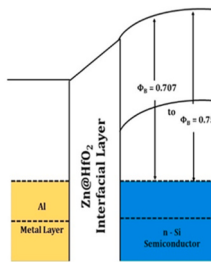
(continued on next page)

Table 1 (continued)

Author Name	Schematic Diagram	Coating Method	Variations	Ideal Parameters	Photodiode Parameters	Energy Level Diagram	Aim and Summary	Ref
Marnadu et.al.,		JNSP	Different concentrations of Zr (0,4,8 wt %)	$n=4.11$ $\Phi_B = 0.665 \text{ eV}$ -	-		activation energy of 0.041 eV and resistivity of $9.7 \times 10^{12} \Omega \cdot \text{cm}$ in the 12 wt% Sn-WO ₃ film. Under light conditions, the diode exhibited a reduced n range 2.35 and it achieved a high D* 12.089×10^{10} Jones and QE of 1971.1% using the 12 wt% nano porous Sn-WO ₃ material. This device structure of MIS diode, making it suitable for photo-detector applications.	[26]
Harish Senthil et.al.,		JNSP	Different composite Concentrations of Sn (0, 5, 10, 15 wt%)	$n = 2.5$ $\Phi_B = 0.779 \text{ eV}$ $I_0 = 5.54 \times 10^{-4} \text{ to } 4.90 \times 10^{-6} \text{ (A)}$	-		The author successfully created an Al/Sn@HfO ₂ /n-Si diode, outperforming a pure Al/HfO ₂ /n-Si diode in rectifier performance, then the addition of Sn, increased grain size from 14 to 36 nm and spectra indicated a monoclinic to orthorhombic phase transition in XRD. Mesoporous and nano porous coral mixtures persisted in the films, as observed in FESEM visuals, then E _g values reduced from 3.8 eV (pure) to 3.2 eV. The XPS spectra indicate the presence of Sn doublet 3d peaks in composite films, with a decrease in Hf 4 f and O1s peaks at 15 wt% compared to pure HfO ₂ , suggesting a strong Sn presence. I-V characteristics show n and Φ_B values ranging from 3.4 to 2.5 and 0.707–0.779 eV, respectively, attributed to spatial indifference of Φ_B . I ₀ values decrease with Sn concentrations. Then the MIS diode (15 wt%) exhibits superior rectifying behaviour compared to the pure MIS	[27]

(continued on next page)

Table 1 (continued)

Author Name	Schematic Diagram	Coating Method	Variations	Ideal Parameters	Photodiode Parameters	Energy Level Diagram	Aim and Summary	Ref
Harish Senthil et.al.,		JNSP	Temperature variation (400, 450, 500, 550, 600) C	n= 3.4. $\Phi_B=0.776$ (eV) $I_0=5.54 \times 10^{-4}$ (A)	- - -		diode, suggesting its suitability for switching applications. Author coated HfO_2 films were evaluated in the $Al/HfO_2/n$ -Si diode using JNSP. XRD revealed a monoclinic crystal structure with enhanced crystallite and FE-SEM micrographs displayed microporous, ball-like grains and also observed tiny porous particles at 600C then the E_g value is around 3.41 eV. In I-V characterization, higher substrate temperatures improved the diode by reducing the value of n, enhancing Φ_B and increasing reverse I_0 . Then the presence of HfO_2 thin films significantly improved the characteristics and performance of the diode at Al and n-Si interfaces. The MIS diode is well-suited for future temperature-dependent electronics applications.	[28]
Harish Senthil et.al.,		JNSP	Different composite concentrations of Zn (0, 5, 10, 15 wt %)	n= 2.2 $\Phi_B=0.759$ (eV) $I_0=5.180 \times 10^{-5}$ (A)	- - -		The $Al/Zn@HfO_2/n$ -Si diode was successfully manufactured, incorporating a Zn composite. XRD spectra revealed a mixed phase of (monoclinic cubic structures) with an increased crystalline size from 14 nm to 38 nm and E_g range from 3.33 eV, also FESEM images displayed intact mixtures of mesoporous and nanorods in the films. XPS spectra show Zn doublet 2p peaks in composite films, decreasing Hf 4 f and O1s peaks at 15 wt% vs. pure HfO_2 . I-V characteristics reveal varying (n) and (Φ_B) ranges of (3.4–2.2) and (0.707–0.759 eV). I_0 values decrease with Zn concentrations, compared to the pure MIS diode, the presence of Zn (5, 10, 15 wt%) in the MIS diode exhibited favourable rectifier characteristics and also the 15 wt% MIS diode is particularly suitable for applications requiring fast switching.	[29]

(continued on next page)

Table 1 (continued)

Author Name	Schematic Diagram	Coating Method	Variations	Ideal Parameters	Photodiode Parameters	Energy Level Diagram	Aim and Summary	Ref
Harish Senthil et.al.,		JNSP	Composite weight variation Of Sr (5,10,15 wt%)	$n=1.9$ $\Phi_B=0.806$ (eV) $I_0=7.85 \times 10^{-6}$ (A)	-		In this work, using JNSP method, successfully deposited the MIS diode structure Al/HfO2-Sr/n-Si. XRD patterns revealed monoclinic, tetragonal, intermediate phases, increased grain size (14–54 nm). FE-SEM analysis, the increasing Sr ratio resulted in irregularly formed porous balls and periodic nanorod structures. UV-Vis spectra, 15% Sr:HfO2 has high absorption, E_g is 3.7 eV. XPS spectra analysis of pure HfO2 and 15% Sr:HfO2 reveals a shift in binding energy and additional OH peaks. Diode characteristics show 15% Sr:HfO2 has superior rectification behaviour, attributed to improved electrical and optical properties of Hafnium oxide with strontium incorporation. And this enhancement suggests potential applications in fast-switching scenarios and diverse diode performance for various applications.	[30]
Bala Subramani et.al.,		JNSP	Doping Weight Variation of W (2,4,6 wt%)	$n=1.68$ $\Phi_B=0.83$ (eV) $I_0=3.57 \times 10^{-4}$ (A)	-		The JNSP approach was successfully used for developing Cu/Sr-W/n-Si-structured SBD with different concentrations of W. The XRD pattern, which primarily orients along (1 1 2) directions, confirms the presence of dual phase (cubic, tetragonal structure). Then this optical study, the minimum E_g of 3.61 eV. The formation of a continuous layer of Sr-W on the n-Si surface and the smooth surface are confirmed by AFM pictures. With a minimum n value of 1.68, the I-V nature of the MIS diode implies enhanced rectifying activity. However, the MIS-structured diode with light condition films shows inconsistent photodiode performance compared to other devices,	[31]
Vivek et.al.,		JNSP	Composite Weight Variation of Zr (0, 5, 10, 15 wt %)	$n=2.98$ $\Phi_B=0.664$ (eV)	-		The author examined MoO3 thin films by varying Zr composite content (0, 5, 10 and 15 wt%) XRD analysis revealed a dual crystal structure (orthorhombic, hexagonal) in MoO3-ZrO2 films with D_{ave} values ranging from 42 to 53 nm, then the plate-like structure with a smooth surface, encouraging grain formation and weak, homogeneous agglomeration in morphological study. For UV characteristics showed that the E_g range (3.8 and 4.0 eV). Also, EDAX confirmed the presence of expected elements in these results and	[32]

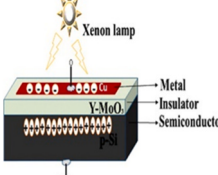
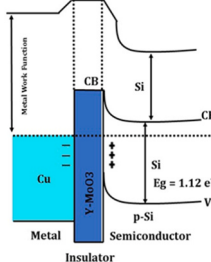
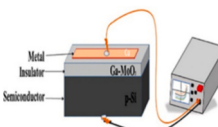
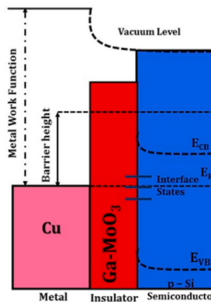
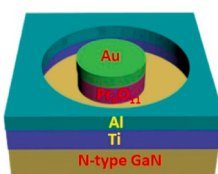
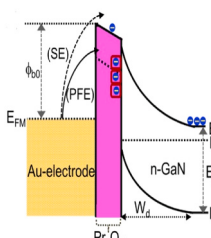
(continued on next page)

Table 1 (continued)

Author Name	Schematic Diagram	Coating Method	Variations	Ideal Parameters	Photodiode Parameters	Energy Level Diagram	Aim and Summary	Ref
Vivek et.al.,		JNSP	Different concentrations of Ba (0, 5, 10 and 15 wt%)	$n=1.92$ $\Phi_B=0.705 \text{ eV}$ $I_0=9.05 \times 10^{-5} \text{ to } 6.48 \times 10^{-3} \text{ A}$	$P_S=5573\%$ - -		increasing Zr concentration led to a drop in electrical conductivities, higher Zr content resulted in increased (Φ_B) and decreased (n). Diode data indicated performance for the 15% wt % composite is the better results compared to the pure one. The outcome suggests that the diode 15 wt % would be suitable for an advanced optoelectronic devices.	[33]
Vivek et.al.,		JNSP	Temperature variation (350,400, 450,500) °C	$n=2.8$ $\Phi_B= 0.894 \text{ (eV)}$ -	$P_S=610.51\%$ $R=35.130 \text{ (mA/W)}$ $QE=136.22\%$ $D^*=1.149 \times 10^{11} \text{ jones}$		In summary, the JNSP technique successfully manufactured the MoO ₃ nanoplate films with varying substrate temperatures. Crystalline structure of orthorhombic, $D_{ave}=42 \text{ nm}$. Surface morphology of nanorod to nanoplate-like structure observed in the films, when the PL analysis of the MoO ₃ nanoplate thin film displayed broad peak at red-shift. Increased transmittance in the visible region and a higher E_g at elevated temperatures. Electrical properties like conductivity, resistivity and activation energy showed temperature-dependent variations. Cu/MoO ₃ nanoplate/p-Si SBDs at 500°C exhibited superior rectification behaviour, a lower n range and enhanced P_S . The MIS diode at 500°C demonstrated remarkable responsivity, quantum efficiency and detectivity, suggesting its suitability for UV photodetector applications.	[34]

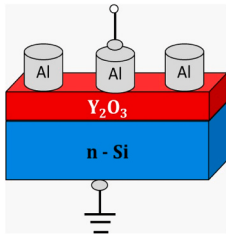
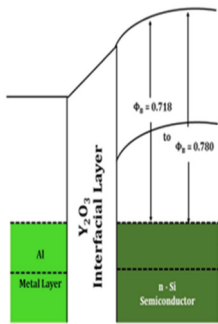
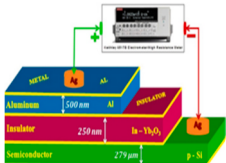
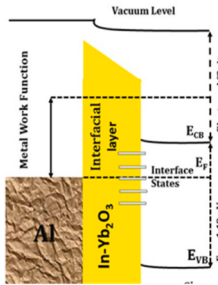
(continued on next page)

Table 1 (continued)

Author Name	Schematic Diagram	Coating Method	Variations	Ideal Parameters	Photodiode Parameters	Energy Level Diagram	Aim and Summary	Ref
Vivek et.al.,		JNSP	Composite weightage variation of Y (5,10,15 wt%)	n=1.70 $\Phi_B=0.732$ (eV) -	$P_S=4496\%$ $R=1584.877$ (mA/cm^2) $QE=614.548\%$ $D^*=9.82 \times 10^{11}$ Jones		This work uses the JNSP technique to deposit MoO_3 nanoplate films, Y composite. It revealing multi-phases crystal size 52.2 nm in the Structural data. Morphology of MoO_3 film exhibited nanoplate structures with clusters then it shows optical analysis of a 3.80 eV of E_g . The DC conductivity exhibited a $5.19 \times 10^{-15} \text{ S}/\text{cm}$ with an activation energy of 0.094 eV and $\rho = 5.77 \times 10^{14} \Omega \cdot \text{cm}$. Cu/ Y-MoO_3 /p-Si diodes displayed current-voltage characteristics with a minimum n range and a higher Φ_B under light conditions. Then the diodes parameters making them suitable for photoelectronic applications	[35]
Vivek et.al.,		JNSP	Change in Ga weight concentration (5, 10 and 15 wt%)	n= 3.07 $\Phi_B= 0.682$ (eV) -	$P_S=20392\%$ $R=36.21$ (mA/cm^2) $QE=13.9\%$ $D^*=12.05 \times 10^{12}$ (jones)		This study successfully deposited Ga-MoO_3 thin films on glass substrates using the JNSP technique. Confirming multi-phase polycrystalline structures and (orthorhombic, monoclinic structure) the highest D_{ave} 78.54 nm was observed in the XRD data and randomly arranged nanoplates and nanorods seen through FE-SEM then the UV absorption spectra indicated E_g ranging from 3.15 to 3.48 eV. Cu/ Ga-MoO_3 /p-Si SBDs displayed good photo conducting properties under light conditions. SBDs with 10 wt% Ga-MoO_3 demonstrated maximum P_S (20,392%), R at (36.21 mA/cm^2), QE (13.9%) and (D^*) reached 12.05×10^{12} Jones for the 10 wt% Ga-MoO_3 MIS diode. It's suggested that MIS SBDs are suitable for photodiode applications.	[36]
Uma et.al.,		EBD	Temperature variations 270–420 K	n=1.42 $\Phi_B=0.93$ (eV) $I_0=1.54 \times 10^{-8}$ (A)	- -		This work focuses on the fabrication, analysis of an Au/ Pr_6O_{11} /n-GaN MIS structure with a Pr_6O_{11} interlayer, exploring its electrical characteristics across temperatures from 270 K to 420 K and the results indicate a temperature-dependent increase in Φ_B , decrease in n range, suggesting potential barrier inhomogeneities at the Schottky interface. Characteristic temperature (T_0) calculations exhibit consistency between different methods, when the thermal coefficient (K_f) is determined as -2.1 mV/K. Interface state density (N_{SS}) rises with decreasing temperature due to thermally-driven restructuring.	[37]

(continued on next page)

Table 1 (continued)

Author Name	Schematic Diagram	Coating Method	Variations	Ideal Parameters	Photodiode Parameters	Energy Level Diagram	Aim and Summary	Ref
Alshahrani et.al.,		JNSP	Temperature variation (300–500 °C)	n= 2.87 Φ _B = 0.780 (eV) I _O = 3.43×10 ⁻⁵ (A)	- - -		Current conduction mechanisms are identified as PFE (270–330 K) and SE (above 330 K). Overall, these findings suggest promising prospects for high-performance MIS devices. This study deposited high-quality Y ₂ O ₃ films using JNSP between 300°C to 500°C. Crystal structure showed a growth transition from (222) to (400) plane after 350°C then the FESEM revealed micro/nano pellet-like grains, also the Energy bandgap values ranged from 4.50 to 4.90 eV. Photoluminescence spectra exhibited UV-visible, blue emissions. Y ₂ O ₃ films showed semiconducting behaviour, the film at 500°C had the highest conductivity (6.2904×10^{-12} S/cm). Al/Y ₂ O ₃ /n-Si heterojunction diodes displayed a semi-logarithmic J-V curve, with the 500°C diode having the lowest (n) of 2.87 and the highest (Φ _B) of 0.780 eV. Series resistance (R _s) values decreased with increasing temperature, suggesting Y ₂ O ₃ films potential for heterojunction diode applications.	[18]
K. S. Mohan et.al.,		JNSP	Variation of doping weight Yb ₂ O ₃ (0,1,5,2.5, 3.5,4.5%)	n=1.791 Φ _B =0.692 (eV) I _O =4.19×10 ⁻⁴ (A)	P _S =3845.58%		In this study investigated Al/In-Yb ₂ O ₃ /p-Si SBDs with varying in doping concentrations of Yb ₂ O ₃ . XRD analysis revealed a mono-crystalline cubic structure, with reduced crystallite size from 14 to 21 nm and also FESEM showed gemstone-like structures with non-uniform surfaces, when In-Yb ₂ O ₃ films exhibited extreme absorption and a wide E _g of 3.75 eV. Elemental composition spectra confirmed the presence of Yb, In and O. Topographic studies demonstrated reduced roughness while increase doping concentration. The PL spectrum indicated strong, broad emission bands at 361 nm with In-Yb ₂ O ₃ films displayed positive photo conducting behaviour, making them suitable for high-speed switching applications.	[38]

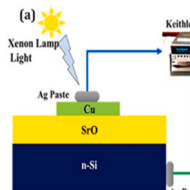
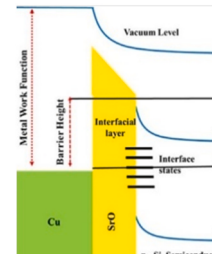
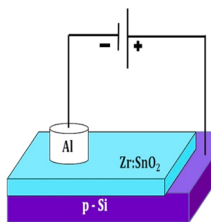
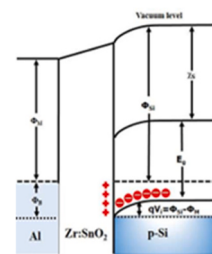
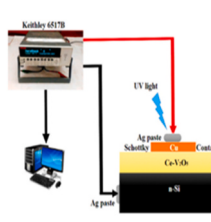
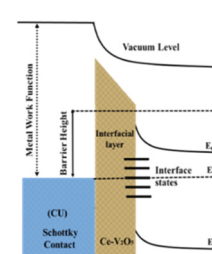
(continued on next page)

Table 1 (continued)

Author Name	Schematic Diagram	Coating Method	Variations	Ideal Parameters	Photodiode Parameters	Energy Level Diagram	Aim and Summary	Ref
K.S. Mohan et.al.,		JNSP	Variation of doping concentration Cu (0,1.5, 2.5, 3.5, 4.5 wt%)	$n=1.757$ $\Phi_B=0.754$ (eV) $I_0=5.82\times10^{-5}$ (A)	- - -		The author successfully the fabrication of Al/Cu-Yb ₂ O ₃ /p-Si (MIS) SBDs with varying Cu doping concentrations in Cu-Yb ₂ O ₃ films. XRD patterns revealed a polycrystalline of cubic system, with a mean crystallite size of 31 nm and FESEM depicted the randomly oriented crack free, smooth surface of the fine tiny globular structure. Then the films showed extreme absorption and the smallest E _g of 3.14 eV in Optical parameter, EDX confirmed Cu presence in this film and also it indicated higher roughness of the film. PL spectra exhibited strong, broad emission bands at 364 nm. DC electrical study demonstrated enhanced conductivity, minimum activation energy at higher doping concentrations. Then the experimental results from MIS SBDs highlighted improved Φ_B and decreased n values, suggesting their suitability for advanced optoelectronic, microelectronic, high-speed switching device applications.	[39]
Lazar et.al.,		JNSP	Different Mole concentration of MoO ₃ (0.02, 0.04, 0.06, 0.08)	$n=3.4696$ $\Phi_B=0.894$ (eV)	$P_S=95.51\%$ - -		This work focused on MoO ₃ thin films prepared through the JNSP technique with varying molar concentrations (0.02 M, 0.04 M, 0.06 M and 0.08 M). X-ray diffraction confirmed the orthorhombic crystal phase (α -MoO ₃) with D_{ave} ranging from 21.71 nm to 42.06 nm, then the surface morphology of the film exhibited a nanorod-like structure with porosity, enhancing light harvesting. Optical E _g values ranged from 3.21 to 3 eV. DC conductivity of the film was analysed with the MIS diodes exhibited favourable for I-V properties, the lowest n value. The high P _S was observed in 0.08 M, these findings	[17]

(continued on next page)

Table 1 (continued)

Author Name	Schematic Diagram	Coating Method	Variations	Ideal Parameters	Photodiode Parameters	Energy Level Diagram	Aim and Summary	Ref
Bala Subramani et.al.,	(a) 	JNSP	Temperature variation (350,400, 450,500) °C	n= 1.73 Φ _B = 0.82 (eV) I _O =7.85–1.37 10 ⁻⁴ (A)	- - -		suggest the potential of Cu/MoO ₃ /p-Si diodes for optoelectronic applications. A highly photosensitive Cu/SrO/n-Si SBDS was successfully fabricated using the JNSP technique, then the impact on SrO films in the crystal size range from 84.44 to 72.73 nm structural parameters, optical properties in the surface roughness was investigated. AFM images confirmed a fairly smooth surface with hillock structures, with the formation of an unbroken SrO layer on the n-Si surface. Then the I-V characteristic diode parameters demonstrated a colossal photosensitive enhancement under light irradiation, the maximum (Φ _B) was observed at 0.82 eV and (n) was found 1.73. Overall, the fabricated diodes are deemed suitable for the development of high-quality photodiodes and optoelectronic applications.	[40]
Ravi Kumar et.al.,		SGSC	Different doping concentration of Zr 0, 2, 4, 6 and 8 wt%	n=2.78 Φ _B =0.96 (eV) I _O =3.21–2.78 (A)	- - -		This study explores Zr-doped SnO ₂ films via sol-gel spin coating for Zr: SnO ₂ /p-Si SBDS. XRD analysis confirmed tetragonal crystal system, with enhanced performance. Crystallite sizes ranged from 2 to 5 nm and FE-SEM showed Zr interruption in grain growth, improving film compactness, then the films had low absorbance and high transmittance, E _G estimates for Zr:SnO ₂ films ranged from 3.90 to 3.96 eV. Doping with 8 wt% Zr resulted in higher electrical conductivity ($\sim 7.8 \times 10^{-7} \Omega^{-1} \cdot \text{cm}^{-1}$), it has displayed favourable for n range and increased Φ _B , then the 8 wt% Zr-doped SBDS demonstrated minimal series resistance, suggesting high suitability for optoelectronic applications.	[10]
Bala Subramani et.al.,		SGSC	Doping Weightage Variation of Ce (0, 2, 4 and 6) %	n=1.73 Φ _B =0.82 (eV) I _O =5.06 × 10 ⁻⁴ (A)	P _S =96090.78% R=65.86 (mA/cm ²) QE= 25.34%		In this study, a highly sensitive Cu/Ce-V ₂ O ₅ /n-Si structured SBDS was successfully fabricated with varying concentrations of Ce. Structural analysis revealed an enhancement in crystallite size from 42.07 to 63.32 nm, maintaining a tetragonal crystal structure, FE-SEM images displayed irregularly arranged nanorod and nanoplate-like structures, with Ce incorporation reducing surface roughness to a	[41]

(continued on next page)

Table 1 (continued)

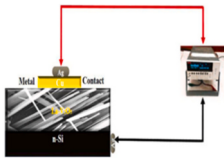
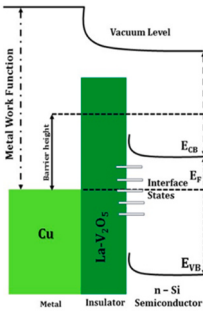
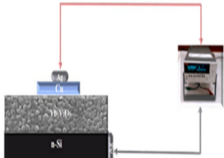
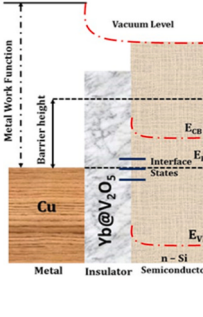
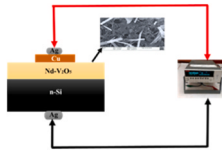
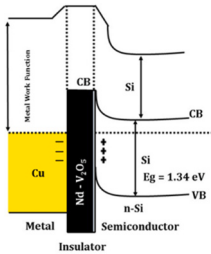
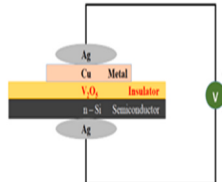
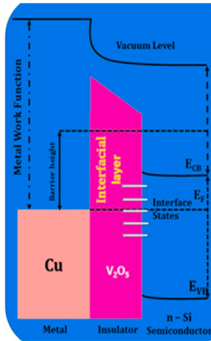
Author Name	Schematic Diagram	Coating Method	Variations	Ideal Parameters	Photodiode Parameters	Energy Level Diagram	Aim and Summary	Ref
Bala Subramani et.al., [42]		SGSC	variation of doping weight concentration in La (0,2,4,6 %)	n=4.15 $\Phi_B=0.83$ (eV) $I_0=1.95\times10^{-4}$ (A)	$P_S=3327.5\%$ $R=33.39$ (mA/W) $QE= 35.41\%$		minimum of 45 nm, then the UV-vis study indicated the Ce concentration exhibited maximum optical absorbance with a reduced E_g of 2.99 eV. The I-V characteristics of the MIS diode demonstrated good performance under light conditions, with the 6 wt% diode achieving a remarkable P_S of 96090.78%, 100 times higher than the pure diode. This work is the presence of the Ce-V ₂ O ₅ layer between Cu and n-Si was found to be suitable for MIS photo detector applications.	In this study, an enhanced photodetector based on Cu/La-V ₂ O ₅ /n-Si MIS (SBDs) was successfully fabricated through La doping using the spin coating method, then the diffraction pattern revealed a tetragonal crystal structure in La-doped V ₂ O ₅ films, FE-SEM images showcased the formation of nanorods and EDX confirmed elemental composition. La doping, particularly at 4 wt%, resulted in higher absorbance and a reduced E_g and I-V characteristics indicated the minimum activation energy for the 4 wt% La-doped film. All MIS SBDs exhibited festive photo conducting behaviour under illumination, with the 4 wt% La-doped SBDs demonstrating good diode parameters. The study suggests that the 4 wt% MIS SBDs are suitable for ON/OFF switching device applications.
Bala Subramani et.al., [43]		SGSC	variation of doping weight concentration in Yb (2,4,6 wt %)	n=2.03 $\Phi_B=0.93$ (eV) -	$P_S=75545.70\%$ $R= 37.90$ (mA/W) $QE=25.93\%$ $D^*=9.97\times10^{10}$ (jones)		In this work Cu/Yb@V ₂ O ₅ /n-Si MIS structure (SBDs) was successfully fabricated by the spin coating method. XRD resulting in tetragonal, orthorhombic structures in the doped films. Morphological studies revealed nanorods to nanoplate-like structures, then the coated thin films exhibited an E_g ranging from 3.23 to 3.31 eV. The electrical properties of MIS SBDs demonstrated good photodiode performance under lighting conditions compared to darkness. Remarkably, a high P_S of 5545.70% was achieved for the diode with 2 wt% Yb@V ₂ O ₅ , making it applicable candidate for the	(continued on next page)

Table 1 (continued)

Author Name	Schematic Diagram	Coating Method	Variations	Ideal Parameters	Photodiode Parameters	Energy Level Diagram	Aim and Summary	Ref
Bala Subramani et.al.,		SGSC	Doping of Nd weight variations (2,4,6 wt%)	$n=2.45$ $\Phi_B=0.85$ (eV) $I_0=10.87-2.77 \times 10^{-9}$ (A)	$P_S=1942$ 7.80% $R=23.79$ mA/W $QE=14.10\%$		development of photodiodes for optoelectronic applications. In this study, pure vanadium and Nd-V ₂ O ₅ nanorods were successfully deposited on glass substrates through spin coating and Nd-V ₂ O ₅ nanorods were further utilized as an interfacial layer in constructing a MIS SD. XRD analysis confirmed a tetragonal structure for all three films, with RE-ion doping notably improving morphology, optical studies indicated a red shift with E_g around 3.12 eV. I-V characteristics of MIS diode is good in ideal parameters. Photodiode performance under illumination surpassed that in darkness, suggesting the MIS structure SBDs feasibility for photonic devices and its high potential for UV photodetector applications.	[44]
Bala Subramani et.al.,		SGSC	Temperature variation (300,400, 500) °C	$n=5.26$ $\Phi_B=0.46$ (eV) -	- - -		This work focuses on Cu/V ₂ O ₅ /n-Si SBD, employing V ₂ O ₅ thin films as interfacial layers fabricated through spin coating. XRD analysis revealed structural changes from amorphous to polycrystalline V ₂ O ₅ films with a tetragonal phase a D_{av} of 42.07 nm then the FE-SEM images showcased rod-shaped surfaces with particle sizes ranging from ~10 to ~45 nm. AFM analysis indicated increased surface roughness with higher annealing temperatures, reduced film thickness. UV analysis demonstrated higher absorbance for films annealed at 500 °C, then the (E_g) values ranged from 3.95 to 3.77 eV, with the 500 °C annealed film displaying high conductivity (9.11×10^{-10} S cm ⁻¹) and low activation energy (E_a) of 0.0747 eV. Forward bias I-V characteristics revealed good diode performance for the 500°C annealed sample, with a minimum Φ_B of 0.46 eV, n value of 5.26, when V ₂ O ₅ thin film as an interface layer demonstrated good rectifying behaviour, making it suitable for temperature-dependent MIS structure diodes and optoelectronic switches.	[45]

(continued on next page)

Table 1 (continued)

Author Name	Schematic Diagram	Coating Method	Variations	Ideal Parameters	Photodiode Parameters	Energy Level Diagram	Aim and Summary	Ref
Sasikumar et.al.,		SGSC	Variation of organic additives: ZrO ₂ thin film	$n=3.21$ and 2.69 $\Phi_B=1.05\text{--}0.96$ (eV) $I_0=1.23 \times 10^{-11}$ to 7.45×10^{10} (A/cm ²)	- - -		This study explored the influence of organic additives on spin-coated ZrO ₂ thin films. From XRD revealing monoclinic crystal structures with reduced crystallite sizes 4.279 nm and the PEG:ZrO ₂ exhibited rod-shaped, square-shaped grains in the SEM analysis, with a lowered E_g range 5.66 eV in the UV-Vis investigation. EDAX confirms the elemental presence of the film in Zr and O, this film demonstrated enhanced conductivity 2.48×10^{-13} S/cm and reduced activation energy 0.090 eV attributed to increased oxygen vacancies, Al/PEG: ZrO ₂ /p-Si SD exhibited improved J-V characteristics with lower Φ_B (0.83 eV), J_s (6.88×10^{-10} A/cm ²) compared to pure ZrO ₂ /p-Si. Then the results suggested that Al/PEG: ZrO ₂ /p-Si SBD are suitable for optoelectronic device applications.	[46]
Sasikumar et.al.,		Spin coating	Variation of rare earth metals (Ce, Gd, Y) with pure ZrO ₂	$n=2.48\text{--}3.24$ $\Phi_B=1.04\text{--}0.97$ (eV) $I_0=6.494 \times 10^{-12}$ to 1.313×10^{-10} (A)	- - -		In this work Rare earth (Ce, Gd and Y) doped ZrO ₂ thin films were prepared using spin-coating, leading to monoclinic phase its $D=6.752$ nm, this partial tetragonal phases with varying crystallite sizes. Gd: ZrO ₂ in XRD data, SEM exhibited square-shaped grains due to crystallite agglomeration at 600 °C. EDX analysis verified the presence of Zr, O, Ce, Gd and Y elements, when the E_g decreased from 5.64 eV (undoped ZrO ₂) to 5.25 eV (Gd:ZrO ₂) and the highest electrical conductivity ($\sigma_{dc}=1.172 \times 10^{-7}$ S/cm) was observed for Ce:ZrO ₂ . The MIS SD based for the high fast switching and optoelectronic applications.	[47]
Sasikumar et.al.,		Spin Coating	Temperature variation (300,400, 500,600) °C	$n=3.772\text{--}3.442$ $\Phi_B=1.12\text{--}1.05$ (eV) $I_0=8.483 \times 10^{-13}$ to 1.235×10^{-11} (A)	- - -		In this work ZrO ₂ thin films were investigated for Al/ZrO ₂ /p-Si MIS. XRD revealed an amorphous nature at 300 °C, transitioning to a highly oriented monoclinic phase with reduced crystallite size the spin-orbit doublet components (Zr 3d _{5/2} and Zr 3d _{3/2}) energy split of 2.4 eV indicated Zr ⁴⁺ oxidation state. SEM images depicted increasing grain size, this film exhibited sub-micro-sized, square-shaped grains at 600°C, (Φ_B , n) values for MIS diodes ranged from 1.12 to 1.05 eV and 3.772–3.442. Both Cheung's and conventional J-V	[48]

(continued on next page)

Table 1 (continued)

Author Name	Schematic Diagram	Coating Method	Variations	Ideal Parameters	Photodiode Parameters	Energy Level Diagram	Aim and Summary	Ref
Priya et.al., 14		CMP	Different concentrations of In (0,5, 7.5 and 10) %	$n=3.89\text{--}2.88$ $\Phi_B=0.744 \text{ (eV)}$ $I_0=1.87\times 10^{-7} \text{ (A)}$	- - -		methods showed consistent results, then the decreased with rising temperature, attributed to a decrease in interface states. The MIS-type SBDs exhibited better J-V performance at 600 °C is suitable for the device applications. This study fabricated LaPO ₄ nanoparticles and doped in-LaPO ₄ through co-precipitation. XRD analysis revealed a monoclinic crystal structure with an increased crystallite size from 10.82 to 15.14 nm, SEM images exhibited spherical agglomerates and irregularly shaped nano blocks. UV spectroscopy indicated a decrease in E _g values from 3.24 to 2.93 eV, MIS structure SBDs showed high rectification behaviour with improved electrical parameters under both dark and light conditions. In the light conditions, minimum n values of 2.88 and Φ_B 0.74 eV. These findings suggest in In-LaPO ₄ suitability for photodiode applications.	[49]
Marnadu et.al., [22]		JNSP	Change in Composite Concentrations of Ce (0,4,8 and 12 wt.) %	$n=2.15$ $\Phi_B=0.686 \text{ (eV)}$ $I_0=4.59 \times 10^{-9} \text{ (A)}$	$P_S=17509.62\%$ $R=20.61 \text{ (mA/W)}$ $QE= 9.72\%$ $(D^*) = 2.7 \times 10^8 \text{ (jones)}$		The authors successfully created a highly Sensitive MIS diode with positive photo response using the JNSP technique. An average crystal size D _{ave} of 42.1 nm and higher FWHM ($B=0.00492$), with a high number of small crystallites clusters were formed on the surface of nanoplate. Then the lower surface roughness of 116 nm in the FE-SEM and Band gap (E _g) was measured at 3.1 eV in the optical studies. The I-V characteristics of the MIS diodes indicated superior photoconducting properties under illumination. Specifically, the MIS diode with 12 wt% Ce exhibited a low value of (n), strong Photo sensitivity (P _S) and achieved maximum QE at 130 mW/cm ² of light. In dark conditions, the Ce-based diode demonstrated a high Detectivity (D*) = 2.7×10^8 jones. The results identified Ce-WO ₃ films with 12 wt% Ce as optimal. Ultimately, the Cu/Ce-WO ₃ /p-Si type diode produced was deemed highly suitable for photonic-sensitive device applications	[22]

Table 2

Ideal Parameter Comparison of MIS Diodes: A Comprehensive Analysis.

Author Name	Technique	Device Structure	Ideality Factor (n)	Barrier Height Φ_B (eV)	Aim and Summary	Ref
D.E. Yildiz et.al.,	ALD (Atomic Layer Deposition)	Au/Ti/n-GaAs	1.30	0.94	The study focuses on Au/Ti/HfO ₂ /n-GaAs & Au/Ti/n-GaAs fabricated the MIS structures the (Φ_B) is 0.94 eV with an (n) of 1.30. In contrast, the reference diode has Φ_B of 0.77 eV with an of 1.07. The HfO ₂ layer in the MIS structure increases Φ_B and reduces leakage current. Analysing C-V and G-V characteristics at 1000 kHz, the study explores temperature-dependent D_{it} , R_s (series resistance), Z, Z', Z'' and phase angle values. Results indicate an increase with temperature for G, C and R_s , while D_{it} , Z and Z' increase with decreasing temperature within the 60–320 K range. The research emphasizes the influence of the HfO ₂ layer on electrical parameters and temperature-dependent characteristics in MIS structures.	[50]
Turut et.al.,	ALD	Au/Ti/HfO ₂ /n-GaAs	1.08 and 2.58	1.19	The MIS diodes were fabricated using the ALD technique for effective HfO ₂ deposition, as confirmed by AFM images showing a uniform and smooth morphology then the electrical properties, including n, Φ_B , R_s , Z and phase angle, depend on both applied voltage and temperature. The decrease in n with increasing temperature is linked to the distribution of interface states and the insulator layer between metal and semiconductor. Incremental n= 1.08, 2.58 and Φ_B = 1.19 eV values with temperature and reduction in n suggest deviation from TE theory. C, G and R_s decrease with temperature, while Z decreases with increasing temperature. The MIS diode exhibits more capacitive behaviour in the bias voltage range of -3 V to about 0.4 V. D_{it} , Q_{eff} and N_{eff} values decrease with increasing temperature in the range of 60–320 K.	[9]
Kaymak et.al.,	ALD	Al/ZnO/p-Si	1.75	0.73	The electrical characteristics of Al/ALD-grown ZnO/p-Si SBDs were investigated using standard TE theory, Norde's function and Cheung method. I-V characteristics were measured in the dark at room temperature for these diodes, n and Φ_B values from TE method were respectively for D1, D2 and D3 diodes (1.44, 0.73 eV), (1.75, 0.73) and (1.64, 0.72). Φ_B from Cheung method was 0.76 eV. Φ_B from Norde's function matched those from the Standard method. The fabricated diode is suitable for NIR Schottky photodetector applications.	[51]
Abdulkerim Karabulut et. al.,	ALD	Au/Ti/HfO ₂ /n-GaAs	1.23	1.06	Au/Ti/n-GaAs structures with an HfO ₂ interfacial oxide layer were prepared by ALD. The series resistance from forward bias I-V characteristics in the (60–400 K) range decreased with decreasing temperature, a positive result for MOS capacitor devices. The Φ_B for MIS Au/Ti/HfO ₂ /n-GaAs at 300 K is 0.94 eV to 0.77 eV, higher than the 0.77 eV for the Au/Ti/n-GaAs diode at 300 K. This suggests that the HfO ₂ thin layer at the metal/GaAs interface can modify Φ_B , serving as a gate insulator in GaAs MOS capacitors and MOSFETs, addressing the crucial need for large band offsets at MIS interfaces.	[52]
Turut et.al.,	ALD	Au/Ti/Al ₂ O ₃ /n-GaAs	2.45	1.18	This study focuses on the Ti/Al ₂ O ₃ /n-GaAs diode, revealing a higher Φ_B of 1.18 eV compared to conventional Ti/n-GaAs diodes reported in literature, essential for effective FET operation. Emphasizing the crucial role of BH modification in MS devices, the Correction for series resistance was crucial for accurate extraction of information from measured admittance. The correction results in a significant difference between corrected and non-corrected admittance data, highlighting the necessity of considering series resistance, particularly in the accumulation and a portion of the depletion region. Peaks in G-V curves post-	[53]

(continued on next page)

Table 2 (continued)

Author Name	Technique	Device Structure	Ideality Factor (n)	Barrier Height Φ_B (eV)	Aim and Summary	Ref
C.S. Guclu et.al.,	ALD	(Au/Ti)/Al ₂ O ₃ /n-GaAs	5.59	0.48	correction indicate the importance of series resistance correction and also device exhibits more capacitance at the reverse bias voltage range, with a nearly constant phase angle of 90° at all frequencies of MIS structures.	
					The study focuses on analysing Φ_B and possible current conduction mechanisms (CCMs) in the reverse bias I-V characteristics of (Au/Ti)/Al ₂ O ₃ /n-GaAs (MIS) type of SBDs across a wide temperature range. Forward and reverse bias BHs are compared, revealing an increase with temperature. BH values obtained from reverse bias are consistently lower than those from forward bias for each temperature, attributed to the electric field dependence of BH. Various current conduction mechanisms, including PFE and Schottky emission, did not yield realistic values for physical parameters. The TAT mechanism was employed, indicating an ohmic conductive mechanism for MIS structure SBDs.	[54]
S. Alialy et.al.,	ALD	Au/TiO ₂ /n-4 H-SiC	5.09–2.68	0.519–0.959	In this study, Au/TiO ₂ /n-4 H-SiC MIS SBDs were fabricated and their forward bias current-voltage-temperature (I-V-T) characteristics were investigated in the temperature range of 200–380 K. Electrical parameters (c , R_s , R_{sh}) varied significantly with temperature. Notably, semi-logarithmic forward bias I-V plots showed a parallel behaviour at moderate applied bias voltages, indicating a constant slope independent of temperature and the tunnelling parameter E_0 suggested that the FE mechanism dominates in Au/TiO ₂ /n-4 H-SiC SBDs. A plot of Φ_B vs $q/2kT$ revealed evidence of a GD of Φ_B . GD mechanism was confirmed as the main current conduction mechanism in Au/TiO ₂ /n-4 H-SiC SBDs. The energy density distribution profile of interface states (N_{ss}) was extracted from forward-bias I-V data, showing suitable values for electronic devices.	[55]
Turut et.al.,	ALD	Au/Ti/Al ₂ O ₃ /n-GaAs	1.10	0.76	The study reveals that the (MIS) structure, utilizing a high- κ Al ₂ O ₃ gate dielectric grown through (ALD) on an n-GaAs substrate, demonstrates outstanding electrical properties and this structure exhibits minimal hysteresis across the entire bias range, no frequency dispersion in the reverse bias (C-V) curves for all frequencies tested. With an ultrathin film thickness of approximately 3 nm, this Al ₂ O ₃ gate dielectric emerges as a highly promising candidate for future ULSI devices. These results suggest the potential for advanced electronic applications leveraging the excellent performance of ALD-grown high- κ dielectrics on GaAs substrates. Then the $n = 1.10$, $\Phi_B = 0.76$ are found it's suitable for diode applications.	[56]
Esra Balci et.al.,	RF Magnetron sputtering	Au/ZnSe/Si Ag/ZnSe/Si Al/ZnSe/Si	3.18	0.718	Subsequently, Au/ZnSe/Si, Ag/ZnSe/Si and Al/ZnSe/Si MIS structures were fabricated and examined. Then the ZnSe thin films of varying thicknesses were deposited on Si substrates using the sputtering technique. Characterization results led to the fabrication of MIS structures. The study revealed an increase in particle size from 11.14 to 34.63 nm with film thickness, accompanied by a decrease in strain, indicating improved crystallinity. Surface morphology measurements showed a rise in particle size from 16 to 45 nm as the film thickness increased. XPS spectra analysis confirmed Zn/Se stoichiometry in ZnSe, with an obtained ratio of 0.98. Electrical characterization demonstrated superior performance in the Au/ZnSe/Si SD with $n = 3.81$, $\Phi_B = 0.718$ eV and $R_s = 239 \Omega$, making it suitable for optoelectronic applications.	[57]

(continued on next page)

Table 2 (continued)

Author Name	Technique	Device Structure	Ideality Factor (n)	Barrier Height Φ_B (eV)	Aim and Summary	Ref
V. Rajagopal Reddy et.al.,	PLD	Au/ZrO ₂ /n-GaN	2.13	0.94	In this study, the surface composition and depth profile of pulsed laser-deposited high-k zirconium oxide (ZrO ₂) on n-type GaN are explored to form. The Au/ZrO ₂ /n-GaN (MIS) junction is fabricated, demonstrating good rectification with lower leakage current compared to the (MS) junction. Statistical analysis estimates an average Φ_B and n, revealing values 0.94 eV and 2.13 for MIS junctions. Cheung's and Norde functions confirm comparable Φ_B values. Then the MIS junction shows a lower interface state density (N_{SS}) than the MS junction, indicating effective reduction of dangling bonds on the GaN surface by the ZrO ₂ insulating layer. This study concludes that the current conduction mechanism in both junctions is governed by PFE in reverse bias. The deposited ZrO ₂ thin insulating layer is identified as a promising dielectric for MIS-based electronic device applications.	[58]
Venkata Prasad et.al.,	LPD	Au/Y ₂ O ₃ /n-GaN	2.09	0.96	In this study, the electrical and current transport properties of Au/Y ₂ O ₃ /n-GaN (MIS) diodes, featuring high-k Y ₂ O ₃ as an interlayer, are investigated and compared with Au/n-GaN (MS) diodes. Current-voltage (I-V) and capacitance-voltage (C-V) techniques are employed to explore the electrical characteristics at room temperature and the mean Φ_B and n are determined as MIS diode, respectively. This device exhibits a higher Φ_B compared to the MS diode. Cheung's functions, Norde method are utilized to determine Φ_B , R _s and n, showing parameters that are compared between the two diodes. Additionally, the interface state density (N_{SS}) is estimated, indicating a lower N_{SS} for the MIS diode, suggesting that the Y ₂ O ₃ interlayer reduces the interface state density and it concludes that PFE is the dominant conduction mechanism in the reverse bias region for Au/Y ₂ O ₃ /n-GaN MIS diodes.	[59]
S. Sai Krupa et. al.,	EBD	Ti/CaTiO ₃ (CT)/p-InP	1.22	0.84	This study presents the of high-k CaTiO ₃ (CT) on a p-InP substrate, examining its surface using AFM, XRD and XPS. The CT layer, confirmed by XRD, XPS, exhibits smooth surface roughness. Ti/CaTiO ₃ (CT)/p-InP MIS diode and Ti/p-InP SDs were prepared and electrical features were measured. The MIS diode shows superior rectifying behaviour compared to the SDs. Higher Φ_B (0.84 eV (I-V) and 1.15 eV (C-V) is observed for the MIS diode than the SDs (0.72 eV (I-V) and 0.92 eV (C-V), indicating the CT layer modifies the SDs Φ_B . I-V, Cheung's and $\alpha(V)-V$ approaches extract Φ_B , n and R _s of the SDs and MIS diode, showing close agreement. The lower N_{SS} for the MIS diode suggests the CT layer significantly alters the potential density of states of the SDs. The CT layer holds promise for high-performance InP-based (MIS) devices.	[60]
M.Uma et.al.,	EBD	Au/La ₂ O ₃ /n-GaN	1.72	0.76	This study investigates the influence of a La ₂ O ₃ insulating layer on Au/n-GaN Schottky junctions by introducing an Au/La ₂ O ₃ /n-GaN (MIS) junction. Structural and chemical analyses confirm the successful formation of the La ₂ O ₃ film on the n-GaN surface. Electrical evaluations through I-V and C-V measurements reveal that the Au/La ₂ O ₃ /n-GaN MIS junction exhibits superior rectification and lower reverse leakage current compared to the Schottky junction. Higher Φ_B in the MIS junction (0.76 eV (I-V)/ 0.95 eV (C-V)) are observed, suggesting the beneficial impact of the La ₂ O ₃ layer and consistency in Φ_B values from different methods validates the reliability of the experimental techniques. Then the estimated interface state density (N_{SS}) is lower in the MIS junction,	[61]

(continued on next page)

Table 2 (continued)

Author Name	Technique	Device Structure	Ideality Factor (n)	Barrier Height Φ_B (eV)	Aim and Summary	Ref
Rehab Ramadan et.al.,	EBD	Al/Si/TiO ₂ /NiCr	2.12	0.87	indicating the involvement of La ₂ O ₃ in reducing N _{ss} . Overall, the study suggests that La ₂ O ₃ films could be promising dielectric materials for enhancing the performance of MIS devices. The study aimed to assess the potential of three MIS SBDs for photovoltaic solar cells by analysing AC and DC electrical conduction properties. AC properties were characterized using electrochemical impedance spectroscopy and capacitance–voltage measurements, proposing an equivalent electric model. Mott–Schottky analysis determined flat-band potential, carrier doping density and conduction type (p or n). DC properties from current–voltage measurements revealed key diode parameters. Modifications to the Al/Si/TiO ₂ /NiCr MIS diode, including Si surface etching for nano PS layers and silver nanoparticles in nano PS layers, enhanced electrical conduction properties. The improvements also enhanced optoelectronic performance, making these devices suitable for photovoltaic applications.	[62]
Somnath Mahato et.al.,	CVD	Au/MoO ₃ —x/n-Si	1.92–1.55	0.718–0.995	In summary, the thermal evaporation process reduced molybdenum trioxide (MoO ₃) to non-stoichiometric MoO ₃ —x, altering Mo's oxidation state from Mo ⁺⁶ to Mo ⁺⁵ . This reduction induced defects in the film, influencing charge transports. Photoluminescence measurements at low temperatures confirmed the presence of defects, with a shift toward longer wavelengths as temperature increased. At ≤ 165 K, MoO ₃ —x behaved as an insulator due to insufficient thermal energy then the results revealed an increase in Φ_B with temperature, while C-V-T showed inverse characteristics, indicating the presence of interface barrier inhomogeneity affecting device performance. The modified RP, considering a double GD for SBDs, yielded a RC of 155 A·cm ⁻² K ⁻² , close to the theoretical value for n-Si, aligning well with TE theory.	[63]
V. Manjunath et.al.,	EBD	Au/Sm ₂ O ₃ /n-GaN	1.64	0.81	This study focuses on the deposition of high-k samarium oxide (Sm ₂ O ₃) thin films on n-type GaN by e-beam evaporation. Chemical properties, assessed using (XPS), confirm the presence of Sm 3d _{3/2} , Sm 3d _{5/2} and O 1 s peaks. An Au/Sm ₂ O ₃ /n-GaN (MIS) junction is fabricated and compared with an Au/n-GaN (MS) junction. Then the MIS junction demonstrates superior rectification and lower leakage current, attributed to a higher Φ_B (0.81 eV (I-V)/1.0 eV (C-V)) compared to the MS junction (0.68 eV (I-V)/0.90 eV (C-V)). Analysis using different methods yields consistent results for Φ_B , n, R _s and insulating layer effectively reduces interface state density, suggesting a promising application for MIS-based devices. Capacitance measurements reveal bias voltage and frequency dependencies, while forward bias I-V characteristics indicate ohmic behaviour at lower biases and space-charge limited current at higher voltages for both junctions. Reverse leakage current is governed by PFE in both MS and MIS junctions. The findings affirm Sm ₂ O ₃ as a suitable dielectric material for electronic applications.	[64]
R. Padma et.al.,	EBD	Au/Fe-ZnO NS/n-InP	1.90	0.90	The impact of an Fe-doped ZnO NS interlayer on the electrical properties of Au/n-type InP Schottky structure was investigated. Surface analysis (FESEM, AFM) revealed a smooth Fe-ZnO NS on InP. XRD determined an average grain size of 12.35 nm. The Au/Fe-ZnO/n-InP MIS Schottky structure exhibited superior rectifying behaviour compared to Au/n-InP Schottky, Φ_B were 0.79 eV (I-V)/0.89 eV for Au/n-InP MS and 0.90 eV (I-V)/1.06 eV (CeV) for Au/Fe-ZnO/n-InP. Fe-ZnO NS	[65]

(continued on next page)

Table 2 (continued)

Author Name	Technique	Device Structure	Ideality Factor (n)	Barrier Height Φ_B (eV)	Aim and Summary	Ref
Necati Basman et al.,	Electro Chemical method	Au/S-DLC/p-Si	3.3–0.90	0.62–0.92	<p>effectively modified the interfacial potential barrier and interface state of Au/n-InP Schottky, resulting in increased effective Φ_B and decreased interface state density. Norde and Cheung's functions determined n, Φ_B, R_s revealing lower N_{ss} values for MIS. PFE conduction dominated at lower biases and Schottky emission at higher biases for both structures. Experimental results suggest Fe-ZnO NS as a promising candidate for Schottky rectifiers in electronic devices.</p>	[66]
Balasubramani et.al.,	JNSP	Al/n-MDC/p-Si	10.35–10.8	-	<p>This study explores sulfur-doped diamond-like carbon (S-DLC) nanocomposite films deposited on a p-type silicon substrate via electrochemical methods, Au/S-DLC/p-Si MIS diodes were fabricated and compared with Au/p-Si diodes. This include the superior thermal stability of the MIS diode, maintaining rectification at 700 K compared to the Au/p-Si diode, which lost rectification at 500 K. Post temperature-dependent measurements revealed a structural transformation in the S-DLC interlayer, enhancing rectification at room temperature. The S-DLC interlayer acted as a Φ_B modifier, exhibiting a lower Φ_B before annealing and a higher Φ_B after annealing than the Au/p-Si diode. Both diodes displayed temperature-dependent parameters, with increased Φ_B and decreased n as temperature rose, attributed to inhomogeneities in Φ_B. Non-linearity in the RP was explained by a GD of Φ_B. Electrodeposited S-DLC films show promise for high-temperature diode applications.</p>	[67]
M.Uma et.al.,	EBD	Au/Pr ₆ O ₁₁ /n-GaN	1.51	0.83	<p>The successful fabrication of NS Honeycomb-like and Foam-like Manganese-Doped Cerium films on high-quality glass using JNSP. The incorporation of Mn atoms into the CeO₂ films has profound implications for optical properties, impacting parameters such as band gap, refractive index optical conductivity. Emission analysis disclosed three distinct bands in the visible region, showcasing vibrant colours in violet, blue and green at 394 nm, 425 nm and 467 nm then the crystal structure of the Manganese-Doped Cerium film, characterized by a polycrystalline nature and a single-phase cubic fluoride structure oriented preferentially along the (200) direction. FTIR confirmed the presence of terminal stresses (CeO) and phonon bands (Ce-O) within the iron oxide. Morphological analysis revealed the formation of intricate structures, with fine particles converging to create spherical formations, including honeycombs, foams, rings and voids. XPS indicated a higher Mn ion content on the film's surface, with successful doping of Mn ions into the interior of the CeO₂ lattice. The n range suggested the existence of a natural oxide layer comprising Manganese-Doped Cerium and an inorganic semiconductor, specifically p-type silicon. Beyond fundamental characteristics, the films demonstrated practical utility in optoelectronic applications, showcasing high electrical properties and rapid responsiveness to light. In conclusion this structure of diode is good for the applications in optoelectronics, electronics and sensor technologies.</p> <p>This study focuses on growing a high-k Pr₆O₁₁ thin film on an n-GaN surface using the e-beam technique, characterized by XRD and XPS. An Au/Pr₆O₁₁/n-GaN MIS junction with a Pr₆O₁₁ insulating layer is fabricated. Electrical properties, assessed through I-V and C-V measurements, demonstrate excellent rectifying behaviour and low reverse leakage current for MIS junction. The MIS junction exhibits a higher Φ_B (0.76 eV (I-V)/1.19 eV (C-V)) compared to</p>	[68]

(continued on next page)

Table 2 (continued)

Author Name	Technique	Device Structure	Ideality Factor (n)	Barrier Height Φ_B (eV)	Aim and Summary	Ref
M.Uma et.al.,	Electro chemical deposition	Au/Fe ₃ O ₄ /n-GaN	1.87	0.84	<p>the SE (0.71 eV (I-V)/0.90 eV (C-V)), indicating modification of the Φ_B by the Pr₆O₁₁ insulating layer. Various analysis methods, including Cheung's, Norde functions and $\Psi_{S,V}$ plot, were employed to extract Φ_B, n and R_s, showing consistent results. This MIS junction exhibited a lower interface state density (N_{ss}) than the SE, highlighting the significant role of the Pr₆O₁₁ insulating layer in reducing N_{ss}. The observed PFE suggested that the Pr₆O₁₁ thin film holds promise as a high-k insulating material for developing GaN-based MIS devices.</p> <p>This study investigates the statistical distribution of Φ_B, reverse current conduction and capacitance-frequency (C-f) and conductance-frequency (G-f) characteristics in the Au/Fe₃O₄/n-GaN heterojunction. Statistical analysis reveals higher average Φ_B for the HJ (0.84 eV) compared to the Au/n-GaN Schottky junction (0.70 eV), attributed to the Fe₃O₄ interlayer insertion. This SJ undergoes a transition from PFE to Schottky emission with increasing voltage, while the HJ exhibits PFE throughout the voltage range. Higher capacitance at lower frequencies suggests excess capacitance from interface states in equilibrium with n-GaN. Then the conductance remains nearly constant at 10³-10⁵ Hz, then sharply rises with increasing frequency. Interface state densities and relaxation times extracted from C-f and G-f characteristics indicate the potential of the Fe₃O₄ interlayer for (MIS) device applications.</p>	[69]
M. Chandra Sekhar et.al.,	DC MS	Al/(Ta ₂ O ₅) _{0.85} (TiO ₂) _{0.15} /p-Si	2.20–1.95	0.71–0.76	<p>This study explores the impact of negative bias voltage (0 to -150 V) on (Ta₂O₅)_{0.85}(TiO₂)_{0.15} thin films deposited on p-Si (100) and quartz substrates using dc reactive MS. Then this film exhibits improved crystallinity with orthorhombic β-Ta₂O₅ phase under a suitable negative bias and the optical E_g decreases from 4.49 to 4.39 eV with increasing bias voltage. Al/(Ta₂O₅)_{0.85}(TiO₂)_{0.15}/p-Si MIS Schottky devices were fabricated with bias voltages from 0 V to -100 V, revealing superior Schottky barrier parameters for the sample biased at -100 V, including a higher Φ_B, lower n and lower R_s. Discrepancies in Schottky barrier height measurements from I-V and C-V methods were explained by interface inhomogeneities. In conclusion, negative substrate bias voltage enhances the structural, optical and electrical properties of MIS devices.</p>	[11]
R. Ertugrul-Uyar et.al.,	RF MS	Au/TiO ₂ /n-Si	2.57–2.11	0.62–0.669	<p>In this paper investigates the impact of gamma radiation on the Au/TiO₂/n-Si (MIS) structure was explored through current measurements at various irradiation doses. Results indicate that radiation induces defect states in the insulator layer, leading to a reduction in reverse current, attributed to a decline in minority carriers due to radiation-induced defects. Calculated interface state density (N_{ss}) values decrease with irradiation and electrical parameters of the MIS structure are dose-dependent, suggesting the potential application of this gamma-sensitive MIS structure as a solid-state radiation detector.</p>	[12]
A. Buyukbas Ulusan et.al.,	RF MS	Au/Si ₃ N ₄ /p-GaAs	2.41	0.79	<p>This paper investigates the electrical characteristics and current conduction mechanisms of the Au/Si₃N₄/p-GaAs (MIS) diode were investigated at room temperature. Using the TE theory, I-V characteristics were explained and diode parameters such as Φ_B, n and R_s were obtained. The Φ_B value was determined using Norde's method and matched with the TE method. N_{ss} was calculated from forward bias I-V measurements. Current conduction mechanisms</p>	[13]

(continued on next page)

Table 2 (continued)

Author Name	Technique	Device Structure	Ideality Factor (n)	Barrier Height Φ_B (eV)	Aim and Summary	Ref
H. Tanrihulu et. al.,	RF MS	Au/TiO ₂ /n-Si	5.31–1.75	0.55–0.75	were analysed under both forward and reverse bias, involving ohmic, TCLC, SCLC under forward bias and Schottky emission under reverse bias. Results suggest the MIS diode is suitable for capacitor applications.	[14]
Arjun Shetty et. al.,	RF MS	Pt/HfO ₂ /n-GaN	3.6–1.2	0.3–0.79	This work reports an experimental investigation of the electrical characteristics of a MS -fabricated Au/TiO ₂ /n-Si. Diode and this diode's I-V and C-V properties were examined by authors at different frequencies and temperatures. They found that the n and Φ_B changed with temperature, which was explained by barrier inhomogeneities. The diode's interface state density and R_s were determined, together with the RC, activation energy and Φ_B is suitable for diode application. The author revealed that the Gallium nitride films, 300 nm thick, were grown on sapphire substrates using plasma-assisted molecular beam epitaxy. The film crystalline qualities were confirmed through High Resolution-XRD and their optical properties were assessed using photoluminescence measurements. MIS diodes were fabricated and diode parameters such as Φ_B and n were extracted, then the addition of HfO ₂ as an insulator layer improved diode performance, enhancing rectification ratio (5.1–8.9), increasing Φ_B (0.3 eV to 0.79 eV) and reducing n (2.1–1.3). Temperature-dependent I-V measurements of the Pt-HfO ₂ -GaN SDs revealed increased Φ_B and decreased n with rising temperature, indicating an inhomogeneous Schottky contact. A modified RP yielded an actual Φ_B of 0.85 eV with a standard deviation σ^2 of 0.013. In conclusion, HfO ₂ proved effective as an interfacial layer, enhancing Pt/n-GaN SDs parameters and demonstrating inhomogeneity at the Pt/HfO ₂ /n-GaN interface.	[15]
B. Prasanna Lakshmi et.al.,	RF MS	Au/Ta ₂ O ₅ /n-GaN	1.13	1.03	This study investigates the electrical characteristics of Au/Ta ₂ O ₅ /n-GaN (MIS) structures, focusing on the impact of annealing temperature. Leakage current significantly decreases to 1.42×10^{-10} A at –2 V after annealing at 500 °C. As-deposited contact exhibits a Φ_B of 0.93 eV and an n of 1.13. Annealing at 500 °C increases Φ_B and n to 1.03 eV and 1.13, respectively, while a slight decrease is observed at 600 °C (Φ_B is 0.99 eV). Norde's and Cheung's methods estimate Φ_B , n and R_s , revealing SE dominance with PFE in high voltage regions. The annealed MIS diodes with the interfacial layer exhibited lower density of interface states compared to the as-deposited MIS diode with the interfacial layer.	[16]
Marnadu et.al.,	JNSP	Cu/Sr-WO ₃ /p-Si	2.39	0.57	In this study, WO ₃ and Sr-WO ₃ composite films were grown using the JNSP technique at an optimized substrate temperature of 400 °C and their structural, optical and electrical properties were analysed. XRD results showed a higher D_{ave} for 12 wt% Sr-WO ₃ film. FE-SEM revealed changes in the surface microstructure, transitioning from spheroid pan to seashell-like structures for 12 wt% Sr-WO ₃ films. AFM analysis indicated higher surface roughness for higher Sr concentration. EDX spectra confirmed the presence of W, O and Sr. Then the composite film with 12 wt% Sr-WO ₃ exhibited maximum absorption, minimum E_g of 3.60 eV. I-V characteristics revealed the highest electrical conductivity and the lowest activation energy for 12 wt% Sr. In MIS SBDs, 12 wt% Sr-WO ₃ showed the lowest n and a favourable forward bias value, indicating better device performance. This study suggests that MIS SBDs have promising	[70]

(continued on next page)

Table 2 (continued)

Author Name	Technique	Device Structure	Ideality Factor (n)	Barrier Height Φ_B (eV)	Aim and Summary	Ref
B. Guzeldir et.al.,	Successive Ionic Layer Adsorption and Reaction (SILAR)	Cu/Cu ₃ Se ₂ /n-GaAs	4.97–1.14	0.21–0.83	applications in optoelectronics, microelectronic and high-speed switching devices. In this study, copper selenide films were deposited on GaAs substrate using the SILAR method. Structural and morphological properties were investigated using XRD, SEM and AFM. A Cu/Cu ₃ Se ₂ /n-GaAs/In structure was fabricated and its I-V characteristics were analysed from 60 to 400 K. SDs parameters, such as n and Φ_B , exhibited temperature dependencies attributed to barrier inhomogeneity at the MS interface. Then they decrease in Φ_B potential and increase in n with decreasing temperature were explained by the TE with GD of the Φ_B . The study suggested that the dominance of TFE could be linked to lateral variations in Φ_B , impacting the transmission probability and electric field distribution.	[71]
O. Gullu et.al.,	Simple cast method	Al/DNA/p-Si	1.344–1.704	0.753–0.605	This work explores DNA molecules as a potential organic thin film for MIS devices were studied for I-V characteristics in the temperature range of 200–300 K. The non-ideal behaviour of the diode was observed, with n of 1.34 ± 0.02 at 300 K and 1.70 ± 0.02 at 200 K and the Φ_B decreased from 0.75 ± 0.01 eV at 300 K to 0.61 ± 0.01 eV at 200 K. VF-T characteristics were linear for different activation currents and temperature coefficients of the forward bias voltage (dVF/dT) were determined as -2.30 mV K ⁻¹ , -2.60 mV K ⁻¹ and -3.26 mV K ⁻¹ for varying currents. The Al/DNA/p-Si SDs is suggested as a cost-effective alternative to Si p-n junctions for temperature sensing, demonstrating 42% higher sensitivity.	[72]
Engin Arslan et. al.,	Metal organic chemical-vapor deposition (MOCVD)	Al _{0.22} Ga _{0.78} N/AlN/GaN	Sample B 2.54 Sample C 0.89 4.05	Sample B 0.95 Sample C	This paper investigates (SBDs) on Al _{0.22} Ga _{0.78} N/AlN/GaN heterostructures with and without an insulator layer. Forward and reverse bias I-V, C-V and G/ ω -V characteristics were measured to analyse key electrical parameters at room temperature, including n, zero-bias Φ_B , R _s and interface-state density (N _{ss}). Then the study reveals that the insulator layer thickness and R _s significantly impact the main electrical parameters. R _s values, obtained using Cheung's method and conductance method from forward bias I-V characteristics, show dependence on the insulator layer thickness. This energy distribution profile of N _{ss} , derived from forward bias I-V characteristics and considering bias dependence, along with low-high frequency C-V characteristics, demonstrates a decrease in N _{ss} values with increasing insulator layer thickness and the findings contribute to understanding the effects of insulator layers on the electrical performance of SBDs in AlGaN/GaN heterostructures.	[73]
Souvik Kundu et. al.,	hot probe technique	Al/MEH-PPV/p-GaAs poly [2-methoxy-5-(2/-ethyl-hexyloxy)-1,4-phenylene vinylene] (MEH-PPV), as an interfacial layer.	1.17	0.87	In this study, we developed a GaAs-based (MIS) device with MEH-PPV, an organic material, serving as an interfacial layer to enhance the Φ_B . The band diagram of p-GaAs/p-MEH-PPV was proposed, aiming to understand the dominant current transport mechanism and the MIS device exhibited a significantly reduced leakage current of 5.3×10^{-8} A at 0.50 V compared to 1.1×10^{-6} A in the (MS) device. Then the introduction of MEH-PPV increased the Φ_B by 0.22 eV, confining charge carriers effectively. MEH-PPV demonstrated stability, contributing to a high-quality organic/inorganic interface with low hysteresis voltage and interface states. Additionally, C-f characteristics revealed a high transition frequency, indicating low density of interface states. Then the MIS photovoltaic device exhibited promising characteristics with a V _{oc} of	[74]

(continued on next page)

Table 2 (continued)

Author Name	Technique	Device Structure	Ideality Factor (n)	Barrier Height Φ_B (eV)	Aim and Summary	Ref
Mustafa A. Ahmed et.al.,	SGSC	Pd/ZnO/n-Si/AuSb	1.06	0.750	1.10 V, I_{sc} of 0.52 mA and efficiency of 5.92% under AM 1.0 and V_{oc} of 1.15 V, I_{sc} of 0.43 mA and efficiency of 5.45% under AM 1.5. These findings position MEH-PPV as a favourable organic material for the development of organic-based electronic and photovoltaic devices. From this work, SDs based on undoped and (Ce, Sm) co-doped ZnO nanorods were successfully fabricated on an n-Si substrate using chemical bath deposition and SGSC techniques. XRD results confirmed the crystalline nature of the nanorods, with preferential growth along the x-axis. The nanorods maintained their hexagonal structure, as observed in FESEM images. Raman spectroscopy indicated a shift in the E2 high peak, decreased intensity after doping. XPS analysis detected Ce and Sm in higher doping concentrations, along with the presence of oxygen vacancies. Photoluminescence spectra exhibited weak UV and strong deep-level emissions, with the latter decreasing up to 0.4 at% doping and increasing at higher concentrations. SDs showed rectification behaviour and the n decreased with increasing doping. Then the current transport mechanism involved ohmic conduction at lower voltages and SCLC and TFL at higher voltages, indicating enhanced generation-recombination processes in co-doped nanorods.	[75]
F. Yigiterol et.al.,	Hill-Coleman	Au/Si ₃ N ₄ /4 H n-SiC	2.50	0.98	In this study, an Au/Si ₃ N ₄ /4 H n-SiC MIS diode was fabricated and its electrical properties were investigated through temperature-dependent I-V, frequency- and temperature-dependent C-V and G-V measurements. The forward I-V behaviour was modelled using TE theory with a GD of Φ_B due to inhomogeneity at the interface. The calculated values for Φ_B and R_S were 1.43 eV and 0.169 eV, respectively. Considering BH inhomogeneity, the corrected RC was determined as 141.648 A/cm ² K ² . Cheung's model revealed a decrease in R_S with increasing temperatures. C-V, G-V plots indicated sensitivity to high temperature and low frequency, suggesting possible interface restructuring under thermal effects. The Hill-Coleman method was employed to evaluate the capacitance of the insulator layer, D_{it} values were calculated based on variations in frequency and temperature.	[76]
S. Zeyrek et.al.,	nitride passivation	Al/Si ₃ N ₄ /p-Si	6.17	0.714	The Al/Si ₃ N ₄ /p-Si MIS SBDs were studied for (I-V) and (C-V) characteristics in the temperature range of 80–300 K. The decrease in zero-bias (Φ_B) and increase in n at lower temperatures suggest significant changes, attributed to Schottky barrier inhomogeneities with a GD of Φ_B at the interface. A plot of Φ_B versus $q^2/2kT$ revealed a mean Φ_B of 0.826 eV and standard deviation (σ_ϕ) of 0.091 V. Values of Φ_B and RC (A^*) obtained from a modified ln $(I_0/T^2) - q^2\sigma_\phi^2/2(kT)^2$ Vs q/kT plot were 0.820 eV and 30.273 A/cm ² K ² , respectively. The disagreement between SBH values from I-V and C-V measurements is attributed to dominance of low SBH regions at low temperatures in I-V. The interface state density (N_{ss}) increased with temperature, while the N_{ss} distribution profile decreased, showing thermal restructuring and reordering of the Si-Si ₃ N ₄ interface.	[77]
Ali Riza Deniz et. al.,	Spin Coating method	Au/CoO/p-Si/Al	1.19	0.82	In this paper, I-V measurements of reference Au/p-Si/Al and Au/CoO/p-Si/Al diodes produced under the same conditions were analysed. The CoO material used as the interface material has changed the diode characteristics. As the n value decreased, the Φ_B value increased. It was determined that the n, Φ_B and R_S values calculated from the temperature dependent I-V	[78]

(continued on next page)

Table 2 (continued)

Author Name	Technique	Device Structure	Ideality Factor (n)	Barrier Height Φ_B (eV)	Aim and Summary	Ref
Mustafa Okutan et.al.,	Vacuum Thermal evaporation	Ag/SiO ₂ /n-Si	1.91	0.62	measurements of the Au/CoO/p-Si/Al diode were strongly dependent on the temperature and this was attributed to the inhomogeneous nature of the potential barrier. From the C-V measurements performed for different frequency values of the Au/CoO/p-Si/Al diode, it was determined that the Na, V _d and Φ_B values decreased with increasing frequency and suitable for diode applications.	[79]
M. Siva Pratap reddy et.al.,	MOCVD	Ni/Au/Al ₂ O ₃ /GaN	1.09	0.96	This paper explores the characteristics of a fabricated Ag/SiO ₂ /n-Si MIS diode through I-V and C-V analyses. The observed behaviour suggests a MIS configuration rather than an ideal SBDs for the Ag/n-Si structure and its presence of the interfacial oxide layer induces modifications in the electronic parameters of the Ag/SiO ₂ /n-Si/SDs. The interface state density exhibits a variation, ranging from $1.66 \times 10^{11} \text{ eV}^{-1} \text{ cm}^{-2}$ to $0.18 \times 10^{11} \text{ eV}^{-1} \text{ cm}^{-2}$ it is suitable for photodiode applications.	[80]
S. Ashok et.al.,	Plasma Oxidation	Au/SiO ₂ /nGaAs	1.10	0.91	This study examines the temperature-dependent electrical properties of TMAH-treated Al ₂ O ₃ /GaN MIS diodes. The Φ_B increases then the n value decreases with rising temperature and the temperature range of 150 K to 400 K, (R_S) and interface state density (N_{SS}) of the diode decrease. Carrier transport mechanisms vary with electric fields and temperatures, indicating a transition from PFE at 150 K to 250 K to space-charge-limited conduction SE dominating at temperatures above 300 K. The distinct mechanisms are attributed to different carrier transport phenomena in the TMAH-treated Al ₂ O ₃ /GaN MIS diode, with SE occurring at the dielectric interface and PFE through traps in the bulk of the dielectric suitable for diode applicatiions.	[81]
Ozge Surucu et. al.,	(MOCVD)	Al/Si ₃ N ₄ /p-Si	3.039	0.713	In this work MIS SBDs were created on n-GaAs with a thin plasma-oxidized insulating film. Reference MS diodes were also made on untreated and oxide-stripped GaAs. Then the MIS diode's forward I-V characteristics suggest classical TFE. The reduction in forward current is attributed to an increased Φ_B , we reduced velocity of emitted carriers. Negative charge at the interface increases Φ_B , while recombination in the oxide reduces carrier velocity. Unlike MS diodes, an excess current is observed at low forward voltages due to recombination in the space-charge layer. The reverse current in MIS diodes is attributed to generation in the space-charge layer at low voltages and electric-field modulation of the barrier by the interfacial layer and interface states at higher biases. Interface state density derived from reverse current data aligns with independent evaluation based on C-V data. An anomalous capacitance behaviour in MIS Schottky barriers is discussed and attributed to a non-uniform oxide layer. The study highlights potential errors in Φ_B and doping concentration evaluation from MIS SDs data and proposes criteria for checking parameter reliability, when the modelling methodology is crucial for resolving inconsistencies in MIS SDs with non-uniform oxide layers.	[82]

(continued on next page)

Table 2 (continued)

Author Name	Technique	Device Structure	Ideality Factor (n)	Barrier Height Φ_B (eV)	Aim and Summary	Ref
Dilber Esra Yildiz et.al.,	ALD	Ag/ZnO/p-Si	1.48	0.74	increasing with light intensity. Responsivity and detectivity decrease with higher illumination. The photodiode exhibits stable behaviour in transient experiments, indicating potential for optoelectronic devices.	[83]
D. Esra Yildiz et.al.,	ALD	Al/TiO ₂ /p-Si Al/ZnO/p-Si	12.71 4.80	0.64 0.69	This work explores the ZnO film was deposited on p-Si using ALD method. The fabrication of Ag by using thermal evaporation, forming Ag/ZnO/p-Si MIS SBDs. ZnO displayed absorbance across UV to visible range with a E_g of 3.19 eV. I-V measurements yielded, Φ_B , n and R_s values of 0.74 eV, 1.48, and 8.06 kΩ. The device showed photodiode behaviour under increasing light intensity, with max responsivity and detectivity of 0.28 A/W and 6.54×10^9 . Best performance was at 550 nm wavelength, indicating potential for optoelectronic applications across the visible spectrum.	[84]
Dilber Esra Yildiz et.al.,	ALD	Au/ZnO/n-Si	1.27	0.91	This paper compared the two MIS structure of (Al/TiO ₂ /p-Si and Al/ZnO/p-Si) SBD. TiO ₂ and ZnO interlayers were fabricated by ALD method. The devices underwent I-V and I-t testing across various light conditions. SEM and EDX analysis confirmed uniform morphology and composition. Diode parameters (n, R_s , Φ_B) were determined using TE, Norde, and Cheung methods. Al/ZnO/p-Si showed a higher barrier height (0.69 eV) compared to Al/TiO ₂ /p-Si (0.64 eV). Responsivity was significantly higher for Al/ZnO/p-Si (755 mA/W vs. 21.7 mA/W), with an EQE of 173.08%. According to performance results, Al/ZnO/p-Si exhibited better photodetector performances.	[85]

photo-induced, electron hole pairs ($e^- - h^+$) and the reduction of charge recombination, leading to increased absorption of higher light intensities. Illumination, a key factor for devices like photodiodes, photovoltaics, interacts with parameters such as temperature, voltage, doping and thickness, influencing crucial photodiode characteristics such as ideality factor (n), barrier height (Φ_B), saturation current (I_0), photo-sensitivity (P_S), responsivity (R), quantum efficiency (QE) and detectivity (D) [6]. Despite numerous studies on diode performance under illumination, limited literature exists concerning MIS structured photodiodes operating with inorganic materials as interlayers and inclusion of an organic interlayer in the MS interface can significantly alter the electrical parameters of MIS-type SBDs due to notable tunnelling currents [7].

Organic and Inorganic semiconductors, characterized by sturdy covalent bonds within the lattice, exhibit enhanced charge transport properties, thereby improving the efficiency of MIS diodes [8]. The

unique features of these semiconductor devices make them instrumental in the advancement of photon-focused research, particularly in optimizing the interaction between light and materials for superior device performances. Delving deeper into the fundamental principles, a diode, a two-terminal circuit, facilitates current conduction and electrical reversal, typically in a single direction. Constructed from p-type and n-type semiconductor materials bonded to form a p-n junction, a diode permits current flow from the p-type to the n-type material while blocking current flow in the reverse direction. These inherent properties render diodes invaluable in various electronic applications such as modulation, power control and signal switching. Then the diverse array of diode types, including standard silicon diodes, SDs, Zener diodes and LEDs, each possesses unique characteristics and finds applications across a spectrum of electronic devices, underscoring the indispensable role of semiconductor devices in modern technology [1–4]. Due to its tunable features such as fast response, ultra-high

speed, low current flow, stability and long life have made the research community focus on photon-focused equipment research and there is still much room for improvement in performance, when SDs are used variably in response to different light levels [5].

Various techniques are employed for thin film fabrication, each offering distinct advantages tailored to specific applications. PVD involves vaporizing a material, which condenses onto a substrate, achieved through methods like evaporation or sputtering. Evaporation entails heating a material until it evaporates, while sputtering uses ions to dislodge atoms from a target. CVD relies on the chemical reaction of gaseous precursors to deposit a thin film, widely utilized in semiconductor fabrication. ALD occurs layer by layer, allowing precise control over film thickness through self-limiting reactions, beneficial for conformal coatings on complex surfaces A. *Turut et al.*, [9]. The SGSC Process transforms a colloidal solution into a gel, cost-effectively producing thin films of various materials like ceramics and glasses. K. *Ravikumar et al.*, [10]. Spin Coating dispenses a liquid solution onto a rotating substrate, creating uniform films centrifugal force, commonly used for polymers, photoresists and small-scale applications. Molecular beam epitaxy deposits atoms or molecules in a vacuum, crucial for semiconductor device fabrication, ensuring precise control over layer thickness and composition. RF MS is a thin film deposition process using a target and substrate in a vacuum chamber. Unlike DC MS, RF MS uses a RF power source to generate high-frequency electricity to ionize a rare gas to produce plasma. RF energy increases ionization efficiency and makes synthesis more efficient as in DC MS, the magnetic field produced by the magnetron confines the plasma close to the target surface. Positively charged ions from the plasma bombard the target, causing sputtering and the expelled material is placed on the substrate to form a thin film. RF MS is appreciated for its ability to deposit a variety of materials, including insulators for its excellent control of films, making it suitable for many applications in electronics, optics and advanced systems [11–16]. Laser ablation involves using a laser beam to remove material from a target, suitable for depositing complex materials in superconductors and thin film transistors. Electroplating deposits a metal film onto a substrate through an electric current, cost-effective for large-scale production of metal coatings. The selection of a method depends on factors such as material properties, desired film characteristics and specific application requirements within electronics, optics, energy and materials science. Especially we have discussed about the JNSP technique. T. *Lazar et al.*, [17]. JNSP technology has numerous advantages such as cost effectiveness, modest test setup, high homogeneity, huge coverage area and product cleanliness. T. *Alshahrani et al.*, [18]. Moreover, the main challenge of JNSP technology is the control of film surface morphology, thickness and stoichiometry. A. *Narmada et al.*, [19]. V. *Jagadeesan et al.*, [20]. We can also adjust the discharge temperature, gas pressure and liquid volume throughout the film discharge process. J. *Thangabalu et al.*, [21]. The correction parameters of SBDs include the interface layer temperature. It is caused by the direct transfer of energy from high-energy materials to the lattice atoms in the spray field, which affects the performance of the device. In the JNSP technique the temperature is accompany to 450°C. Because only at this temperature we can obtain a good film with good performance.

Several materials were analysed in this review, such as alkali earth metals, transition metals, lanthanides, metalloids, metals and non-metals. We have found that one best group of materials named transition metals from the various aspects of that materials and likely, followed by the points below. Transition metals offer advantages like high performance, encompassing excellent conductivity, stability and durability. Their versatility spans various applications, from electronics to energy devices. Tailored properties of transition metal thin films allow for customization based on specific application requirements. Transition metals are indispensable in the landscape of thin film technology, propelling progress in electronics, optics, energy and medicine. The interplay of availability, specifications, uses, advantages and disadvantages underscores the intricate considerations for researchers and engineers

harnessing these materials. As technology evolves, so too will the pivotal role of transition metals in shaping the future of thin film technology. Transition metals play a pivotal role in advancing thin film technology, revolutionizing various applications and also exploration delves into the abundance, specifications, applications, merits and drawbacks of key transition metals instrumental in thin film deposition. Abundant in the earth's crust, transition metals like titanium (Ti), zirconium (Zr), tungsten (W) and tantalum (Ta) stand out for thin film applications, offering economic viability for large-scale production, each metal boasts unique specifications. Titanium (Ti), shines in medical implants and protective coatings due to its corrosion resistance and biocompatibility. Zirconium (Zr), finds value in optical coatings and transparent conductive films for its high refractive index. Tungsten (W) excels in high-temperature applications, such as electronics and aerospace, owing to its high melting point [22–26]. Tantalum (Ta), atomic, demonstrates stability in corrosive environments, finding applications in electronic components and medical devices. In terms of applications, these transition metals are integral to electronics, with Ti, W and Ta playing key roles in semiconductors. Zr and Ti contribute to optical coatings, enhancing durability and performance in lenses, mirrors and displays. Titanium compounds are crucial in thin film solar cells, advancing sustainable energy technologies. Also, tantalum recognized for biocompatibility and corrosion resistance, play vital roles in medical implants and devices. However, challenges persist, such as the cost associated with certain metals like tantalum, impacting overall thin film production costs. Additionally, certain transition metals pose processing challenges during deposition, necessitating precise control to achieve desired film properties.

On this overview paper we discussed possibilities of MIS diodes and techniques. The primary standards of MIS it functionalise upon the vital inter-mediate insulator layer within the MIS structure are defined, optical parameters, diode parameters, the aim and summary with the diode structure and energy level diagrams are mentioned in the Table1 and ideal parameters representation it mentioned in the Table2. Then the materials that used for the MIS structured diode fabrication are discussed separately by its groups and, each layer of diodes the best works are found from the specifications of those diodes. Followed by way of a conclusion and dialogue of the generalised approaches for fabricated MIS-based diodes such as precise information at the practise of MIS structures.

2. Interfacial layer coating methods of MIS diodes

Thin film plays an important role in many technical applications, providing versatility and importance in the production of advanced materials and devices. Essentially, a thin film is a layer of nanometre to micron scale material deposited on a substrate that exhibits unique properties that vary in their properties and these films are widely used in electronics, optics, coating and sensing applications, then these thin films can be divided into different types based on their deposition methods, materials, including PVD methods such as evaporation and sputtering, CVD techniques such as spin coating and dip coating. Each method provides the thin films with specific properties that affect its thickness, uniformity and composition. The variety of film types allows equipment to be cut to meet the needs of various technologies, making them an essential part of today's equipment. Thin films are widely used in many industries because of their unique properties, quality and they are components of semiconductor devices in the electronics industry and can be used for insulating, conducting or semiconducting layers. Also, it plays an important role in solar cells by improving energy conversion, they are known in the sensor world for their ability to respond to changes in temperature, pressure and other environmental conditions. Advantages of thin films include the ability to control properties such as thickness, composition, thereby improving the performance of electrical and optical devices. Additionally, the use of thin films often reduces the amount of material, making the process more economical and

1. Air compressor
2. Pressure meter
3. Pressure controller
4. Air flow tube
5. Stand
6. Nebulizer kit
7. Precursors solution
8. Solution flow tube
9. Temperature controller
10. Temperature display
11. Substrat holder
12. Substrate

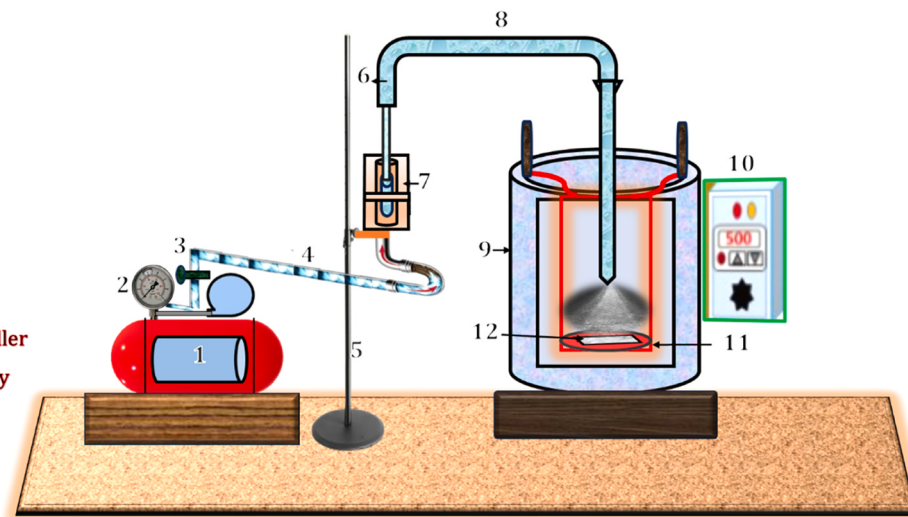


Fig. 1. Representation diagram of the jet nebulizer spray pyrolysis technique.

environment friendly.

2.1. Jet Nebulizer Spray Pyrolysis (JNSP)

In the mid-20th century, when scientists began searching for new ways to control the composition of nanomaterials, combination of atomization and spray pyrolysis principles laid the foundation for technologies that later revolutionized the fields of nanoscience, materials engineering and origins of JNSP can be found in early experiments in spray pyrolysis, a process created by first atomizing a liquid into droplets then pyrolyzing it at ambient temperature. Then the researchers confirmed the potential of this approach for the control of thin films nanoparticles and atomization using a high-pressure jet allows scientists to first obtain the distribution of liquids this is an important consideration in the study of synthetic materials. *R. Marnadu et al.*, [22]. Over the next few years, JNSP was refined became an important component in nanomaterial synthesis laboratories around the world but researchers used the technology's ability to control parameters such as particle size, precursor content, reaction temperature to tailor the properties of nanoparticles and adaptability exterior the way for the synthesis of various nanomaterials. JNSP history is not static; It's a nice ongoing explanation and continuous research aims to refine outdated processes, first discover new knowledge to push the boundaries. This technology is still at the forefront of nanomaterial synthesis, contributing to the continuation of the field of nanotechnology.

Spray pyrolysis is a technique used in material science, nanotechnology for the synthesis of thin films and nanoparticles, it involves creating a chemical precursor containing the desired properties and then atomizing it into a fine spray. Then the spray is sprayed directly onto the heated substrate, where the solvent evaporates, leaving behind a thin film or collection of nanoparticles. In addition, outlet temperature, spray concentration, spray pressure and speed can be adjusted [23]. In this method is often used to create a variety of materials that includes thin-film coatings for electrical and photovoltaic devices.

JNSP technology for film coating consists only of a compressor, a spray gun is L-shaped tube nebulizer made of glass and an open-top oven in which the substrate is mounted on the substrate holder to control the temperature with thermocouple-display. In addition, the main challenge of JNSP technology is to control the film's surface morphology, thickness and stoichiometry [24]. Required surface temperature can be adjusted by temperature control, this technology is used to form thin films. A nebulizer is a small air compressor-powered machine that turns pre-medicated medications into small, mist-like droplets. *R. Marnadu et al.*, [25]. Although it is portable, it requires electricity to run the air

compressor, when the pipe connects the compressor to the small part of the atomizer nebulizer that holds the liquid. It converts liquid into air by applying compressed air to the nebulizer *R. Marnadu et al.*, [26].

There are two types of nebulizers; these are JNSP and ultrasonic nebulizers, while nebulizers are founded on the Venturi principle, ultrasonic nebulizer routine the reverse piezoelectric effect to convert alternating current into high-frequency sound energy, ultrasonic nebulizers do not use airflow to create aerosols. Instead, these nebulizers use ultrasonic waves to create vibrations, that break the liquid into tiny particles. More specifically, these nebulizers use vibrating piezoelectric crystals to produce ultrasonic waves. For both types, the main variables are the operating time required, the size produced and the liquid aerosol released. There are two main parameters to measure the presentation of the nebulizer: aerosol droplet size supply and liquid discharge rate, which are determined by the design of the nebulizer. Higher air pressure from the compressor in the jet nebulizer or the frequency of displacement of the piezoelectric crystal in the ultrasonic nebulizer will reduce small droplets and importance of particle size should better correspond to aerodynamic particle diameters in the range of 1–6 mm. Then the size and flow rate of the drug in the nebulizer mainly depends on the geometry of the nebulizer and the gas carrier pressure, the main driver of the spray nebulizer spraying device is an air compressor with control valve, the air compressor is connected to the pipe with the head from the purification nebulizer. It can be considered that the small distribution of the described micro nebulizer plane is better and more than the products used today. And the power consumption is lower than ultrasonic nebulizer. *P. Harishsenthil et al.*, [27].

It has several important steps: first, atomization of the salt containing liquid, sending the liquid to the thermal substrate, evaporation of the film, solvent formed on its substrate's surface and decomposition of an accumulated substances. In this device, the temperature of the substrate plays an imperative part in the formation of the film. This technology has many advantages: it is possible to create ultra-thin films of various thicknesses; it is easy to add additives to the spray and it is not difficult to prepare the films of a mixture by mixing additives. Associated, with other deposition methods such as thermal evaporation method, sputtering method, pulsed laser deposition method, JNSP technology is an inexpensive method as the total cost is less. Additionally, nebulizer kits, guns, air cylinders, compressors and open-top stoves are easily available at local stores at low cost [86,87]. Owing to JNSP technology is cost-effective, time-saving and more efficient than other (high-cost) technologies [27,28].

Fig. 1. Diagram representing of the JNSP technique. An air compressor functions by converting energy into compressed air,



Fig. 2. Photograph of the jet nebulizer spray pyrolysis (JNSP).

achieving high energy suitable for various applications. When this process involves drawing air through an inlet valve, compressing it using mechanisms like pistons, generating heat in the process and storing the compressed air in a tank. Pressure is regulated and controlled before distribution through a network of pipes, a pressure meter or barometer, measures gas pressure by utilizing a sensing element like a diaphragm or Bourdon tube. Then the pressure change deforms the element, providing a visual or numerical pressure reading. A pressure controller, designed to manage fluid pressure, adjusts output based on the comparison between actual and set-point pressures. And an air flow tube is utilized in scientific or industrial applications for measuring air pressure and directing airflow in ventilation *P. Harishsenthil et.al.*, [29]. Specialized stands, such as reaction racks, provide a stable platform for drug containers during testing, resistant to corrosion. Nebulizer kits use cups to convert liquid medication into aerosol when the precursors solution involves two solutions in semiconductor fabrication processes like deposition, doping and etching, solution flow tubes find applications in chemical analysis systems, while temperature controllers maintain desired temperatures in various applications. Substrate holders play a crucial role in the semiconductor and thin film industries, ensuring the stability and control of the substrate during production *P. Harishsenthil et.al.*, [30]. The term "substrate" generally refers to the base material supporting various industrial processes.

In semiconductor production, the substrate commonly used is a silicon wafer, serving as the foundation for the integrated electronics manufacturing process which involves depositing various materials like semiconductors and insulators onto the substrate, when significance of the substrate extends to thin film deposition technology, where it functions as the surface for the thin film, providing stability, influencing the film's performance. Across different industries, the term "substrate" generally denotes the base or underlying material for processes or deposits *V. Balasubramani et.al.*, [31]. Then the substrate's performance is application-specific, exemplified by its crucial role in the semiconductor industry, where it contributes to the foundational processes of material deposition and integrated electronics manufacturing on silicon substrates.

2.2. Thin Film Deposition

In this technology, the substrate is a surface of the thin film, then the role of the substrate is to provide a stable base for the film, which affects its performance and properties.

A solution of the drug to be coated as a suitable precursor is placed in the drug compartment at the bottom of the nebulizer and bottom of the chamber connects to the compressor pipe then the drug is released into the souk in the form of an aerosol with a particle size of 2–5 nm. Due to rapid discharge, the temperature drops, the droplets cool, the solvent evaporates, condenses, falls onto the substrate, the temperature of the substrate, chemical reactions will occur and the chemical will oxidize to form crystal nuclei. Then the growth of grains occurs in crystal nuclei, leading to the formation of a continuous thin film and L-shaped pipe is used for liquid flow; the horizontal length of the outlet is 25 cm and the

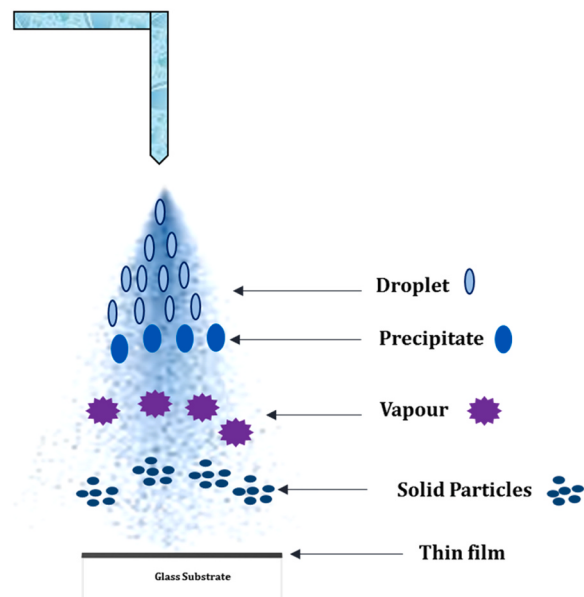


Fig. 3. Photograph of the liquid deposition on the thin film.

vertical length is 15 cm. Bottom of the riser is carefully designed as a nozzle to spray mist evenly onto the substrate and the above tools also include P-N junction diodes, metal insulator-semiconductor diodes, field effect transistor models, etc. It can also be used to create multilayer electronic devices. **Fig. 2.** shows the photograph of the JNSP setup.

According to the above statement, the distance between nozzle and the substrate is optimized by trial and error, starting from 10 to 2 cm, the distance is gradually reduced to 10–7 cm, this means that fog completely disappears due to temperature depending on distance. Below 7 cm, only a light layer is possible, here only fast-moving fog can withstand the heat produced by the stove in the form of steam moves around the glass substrate, after testing it is optimized for 5 cm, when the steam can reach substrate smoothly and completely at a distance of 5 cm. Due to the speed of the air below 5 cm, it spreads out over the substrate. In the static position of the nozzle, the substrate size of the liner will be 1×1 cm per layer, but here a 2.5 cm x 2.5 cm substrate is used for coating, why the process needs to constantly move slightly vertically and horizontally. Water droplets (fog) affect the substrate where the solvent is completely evaporated, resulting in the deposition of a rough film in which the permeability decreases, from an airflow perspective, the size of the air particles is also good. Therefore, the thermal energy obtained from water droplets evaporates on the substrate and forms a beautiful film, in the case of high air flow, the fog particle size will be smaller than visible and the water droplets will completely evaporate above the substrate. Therefore, the reverse reaction occurs in the vapour field, which reduces activity and the molecules condense into thermal crystallites, then they form powdery precipitates on the substrate that reduce transparency.

2.2.1. Advantages and Disadvantages

The advantages of using a jet nebulizer in conjunction with adequate pyrolysis include the ability to achieve uniform coatings on various substrates *P. Vivek et.al.*, [32]. The nebulizer produces fine droplets, resulting in small material particles, making it suitable for applications requiring precise control and high quality. *P. Vivek et.al.*, [33]. The spray method parameters, such as size, pattern and distribution, can be effectively controlled with the jet nebulizer, crucial for successful outcomes. *T. Lazar et.al.*, [17]. JNSP is user-friendly and find applicability in laboratories or factories, offering additional methods for thin film release through spray pyrolysis. *K.S. Mohan et.al.*, [39]. However, there are limitations, such as difficulties in scaling production while

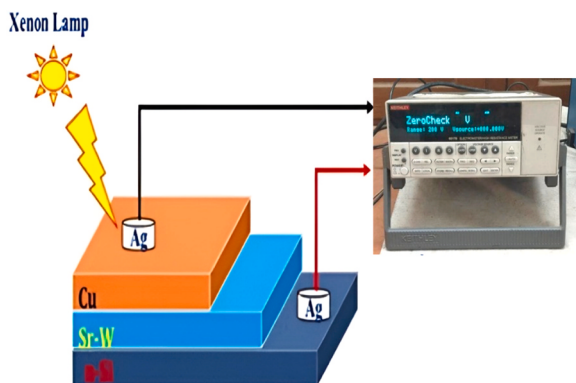


Fig. 4. Schematic diagram of the Cu/Sr-W/n-Si Schottky diode. [31].

maintaining consistency and control over large areas. *P. Vidhya et.al.*, [88]. Then the choice of solvent in the nebulizer can also restrict the effective processing of certain materials that may not dissolve well in nebulizer solvents *P. Vivek et.al.*, [34].

2.2.2. Liquid Deposition on the substrate

Fig. 3. Represents the process of the liquid deposition on the thin film. It shows how the films were formed on the glass substrate.

Compare to all the works done under this technique. We have found the best one from that JNSP method has proven to be very effective in the production of SDs with Cu/Sr-W/n-Si as shown in the **Fig. 4**. structures of different concentration and their performance usability in many areas were demonstrated then the MIS diode implies enhanced rectifying activity. However, the MIS diode with light condition films shows a photodiode performance compared to other devices, as per the final results of the paper. One of the main advantages of JNSP is its high efficiency vacuum-free properties, making it a good choice for many applications and this technology can produce high-quality films using minimal amounts of precursors, thus increasing their profitability and economic viability. In this particular study, the JNSP implementation achieved the best results for SDs with MIS structure. The obtained of $n = 1.68$ and Φ_B of 0.83 eV demonstrates the success of JNSP in achieving excellent device performance. It highlights the importance of JNSP as a promising approach to low-cost, high-quality device manufacturing in semiconductor devices.

2.3. Atomic Layer Deposition (ALD)

ALD is the advanced thin film deposition technique renowned for its unparalleled precision and control at the atomic level, this self-limiting process involves exposing a substrate sequentially to alternating precursor gases in a vacuum chamber. *D. E. Yildiz et.al.*, [50]. The cycle begins with the introduction of the first precursor, which chemically reacts with the substrate surface to form a monolayer, excess precursor is then purged, a second precursor is introduced, initiating a cyclic process that ensures precise control over film thickness and composition. ALD ability to deposit conformal and uniform thin films with exceptional thickness control makes it well-suited for applications in semiconductor manufacturing, nanotechnology and advanced coatings. Among them, ALD technology has become the first choice for thin film deposition due to the characteristics of its sub-substrate deposition mode. MIS methods for deposition of oxide materials in building manufacturing. Since the sub single layer-by-sub mono layer deposition mode characteristic of ALD allows the adjustment of film thickness with monolayer precision, in principle and high conformality and uniformity [89]. In ALD technique, the reactions reach saturation after forming a single atomic layer. This provides accurate, precise and easy thickness control and homogeneous coating. The film thickness depends only on the number of reaction cycles. In this way, it is possible to conformal coat even the most

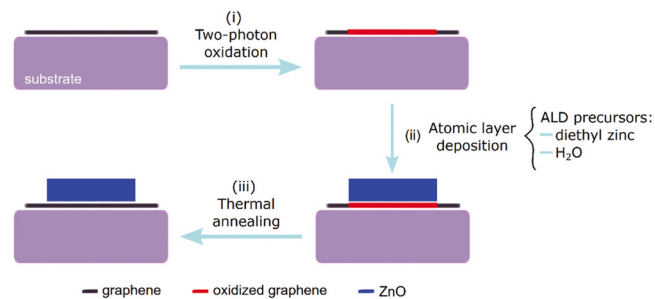


Fig. 5. Scheme of AS-ALD on monolayer graphene. i) Area-activation via two-photon oxidation, ii) atomic layer deposition of ZnO and iii) thermal annealing [92].

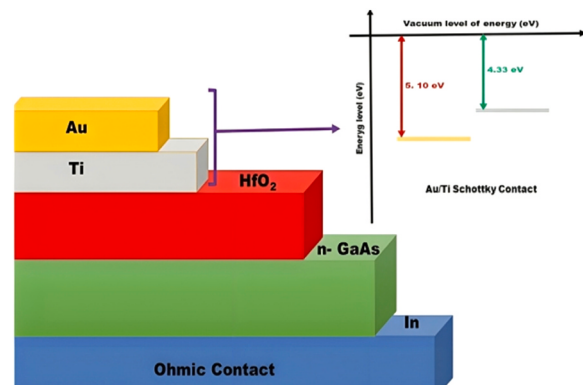


Fig. 6. Schematic representation of the Au/Ti/HfO₂/n-GaAs Diode [50].

challenging geometric shaped surfaces. ALD is a perfect method for depositing thin films with 3D structures and this ALD technique has high performance in the 3D aspect in lofty aspect ratio, it is very compatible substrate surface has many features such as reproducibility, good film density, low-temperature growth, uses very reactive precursors [51,90, 91]. Notably, ALD can coat complex 3D structures and its formation of high-quality, pinhole-free films represents a significant advantage. By placing a single layer of atoms in each designated circle, ALD achieves a uniform, harmonious structure, making it widely utilized across various industries for producing well-controlled films with excellent thickness uniformity and conformability.

Fig. 5. ALD finds widespread application in various industries, notably in the microelectronics and semiconductor sector, where it is extensively utilized to create ultra-thin dielectric layers, metal door frames and other essential components crucial for combining and sustaining small electronic devices. *Abdulkерим Karabulut et.al.*, [52]. Photovoltaics, ALD is instrumental in producing thin-film solar cells, enhancing their performance by depositing thin films with optical and electrical components. *S. Alialy et.al.*, [55]. Then the versatility precision of ALD makes it indispensable across advanced technologies, contributing to progress in electronics, energy, optics and information science. One of its key advantages lies in achieving highly controlled thin film composition, allowing for tailored film properties to meet specific application requirements. *A Turut et.al.*, [56].

Compared with other studies with similar methods, this paper focuses on the ALD technique of MIS structure, especially the Au/Ti/n-GaAs as shown in **Fig. 6**. diode ratio. Studies have shown the Φ_B of the MIS structure is 0.94 eV and the n is 1.30. Then fabricated diode exhibited clear rectifying behaviour and significant zero-biased photo response, photodiode performance under illumination surpassed that in darkness, suggesting the MIS structure SBDS feasibility for photonic devices, combination of high-k dielectrics and metal oxides deposited by ALD is important as a key aspect of MIS also ability of ALD technology

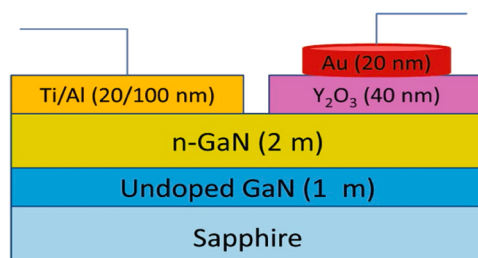


Fig. 7. Schematic configuration of the Au/Y₂O₃/n-GaN metal-insulator-semiconductor (MIS) Schottky diode [59].

with sub-monolayer deposition mode to accommodate different sizes, film thicknesses with a precise layer is highlighted. This work demonstrates the advantages of ALD in depositing high dielectric oxide layers on semiconductor substrates, revealing that it can produce excellent films over large hot and cold substrate areas. Comparative analysis demonstrates the importance of this work, showing that performance is improved by integrating ALD technique into thin films for advanced devices.

2.4. Liquid Phase Deposition (LPD)

LPD is a widely utilized thin film deposition process with applications across diverse industries such as microelectronics, optics, photovoltaics and operating on the principle of chemical reactions occurring in the liquid phase, LPD involves depositing a liquid onto a substrate to form a thin film. *Yi-Shu Hsieh et.al.*, [93]. In materials science and semiconductor manufacturing, LPD employs a liquid-phase reaction solution to control the deposition of thin films on the substrate, utilizing carefully controlled parameters such as reaction temperature, concentration and release time to achieve the desired film thickness and properties. *V. Rajagopal Reddy et.al.*, [58]. *C. Venkata Prasad et.al.*, [59]. However, challenges such as difficulties in film thickness control, the importance of fluid-substrate compatibility, the need for specialized equipment and potential post-processing requirements, like heat treatment, should be considered in the implementation of LPD.

In research using similar techniques, this paper examines and compares the electrical and current transfer properties of as shown in Fig. 7. Au/Y₂O₃/n-GaN MIS diodes with high-k Y₂O₃ interlayer and stands out. Au/n-GaN metal/semiconductor models are available. It is noteworthy that the average Φ_B and n determined in this study are 2.09 and 0.96 eV, respectively. The versatility of the complex coating process and its compatibility with different types of substrates make it useful in this field, in addition of the high-k Y₂O₃ interlayer increases the significance of this work, highlighting its implications for improving device performance. Additionally, this article demonstrates the general use of this method, called LPD, for microelectronics, optoelectronics, solar power generation, ceramics and coatings and the advantages of LPD, such as processing in different fields, the film is not good in large area and the cost of using liquid precursor is cheap, are related to its feasibility and contribute to the advancement of this research in the thin materials industry, film deposition technology.

2.5. Electron Beam Deposition (EBD)

EBD is a thin film deposition method utilizing a focused electron beam to vaporize or sputter material from a source, with the resultant particles condensing on a substrate to form a thin film when the process is conducted in a vacuum to minimize interference from air molecules. *N. Bathaei et.al.*, [94]. Another approach, electron beam lithography, employs a focused beam of light to selectively modify or remove material from the substrate, allowing for nano meter scale pattern creation. Success in the electron deposition method hinges on optimizing

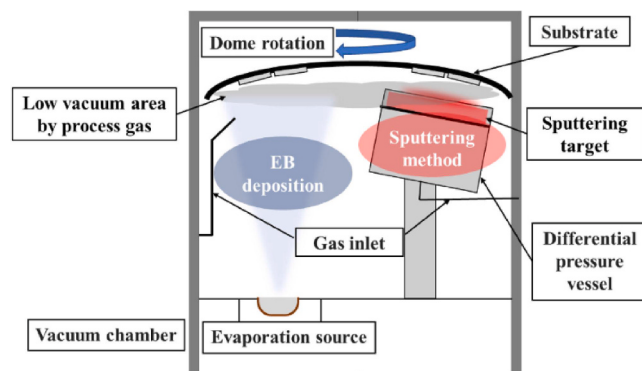


Fig. 8. Schematic diagram of the combination coating equipment (sputtering and EB deposition) [98].

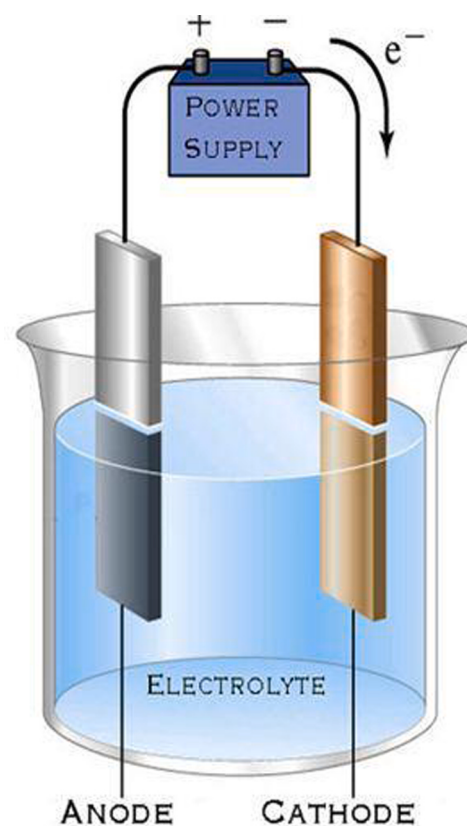


Fig. 9. Photograph of the Electron Beam Evaporation [99].

substrate conditions and controlling the energy and intensity of the electron beam. *M. Nistor et.al.*, [95]. Widely applied in the semiconductor industry, optics and research laboratories, EBD offers high purity film production, precise control over the deposition process and the ability to create uniform coatings on various surfaces, making it essential in the fabrication of microelectronic devices, nanomaterials.

As shown in Fig. 8 and Fig. 9 EBD is a prominent thin film coating technology widely employed in various industries, such as microelectronics, optics and information science. Then the underlying principle of EBD involves the use of high-energy light to heat a material, causing it to thermally evaporate and transform into vapor. *V. Dansoh et.al.*, [96]. This vapor then condenses on a substrate, resulting in the formation of a thin film. The working mechanism of EBD entails creating a high-voltage electric beam directed into a vacuum chamber, where intense electric currents damage the target material, leading to its evaporation or

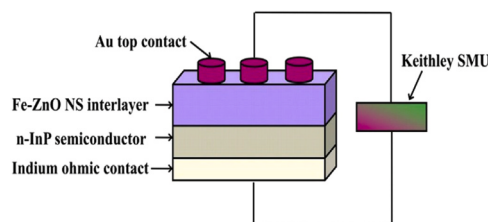


Fig. 10. Schematic diagram of Au/Fe-ZnO NS/n-InP MIS Schottky structure [65].

sublimation. G. Zhang et.al., [97].

The procedures involved in EBD include the preparation of materials, where substances like metals and oxides are loaded into a crucible or substrate. Then the entire process unfolds in a vacuum chamber to eliminate the influence of air molecules, guaranteeing the purity of the deposited film, a key step involves heating an electron beam, producing a focused beam of electrical energy directed at the material's surface, leading to rapid thermal evaporation. T. Zhang et.al., [100]. The evaporated material turns into steam, facilitated by the vacuum and then condenses on the substrate to form a thin film. Then the parameters such as deposition time and substrate temperature allow for precise management of film properties like thickness and uniformity.

In terms of applications, EBD is extensively utilized in microelectronics for depositing thin films in semiconductor devices and it also plays a crucial role in optics, contributing to the production of optical coatings, glasses and other thin film optical components. A. Augustin et.al., [101]. Additionally, EBD is employed in the photovoltaic industry for the production of thin film solar cells.

Among studies using similar techniques, this paper stands out by examining the EBE method, effect of Fe-doped ZnO nanostructure (NS) interlayers on electrical properties of Au/n-type InP SDs. These applications include FET, microwave components, solar photovoltaic energy conversion systems, laser diodes, photodetectors. However, it is to achieve a maximum of 0.9 eV in n-InP-based Schottky junctions due to the stabilization of the surface fermi level caused by the high density of surface states and other factors that do not introduce is-stoichiometric defects ideal value of 2.09 respectively. Then the article describes the EBD process, where the evaporated material condenses on the substrate

via vacuum and forms a thin film and Au/Fe-ZnO NS/n-InP, MIS Structure as shown in Fig. 10. EBD accuracy and sensitivity make it the first choice for thin film deposition in data science and semiconductor manufacturing. This technology enables the bonding of a variety of substrates and can be used in the production of advanced materials devices, optical systems then the article also briefly mentions EBD, another method that relies on an electron beam to release vapor from the material through evaporation and the substrate versatility of the deposition method helps this research advance the importance of thin film technology in many ways.

2.6. Co-Precipitation Method (CPM)

CPM is a highly utilized method for synthesizing nanoparticles, compounds or materials, where in multiple products precipitate simultaneously from a homogeneous solution. E. Endarko et.al., [102]. Then the resulting products often showcase unique properties, making CPM a versatile technique with applications in various fields are valued for its simplicity, cost-effectiveness, ability to control the composition and properties of the final product, CPM involves combining nanoparticles or fine particles of the desired material from a solution. V. H. Choudapur et.al., [103]. In this process, two or more precursor ions are simultaneously precipitated by adding a precipitant, inducing the formation of particles that cause different metal ions or compounds CPM simultaneously. Fig. 11. Shows that the CPM process. V. Manikandan et.al., [104].

This reaction's properties can be fine-tuned by adjusting factors such as reaction temperature, pH and reactant concentration. CPM has found wide application in preparing nanomaterials, catalysts and magnetic materials, offering a versatile and scalable approach to controlled synthesis.

Precipitation methods have many advantages in the field of composites, making them promising for future use its main advantage is the ability to produce nanomaterials with controlled size, morphology, offering a competitive advantage for certain applications in catalysis, sensors and biomedicine. S. Fallahizadeh et.al., [105]. V. S. Kamble et.al., [106].

In a field of research using similar technologies, this particular paper stands out by examining CPM techniques, the fabrication of Cu/In-LaPO₄/n-Si like shown in Fig. 12. structure. More importantly, this study

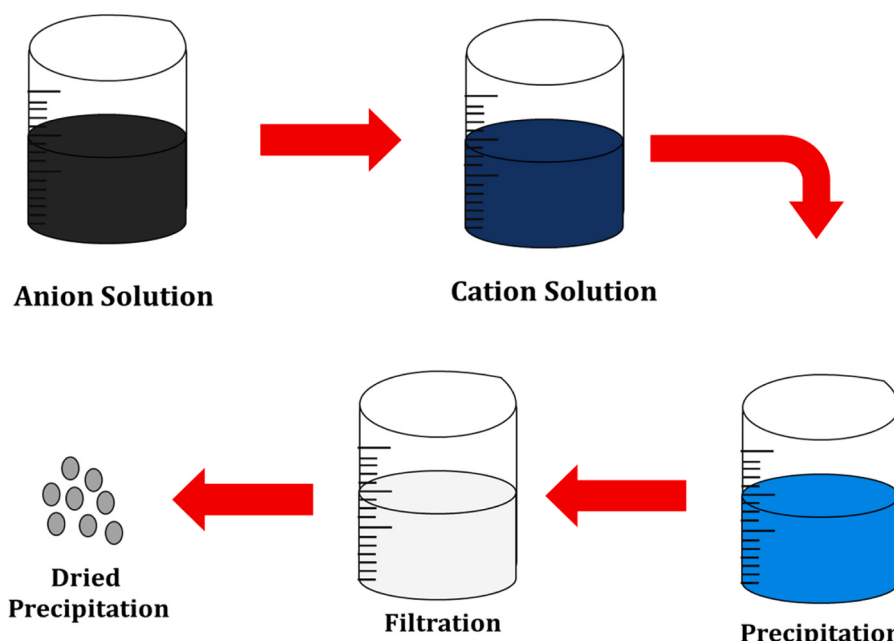


Fig. 11. Photograph of the Co- precipitation method process.

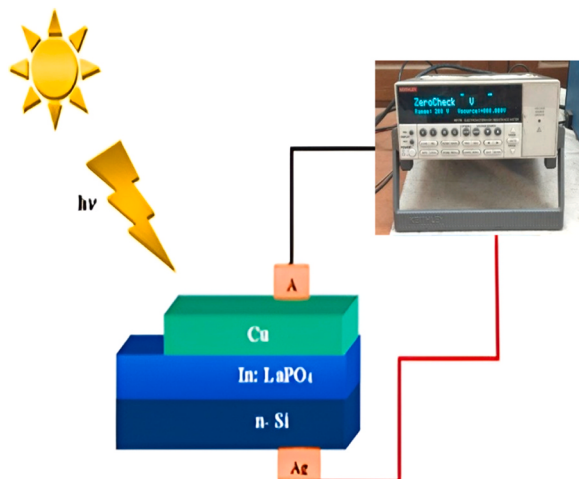


Fig. 12. Schematic diagram of the Cu/In-LaPO₄/n-Si Schottky diode. [49].

demonstrates the effectiveness of n,Φ_B with values of 2.88 and 0.96 eV, respectively. This structure Schottky barrier diode showed high rectification behaviour with improved electrical parameters under both dark and light conditions, which makes this research in unique way that is opens the way to creating versatile products with the right properties by combining many elements into a single nanomaterial, simplicity and cost-effectiveness of this method make it a suitable method for industrial applications, increasing its attractiveness for large-scale production. As researchers continue to develop and explore this approach, its role in advancing nanomaterials science, technology should expand and open new avenues for interactive applications.

2.7. Electrochemical Polymerization Method (EPM)

EPM emerges as a crucial process for producing electronic products by controlled electrical oxidation or reduction of monomers, when polymer materials like polypyrrole, polyaniline and polythiophene exhibit diverse electrical, optical, redox properties, making them suitable for applications in sensors, actuators organic electronics and energy storage. G. A. Kadhim et.al., [107]. This method offers advantages such as simplicity, scalability and the ability to transfer polymers into electronic devices in a controlled manner. The working process of electrochemical polymerization involves several key steps. Firstly, appropriate

monomers, such as pyrrole, aniline or thiophene, are selected based on the desired material properties. An electrical cell, comprising an active electronic component, electrical cabinet and electronic equipment, is then set up with electrodes immersed in an electrolyte solution containing the chosen monomers. S. Saxena et.al., [108]. As shown in Fig. 13. monomers adsorb onto the working electrode upon applying an electric current between the working, counter electrodes, electrochemical oxidation or reduction of monomers occurs, leading to the formation of free radical cations or anions .

These free radicals initiate polymerization, causing polymer chains to grow on the electrode, the polymer film continues to grow, forming a stable adhesion layer whose thickness, shape can be controlled by adjusting parameters like voltage, current and reaction time. R. Miyashita et.al., [110]. The resulting polymer films are characterized for their structure, electrical and electronic properties. EPM provides a versatile and effective means to integrate polymer processing with various materials, facilitating the development of advanced materials for a range of applications. F. Saouti et.al., [111]. Its simplicity, scalability and controllable nature make it a valuable method in the creation of tailored electronic devices and materials. EPM serves various purposes, including the synthesis of nanoparticles with controlled size and composition, making it a significant method in nanomaterial production. It is employed in catalysis, utilizing composite materials with high surface areas and tuneable properties for many chemical processes. In the realm of magnetism, co-precipitation is instrumental in synthesizing magnetic nanoparticles for applications such as data storage, MRI and magnetic hyperthermia. Additionally, EPM is applied in drug delivery systems, where combined materials serve as carriers for controlled release and in environmental treatment to produce materials that remove pollutants from wastewater effluents, supporting environmental remediation. K. Kornaba et.al., [112]. The advantages, applications of co-precipitation span various fields, particularly in nanotechnology for controlled nanoparticle synthesis, catalyst production and the fabrication of magnetic materials its widespread use in water purification for removing heavy metal ions, pharmaceuticals for drug delivery and high-performance materials production attests to its versatility. EPM simplicity, scalability, cost-effectiveness makes it an attractive method for large-scale production, enabling precise control over size, composition and structure. Then this versatility and simplicity contribute to its significance in both scientific and technological domains.

2.8. Successive Ionic Layer Absorption and Reaction (SILAR)

SILAR is a versatile thin film desorption technology widely used in

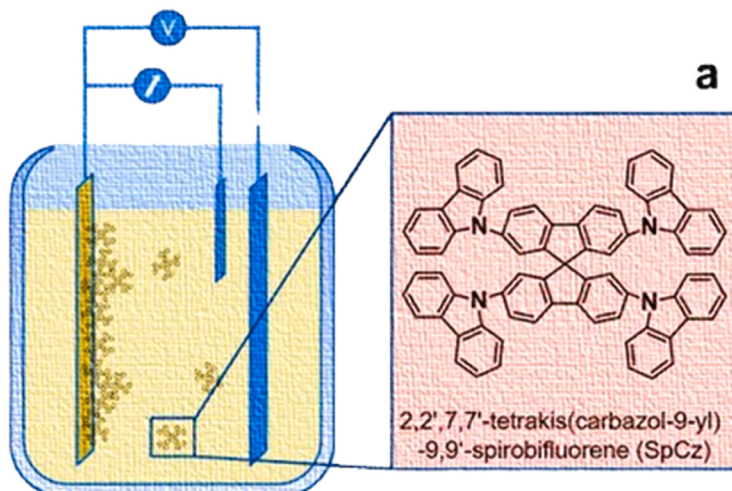
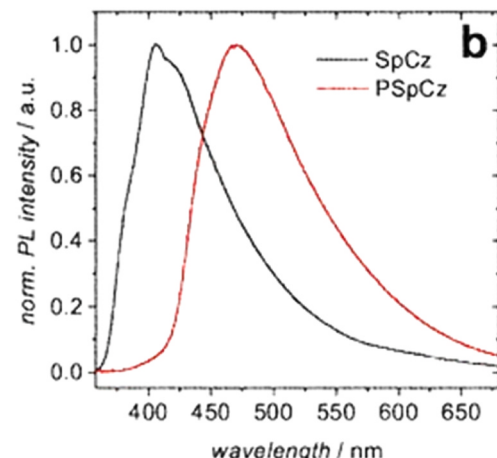


Fig. 13. Represents the Principle of electrochemical polymerization into a microporous network PS p Cz from a solution of the monomer SpCz (a). Photoluminescence (PL) spectra of the resulting microporous PSpCz in comparison to the PL of a thermally evaporated thin film of the monomer (SpCz) [109].



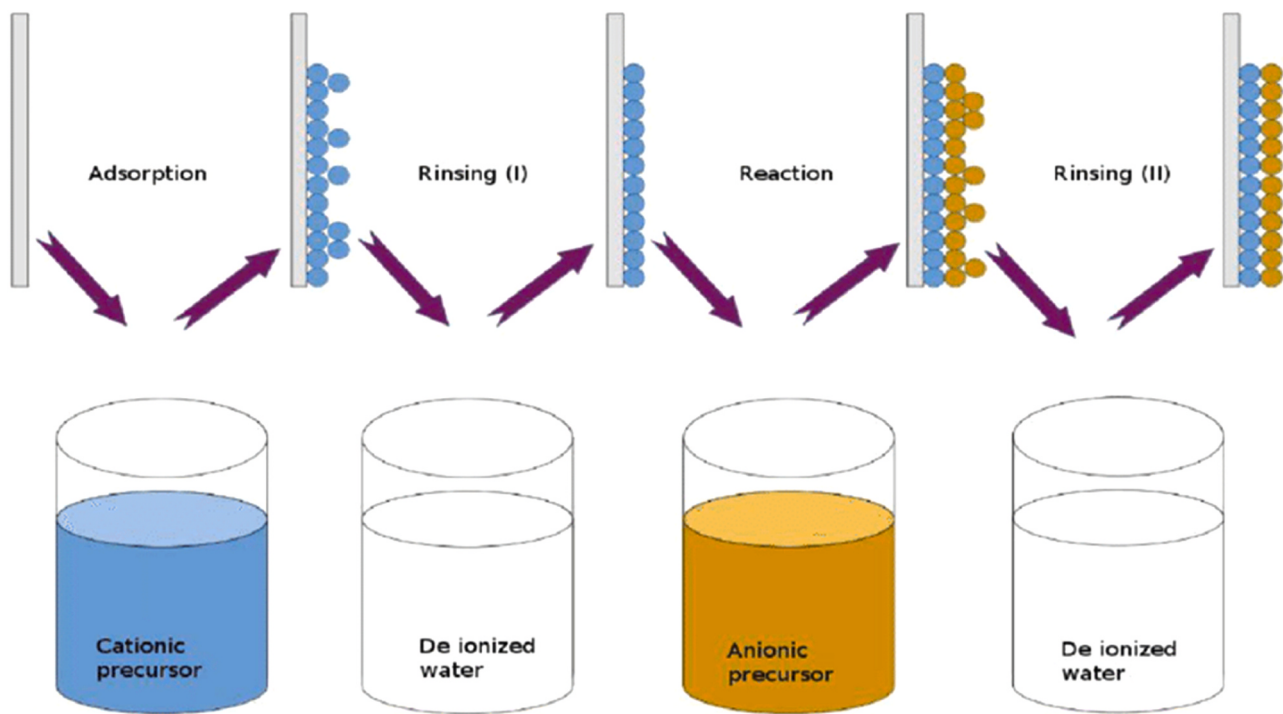


Fig. 14. Schematic illustration of the formation of thin films in SILAR method [118].

the production of various electronic devices, especially thin film solar cells and sensors, this method allows growing films of different thicknesses and compositions by repeating the sequence of ion adsorption and reaction steps in the process begins by immersing the substrate in a solution containing ions of the first product to be deposited. B. Güzeldir *et.al.*, [71]. After, rinsing and drying the substrate to prepare it for the next cycle where it will be exposed to chemicals containing ions of the second product in this combination continues over several cycles, allowing film production with construction materials. G. Yergaliuly *et.al.*, [113]. SILAR is valued for its simplicity, performance and versatility, making it useful in thin film applications (continuous ion layer adsorption and reaction) is an oscillation film involving the diffusion of ions to the surface this process begins by immersing the substrate in a solution containing ions of the first material, causing these ions to adsorb and possibly appear on the surface. B. C. Ghos *et.al.*, [114]. SILAR enables precise control of thin films thickness, composition and is widely used in applications such as thin-film solar cells and electronic devices, has several advantages that make it attractive for thin films. H. S. Min *et.al.*, [115]. As the demand for high-efficiency and commercial thin-film release methods continues to grow, SILAR is poised for further research and integration into various technology areas.

One of the main advantages of SILAR in thin films is its ability to adapt to a variety of materials in this method allows the deposition of thin films of electrodes, oxides and other materials with good properties. E. Jose *et.al.*, [116]. Additionally, SILAR is known for its simplicity and cost-effectiveness compared to other release technologies and then the development of the process with SILAR process is important for cutting the film to ensure uniformity and accuracy in thickness is especially important in applications where the performance of the film is directly affected by its thickness, such as solar cells where light absorption is optimized for energy conversion. A. A. Yatem *et.al.*, [117].

In research using similar techniques, this paper stands out by examining copper selenide films deposited on GaAs substrates using the SILAR method, resulting in the as shown in Fig. 14. Cu/Cu₃Se₂/n-GaAs/In MIS structure model. Then the optimum n = 1.14 and Φ_B of 0.83 eV demonstrate the success of SILAR in achieving the best device. SILAR simplicity, performance allow the thin film to be controlled using

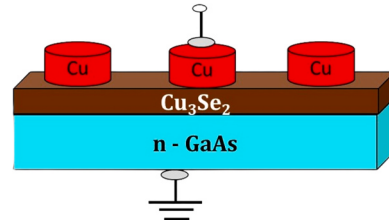


Fig. 15. Schematic diagram of the Cu/Cu₃Se₂/n-GaAs Schottky diode [71].

specialized equipment, making it particularly suitable for applications such as thin-film solar cells and electrification of devices. Its adaptability to a variety of materials and its ability to operate at lower temperatures further increases its effectiveness in many situations in the MIS structure as shown in Fig. 15. Looking ahead, SILAR promising applications include continued research focusing on the development of electronic systems, the advancement of electronic technology and the development of new electronic equipment.

2.9. Sol Gel Spin Coating (SGSC)

SGSC is a complex, widely used technique for depositing thin films with controlled properties and this process begins with the preparation of sol, a colloidal suspension containing metal alkoxides or other precursor molecules. K. Sasikumar *et.al.*, [47]. It is then applied spin coating to the left substrate (usually a flat surface). During the SGSC process, the substrate rotates at high speed, becomes equal to the left surface due to centrifugal force and next important step involves heat treatment, which causes gelation and subsequent solidification of the sol, leading to the formation of a membrane on the substrate and this method allows controlling the thickness, composition and morphology of the deposited films. However, SGSC technology has many advantages, such as low-cost films, stoichiometric control, doping flexibility and large layers [119].

SGSC consists of various methods of thin film deposition in this sol is prepared first and usually contains precursor molecules derived from

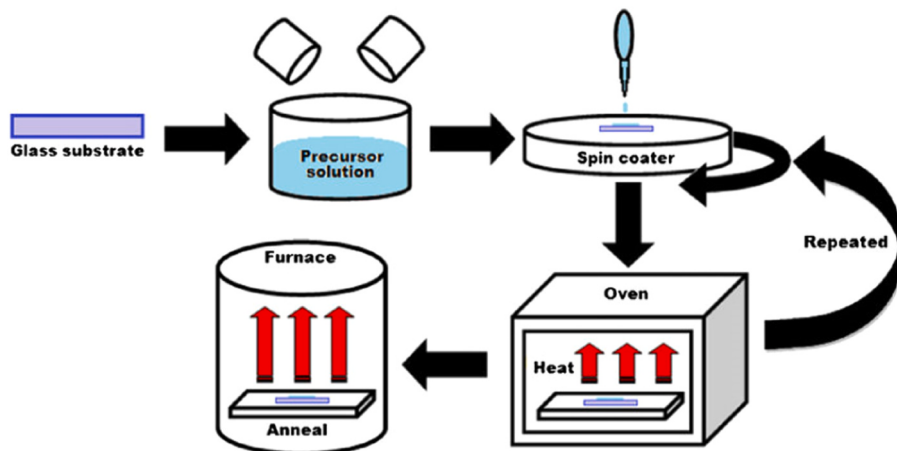


Fig. 16. Representation of the Sol–gel spin coating process [121].

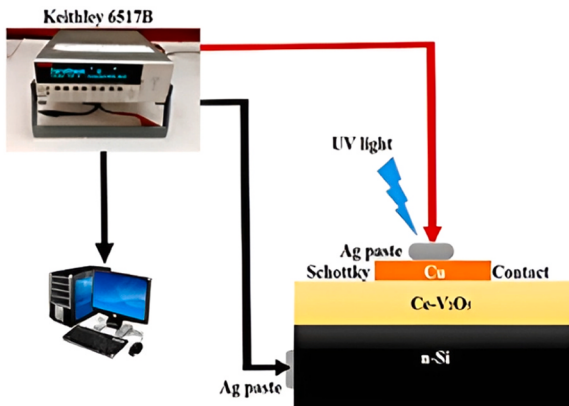


Fig. 17. Schematic diagram of Cu/Ce-V₂O₅/n-Si Schottky barrier diode [41].

metal alkoxides. A sol containing the necessary components for the film is then applied to a substrate, usually a flat surface such as silicone or glass and substrate is spin coated, a dynamic process at high speed in the centrifugal force created by the rotation causes the sol to balance on the surface of the substrate. Due to the SGSC process is more reliable, versatile than many other solutions for the preparation of metal oxide films due to its low cost, high precursor purity, ability to prepare a variety of paper materials, maintaining good stoichiometry and operating temperature [120]. After the layer is separated, the coated substrate is subjected to a heat treatment or annealing process that allows the sol to gel. K. Sasikumar et.al., [46]. In this gelation step is important because it makes the film stronger, forming a thin layer with good properties, then the final film product can be further optimized by controlling parameters such as sol concentration, spin speed and annealing condition, making the SGSC process versatile, precise for film production in many uses. SGSC has many advantages that make it a versatile and popular technique for thin film deposition. A key advantage is the ability to form uniform, pinhole-free films on a variety of substrates, allowing thickness and composition to be controlled. V. Balasubramani et.al., [45]. Then the process is cost-effective as it operates at a lower temperature compared to other deposition processes, making it suitable for hot and cold substrates. V. Balasubramani et.al., [43]. Additionally, SGSC plays an important role in the fabrication of sensors, catalytic materials and biomaterials due to its ability to form customized films with specific functions. V. Balasubramani et.al., [42].

As shown in Fig. 16. SGSC have similarities with other thin film processes such as CVD, PVD and the sol-gel process is good because it is versatile in depositing hard materials such as ceramics and oxides,

providing a uniform film over a large area. Spin coating, meanwhile, stands out for its simplicity, efficiency and ability to form similar films on a variety of materials, including polymers and some non-materials. V. Balasubramani et.al., [41]. In contrast, CVD relies on gas phase reactions to form thin films and allows control of thickness and composition; PVD technology, on the other hand, involves the physicality of the material through methods such as sputtering or evaporation that allow the control of thin films and this choice of this technology depends on the specific equipment, film equipment and available equipment.

Compared to other works using similar techniques, this paper represents a significant advance in thin film fabrication. This work successfully developed high-performance precision as shown in Fig. 17. Cu/Ce-V₂O₅/n-Si structural SDs using SGSC technology. The best parameters were achieved, especially the n of 1.73 and Φ_B of 0.82 eV, making this the best work in its field. SGSC technology has been shown to help achieve good results, such as thickness control, high purity films at low cost, maintenance of proper stoichiometry, flexibility and the ability to control large-scale processes in the region. This work only demonstrates the effectiveness, but also serves as an important factor in producing films and exemplifies the potential for legacy development through careful use of this method. SGSC can be applied to many materials, including ceramics, polymers organic-inorganic hybrid compounds, increasing its versatility it is simple and easy scalable for research and technology. In optics, it is used in anti-reflective coatings, waveguides and filters in the electronics industry, this method is used in semiconductor devices and thin films.

2.10. Magnetron Sputtering (MS)

MS is a film deposition technology widely used in materials science, microelectronics and It is as PVD process that allows accurate and controlled information to be transferred to the substrate, this method is known as a magnetron, a device that creates a magnetic field to enhance the sputtering process. H. Tanrikulu et.al. [14].

In MS, vacuum is used to create a low-pressure environment. The target material, which forms the basis of the coating material, is placed in the chamber along with the substrate to be coated and then the target usually consists of items required for the deposit Shekoofa et.al. [122]. Target materials include metals, semiconductors, insulators and this technique uses a magnet, a material with a magnetic field that creates a magnetic field near the target also magnetic field increases the efficiency of the sputtering process by trapping electrons in spiral orbits around the magnetic field line, thus increasing collisions with gas atoms and then being released into the target. Dybala et.al. [123].

MS is a coating process performed in vacuum and then the target material (usually metal or semiconductor) is placed in the chamber

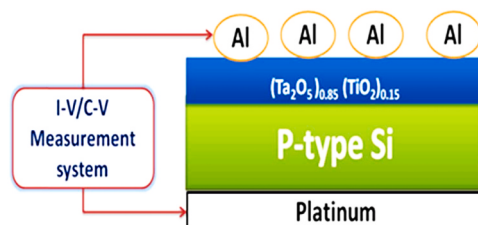


Fig. 18. The schematic diagram of the prepared $\text{Al}/(\text{Ta}_2\text{O}_5)_{0.85}(\text{TiO}_2)_{0.15}/\text{p-Si}$ MIS Schottky barrier diodes. [11].

along with the substrate. DC is applied to the target to produce blood by ionizing a rare gas (usually argon) also plasma is confined by the magnetism of the magnet, making the ions positive at the target, causing scattering and removal of target atoms. Sputtering atoms are deposited on the substrate to form a thin film with controlled properties in this process is widely used in industries such as electronics, optics and coatings as high-quality and non-uniform films can be obtained.

Plasma gas usually introduces argon gas into a vacuum, uses high voltage between the target, substrate and the radiation ionize the gas, creating blood. High-energy ions in the plasma collide with the target surface, causing atoms or molecules to be removed by a process called sputtering. This spray is then passed through a vacuum and deposited on the substrate, creating a thin film and also MS has many advantages, including high deposition rates, high film integrity and the ability to perform complex processes. It is widely used in the production of microelectronic devices, optical coatings, sensors and many other applications where clear controlled thin film is required for operation then the device is versatile can handle a wide range of applications, making it an important technology for modern engineering and manufacturing equipment.

MS offers advantages such as the ability to achieve uniform film thickness control, ensuring consistency across substrate sizes [124]. Its versatility allows for the deposition of various materials like metals, semiconductors and insulators, providing flexibility in thin film applications, then the sprayed films exhibit good adhesion to substrates, enhancing overall coating stability and performance [125]. However, there are drawbacks to consider, including the challenging costly installation and maintenance of the MS system, requiring specialized operational knowledge [126]. Additionally, the sputtering process can lead to material corrosion over time, resulting in a limited target life and necessitating more frequent replacements.

As shown in Fig. 18, compared to other studies using similar techniques, this paper differs by in-depth examination of the effect of negative voltage (-150 V to 0 V) $(\text{Ta}_2\text{O}_5)_{0.85}$ deposited on p by DC reactive MS. $(\text{TiO}_2)_{0.15}$ film. Si (100) and quartz substrate. Then importance of MS in the microelectronics industry is significant because it is widely used to deposit thin films for electronic devices in this method plays an important role in the production of integrated circuits, thin-film transistors and many electronic devices. MS extends beyond microelectronics and can also be used to create optical processes for lenses, glasses, other optical devices, improving their optical properties by controlling film thickness and composition. In data storage, MS helps create thin films for magnetic devices such as hard drives and magnetic tapes. Additionally, in the field of solar energy, magnetron sputtered films are used as photovoltaic cells to help increase the efficiency and effectiveness of solar panels.

2.11. RF Magnetron Sputtering (RF)

RF MS has many advantages, including better film control, improved stepwise substrate geometries and the ability to accumulate more information Ertugrul et al., [12]. It is particularly suitable for applications where control of film properties such as thickness, composition and uniformity are required. Then the technology is widely used in the

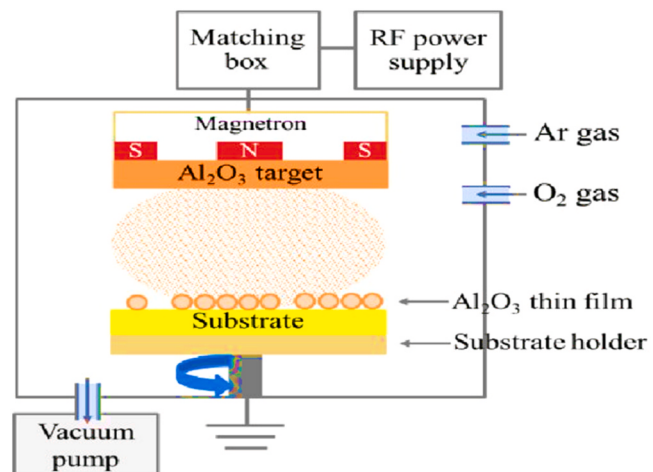


Fig. 19. Illustration of the formation of Al_2O_3 thin films in RF magnetic sputtering method [131].

production of semiconductor devices, optical systems, solar cells and other advanced devices, the performance of thin films is important [127].

In summary, RF MS is a complex and versatile thin film technology, this thin film deposition technology that uses RF energy to improve the sputtering process and its ability to provide precise control, integration makes it useful in the design of many electronic and optical devices [128].

RF MS is a thin film deposition process using a target (usually metal or semiconductor) substrate in a vacuum chamber as shown in Fig. 19. Unlike DC MS, RF MS uses RF power source to generate high-frequency electricity to ionize a rare gas (usually argon) to produce plasma. RF energy increases ionization efficiency and makes synthesis more efficient as in DC MS, the magnetic field produced by the magnetron confines the plasma close to the target surface. Positively charged ions from the plasma bombard the target, causing sputtering and the expelled material is placed on the substrate to form a thin film. RF MS is appreciated ability to deposit a variety of materials, including insulators for its excellent control of films, making it suitable for many applications in electronics, optics and advanced systems.

RF MS has applications in many industries due to its ability to deposit thin films, control properties such as thickness, composition and consistency. RF MS plays a pivotal role in semiconductor manufacturing, particularly in the production of IC. It is utilized to deposit key thin films on semiconductors, contributing to the diversity of these electronic components. In optical applications, such as anti-reflective coatings for lenses, glasses, RF MS enhances light transmission and reduces glare. Then this technology is also integral in glass coating for optical products [129]. When it comes to solar cells, RF MS is crucial in constructing thin film photovoltaics, enabling the creation of efficient and cost-effective photovoltaic devices. Additionally, glass coating, involving reflective coatings on glasses and other optical products, is integral to the manufacturing of optical devices [130]. In the domain of solar cells, RF MS plays a significant role in the construction of thin film photovoltaics, contributing to the creation of efficient and cost-effective solar cells.

Compared to other studies using similar techniques, this paper stands out for its in-depth investigation of the effectiveness of HfO_2 as a layer in improving the poor quality of Pt/n-GaN SDs. More importantly, this work reveals the homogeneity of the as shown in Fig. 20. Pt/ HfO_2 /n-GaN interface, providing insight into the behaviour, with this method, the study achieved the best sensitivity and peak values of 1.2 and 0.79 eV, respectively. In the field of semiconductor manufacturing, the production of integrated circuits relies largely on RF MS, a technology frequently used to deposit thin films important for semiconductors, this provides diversity and improves the electrical properties. RF MS allows

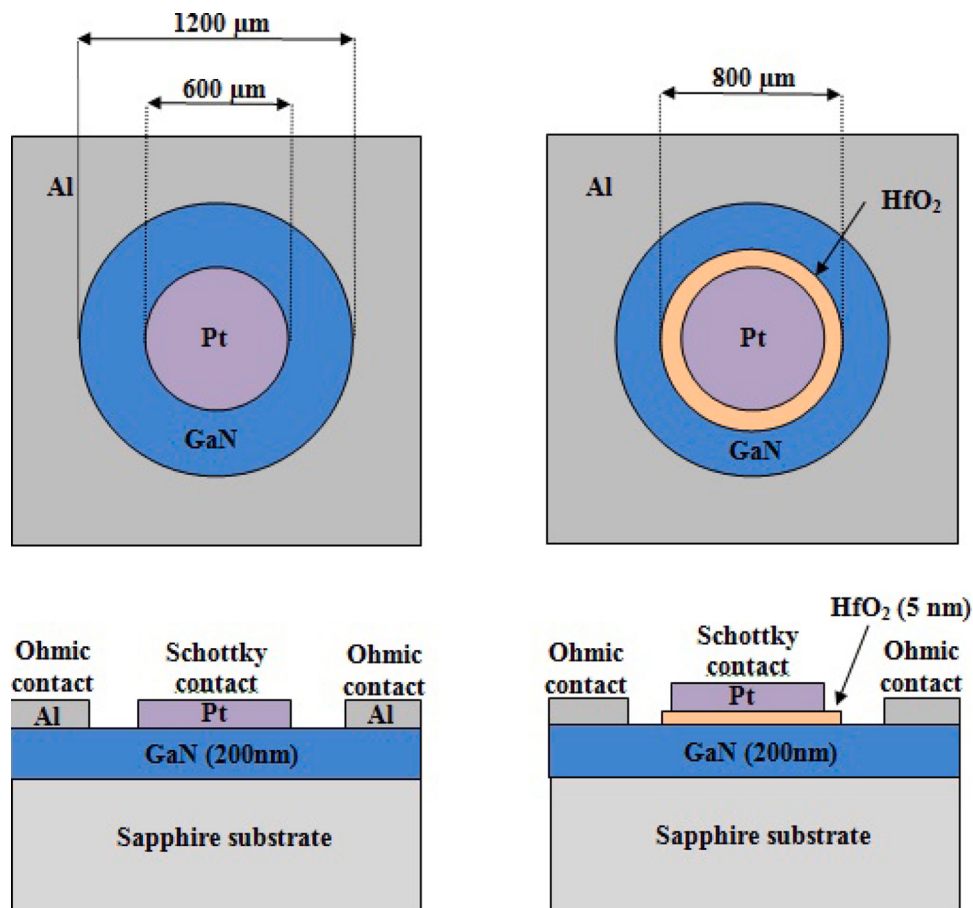


Fig. 20. Schematic diagram representation of this Diode [15].

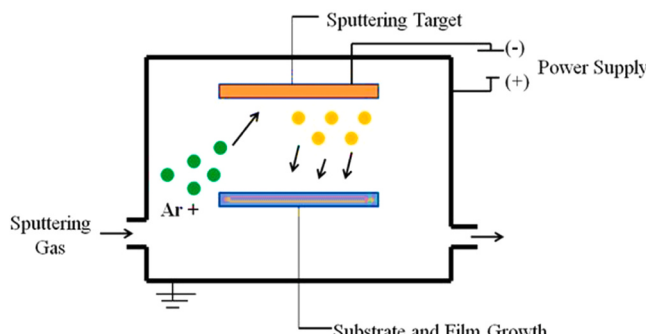


Fig. 21. Schematic illustration of the formation of thin films in DC magnetron sputtering method [137].

the use of anti-interference chemicals on optical components such as lenses and glasses, extending its application to optical processes. This process is designed to improve light transmission and reduce glare, demonstrating the many uses of RF MS in many technological advances.

2.12. DC Magnetron Sputtering

DC MS is a PVD technology used for thin film deposition in various industries such as electronics, optics and coatings. The process involves sputtering material from a target onto a substrate to form a thin film. Below is a brief description of the main concepts and steps involved in DC MS. Irawan et.al., [132].

In DC MS, a vacuum is employed to create a low-pressure field, with the target material (typically metal or semiconductor) placed in the

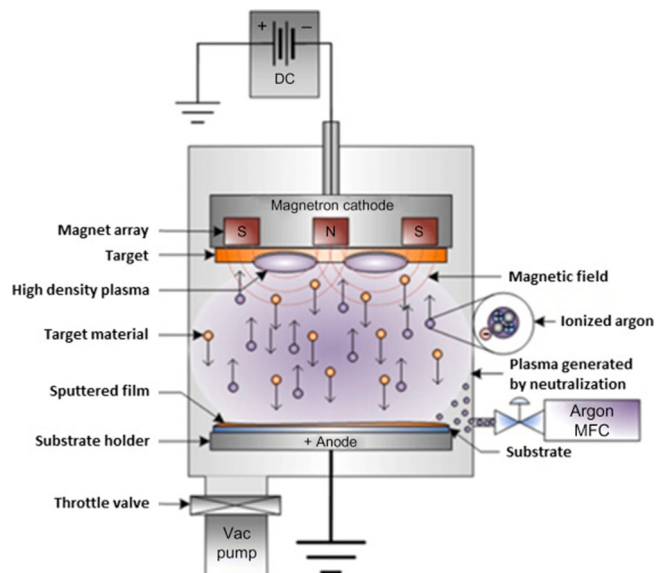


Fig. 22. Photograph of the DC magnetron sputtering [138].

vacuum chamber along with the substrate, where the thin film is deposited. Then the magnetic field generated by the magnetron confines the plasma near the target surface, facilitating ionizing collisions [133]. During the thin film deposition process, electronic material is introduced into the vacuum, ultimately settling on the substrate, carefully positioned to ensure smooth and controlled deposition [134,135]. DC MS



Fig. 23. Represents the graphical map of the All Coating techniques that used for the interfacial layer fabrication.

offers advantages such as high deposition speed, strong film adhesion,

versatility in depositing various materials, especially designed for metals, semiconductors and select dielectric materials. Fig.s 21 and 22. Shows that the DC MS. Its applications span semiconductor manufacturing, optical processes, magnetic materials and fine techniques [136].

In summary, DC MS stands out as a versatile, widely used thin film deposition technology, allowing precise control over thickness, composition and other film properties. Additionally, its low deposition temperature makes it suitable for coating temperature-sensitive substrates and integration into diverse manufacturing processes.

Fig. 23 Represents the graphical map of the MIS coating techniques that used for the interfacial layer fabrication.

3. Metal layer materials of MIS diodes

Metals are a class of chemical substances characterized by their properties of heat, electricity, malleability and ductility. Generally, the metals on the left side of the table have a crystal structure form positive ions in reactions and their common properties include magnetic bonding, which allows electrons to move freely a tendency to lose electrons to form cations. Metals are widely used in many industries due to their strength, electrical conductivity, versatility, playing an important role in construction, manufacturing, electricity transportation and its represent a variety of chemicals, all physical, chemical and they are broadly divided into four main types, these include alkali metals such as lithium and sodium, known for their high activity and tendency to produce alkaline solutions; alkaline earth metals such as magnesium and calcium, which exhibit higher reactivity; transition metals, including elements with varying oxidation resistance, high melting points and the ability to produce mixed colour, such as iron and copper; post transition metals such as lead, whose properties are intermediate between transition metals and metalloids. Together, these metals underscore their important role in shaping the modern world by supporting wide range of

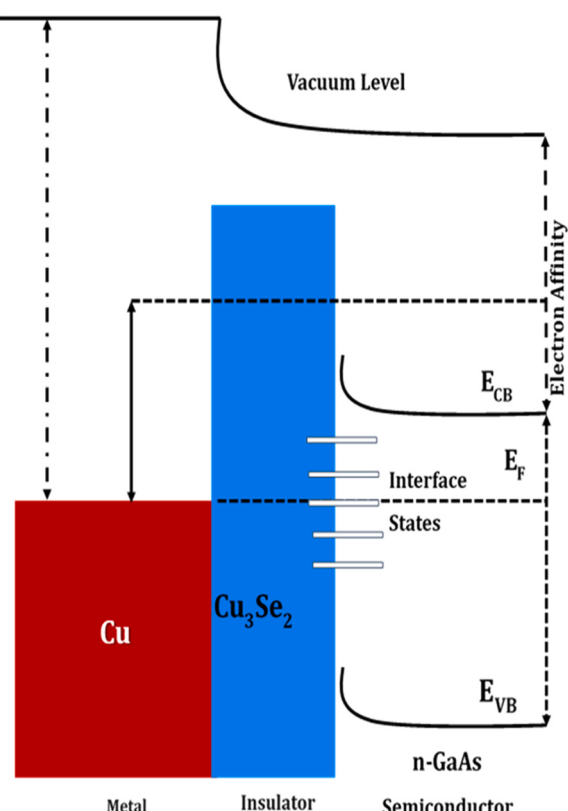


Fig. 24. Energy level diagram of the Cu/Cu₃Se₂/n-GaAs [71].

industrial applications from construction electricity to transportation and medicine. The work function of metal is the minimum energy required to remove electrons from metal surface and it is usually measured in electron volts (eV). Functionality is affected by factors such as metal composition and crystal structure with lower conductivity will release more electricity, when exposed to light or other energy sources also the work function is important in fields such as electricity, where it determines how easily electrons can be removed from a material.

3.1. Copper (Cu)

Copper has many advantages, including excellent electrical and thermal conductivity, making it an ideal material for wires and devices. Its malleability make it easy to construct and install, while its corrosion resistance ensures long life in many applications. Additionally, copper has antibacterial properties that facilitate its use in medicine. However, the main problem is that it darkens easily and needs to be careful in some applications. But copper is widely used in electronics, plumbing, construction and many other industries. Its recyclability further enhances its sustainability properties and reduces environmental concerns associated with its extraction. The advantages of copper's conductivity, durability and antimicrobial properties outweigh its disadvantages, making it a versatile and indispensable product in many areas.

In this work author uses the SILAR method to deposit a copper selenide film on a GaAs substrate to study its structure and determine its morphological properties using XRD, SEM and AFM methods. As shown in Fig. 24, it was formed in the Cu/Cu₃Se₂/n-GaAs structure and its I-V properties were analysed in the temperature range of 60 K - 400 K. The calculated SDs parameters, including the optimum and the height of the barrier, show temperature dependence. The increase in the ideal and the decrease in the Φ_B potential with temperature are due to the inequality of the Φ_B potential of the interface, especially between the metal/semiconductor interface. MIS Electrical measurements on the sample indicate the temperature, which can be explained by TE with the Gaussian distribution of the high barrier. The dominance of hot electron FE is associated with the lateral distribution of the barrier height. This indicates that the increased conduction may be due to a local increase in the electric field causing a local decrease in barrier height.

From the study of this work I-V diagram is constructed using temperature measurements of charge carriers due to lattice interference and junctions in the saturation current region due to series resistance. At high temperatures, reduced lattice distortion allows carrier mobility, which reduces the resistance associated with thick semiconductor materials. This causes the I-V diagram to intersect. Then the experimental value and ideal of Φ_B are determined by the line emerging from forward bias I-V [71].

3.2. Aluminium (Al)

Al representing a light silver-white metal with the advantages of aluminium are its manifold, poor corrosion and high strength-to-weight ratio. This ensures that it does not operate in various industries. Its light weight helps increase fuel efficiency in transportation, especially in the aviation and automotive sectors. Aluminium's corrosion resistance makes it durable, making it a good choice for equipment and packaging such as beverage cans. Additionally, aluminium is perfect and formable, allowing for a wide range of production in these terms of future use, aluminium must play an important role in the development of sustainable technology. Its recycling is based on environmental practices and research is constantly exploring its use in new areas such as heavy equipment, renewable energy and optimal energy products for electric vehicles, highlighting its role in sustainable development and technology-driven priorities for the future [48].

As shown in Fig. 25. When a positive bias is applied on the p-Si relative to the metal, the electrons from Al metal flow out through the RE:ZrO₂ insulating layer and create ionized acceptors above the valence

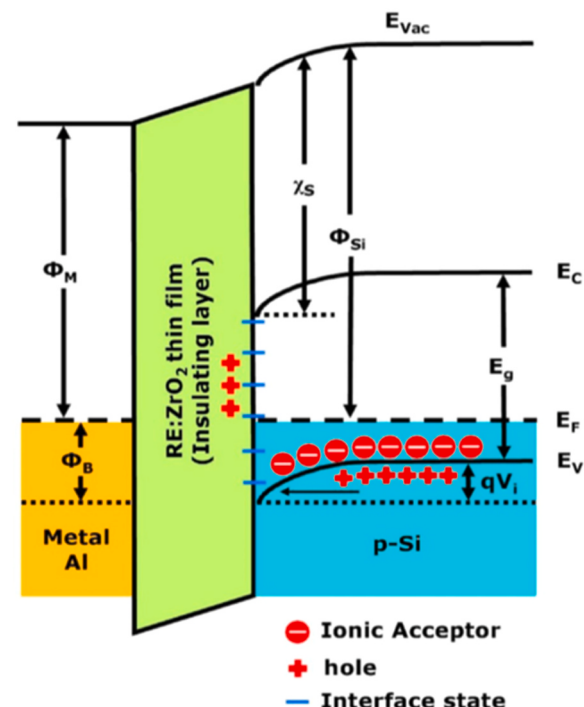


Fig. 25. The energy band diagram of Al/RE:ZrO₂/p-Si SBDs is depicted [47].

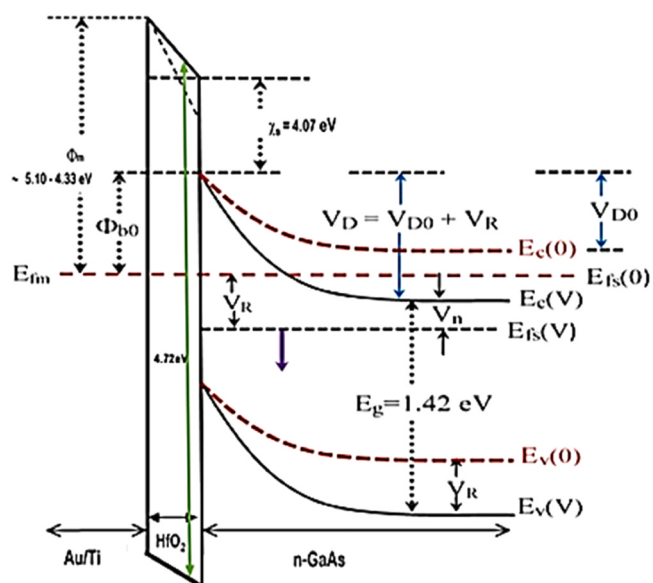


Fig. 26. The energy band diagram of Au/Ti/HfO₂/n-GaAs SBDs is depicted from [52].

band in p-Si. Meanwhile, holes move from the valence band into metal and hence current flows in SBDs.

3.3. Gold (Au)

Au is a valuable and precious metal that has a special place in human history due to its beauty and great value. Known for its performance, corrosion resistance and excellent electrical conductivity, gold has many uses in jewellery, electronics and finance. In addition to its traditional role, gold will also play an important role in future innovations, especially the field of nanotechnology and medicine. Au nanoparticles show promise in drug delivery and delivery technologies and herald a

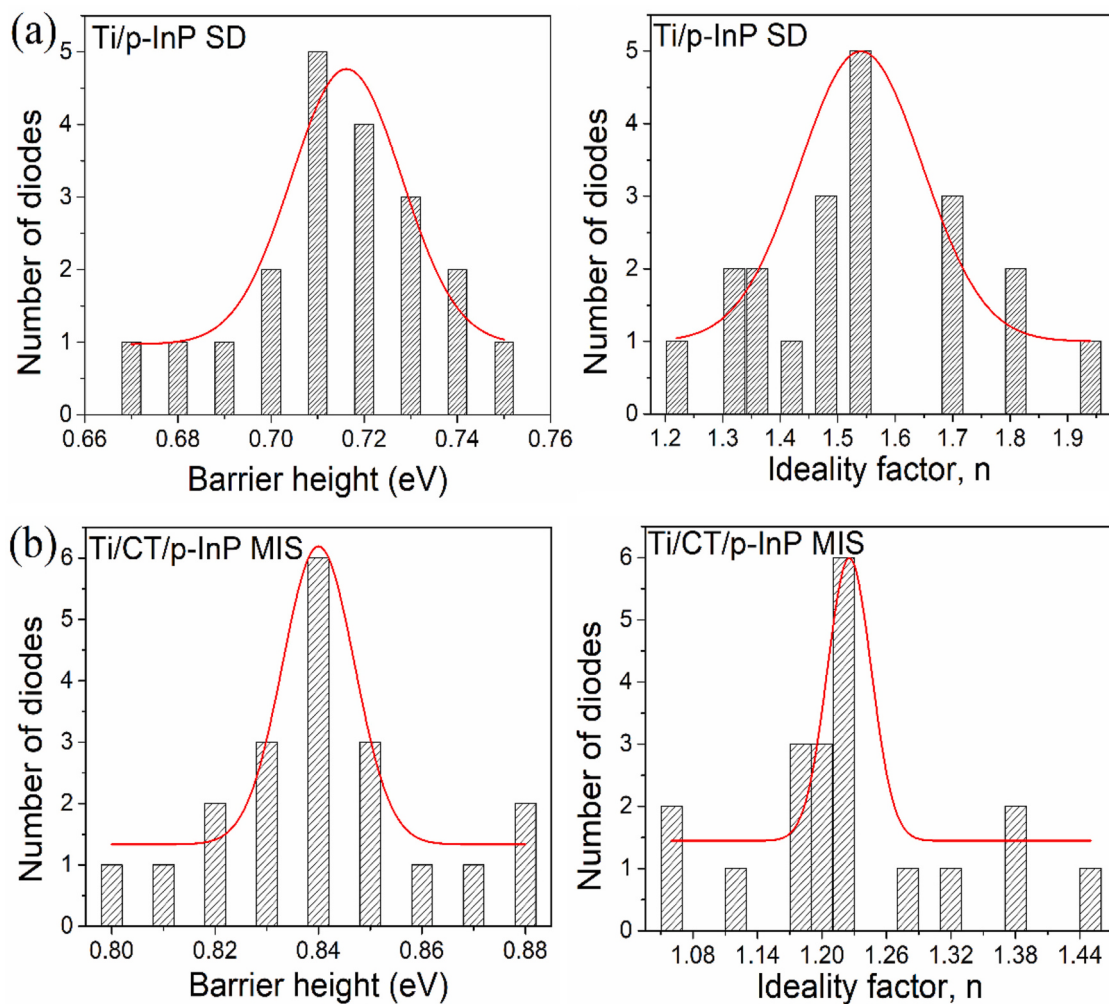


Fig. 27. (a) and (b) depict the statistical distribution of the BHs and n for the SDs and MIS diode and are fitted via the Gaussian function [60].

revolutionary change in healthcare. Additionally, the metal can be used in energy storage and catalysis, in addition to its importance in the development of future technology and security. As a symbol of wealth and versatility, with both its historical significance and modern use, gold is expected to continue to attract and contribute to many industries and play an important role in the development of technology and future research [50].

The Fig. 26. shows energy-band diagram for Au/Ti/HfO₂/n-GaAs diode at under applied and zero-bias condition, where E_{fm} is the Fermi energy level, M is the work function of metal, V_n is the potential difference between fermi energy level and the conduction band bottom, $b_0 = VD_0$. V_n is the effective barrier height at the zero bias, VD_0 is the value at the zero bias of the surface potential, VD is the value under the applied reverse bias of the surface potential and VR is the voltage drop across the depletion region in the reverse-bias case. As shown in, the electron affinity (vs) of n-GaAs is 4.07 eV, the thickness (d) of the HfO₂ is 10 nm and the energy band gap of n-GaAs is 1.42 eV.

3.4. Titanium (Ti)

Titanium is a lightweight and corrosion-resistant transition metal that offers a unique combination of strength and density, making it an important material in many industries. Titanium is widely used in aerospace; automotive, medical applications and its high strength-to-weight ratio makes it ideal for structures where durability and weight are important and it is attracting increasing attention in new areas as well as its applications in traditional industries. In medical applications,

titanium alloys are used in dental implants, prostheses due to their biocompatibility and corrosion resistance. Looking to the future, titanium holds broad promise in high-tech applications such as aerospace, renewable energy, additive manufacturing and special properties make titanium indispensable for progress in construction, improved fuel efficiency and new processes, making it the product of choice to meet the needs of modern technology and sustainability.

From the Fig. 27 (a), (b) depicts the statistical distribution of the Φ_B and n for the SDs and MIS diode and are fitted via the Gaussian function. The acquired mean Φ_B values of SDs and MIS diode are 0.72 eV with a standard deviation of 1.64 meV and 0.84 eV with a standard deviation of 1.02 meV. While, the estimated mean ideality factors are 1.54 with a standard deviation of 0.03 and 1.22 with a standard deviation of 0.08 for the SDs and MIS diode, respectively. Higher Φ_B was acquired for the MIS diode with an excess Φ_B of 0.12 eV than the SDs, implying the CT insulating layer affected the space charge area of the InP substrate. Thus, the CT layer offers a physical barrier, which averts a direct connection between the metal and the p-InP surface. The calculated ideality factor value deviated from unity for the investigated SDs and MIS diode, which may be due to the occurrence of interface dipoles as a result of an interlayer, an explicit interface structure or the occurrence of defects at the interface during the fabrication process. Additionally, the spreading of interface states, the recombination-generation process, the image force effect and the tunnelling effect can cause a deviation in the ideality factor. Tung suggested that the higher ideality factor would be because of the occurrence of a wide spreading of low Schottky barrier height areas pretentious by a laterally inhomogeneous Φ_B [60].

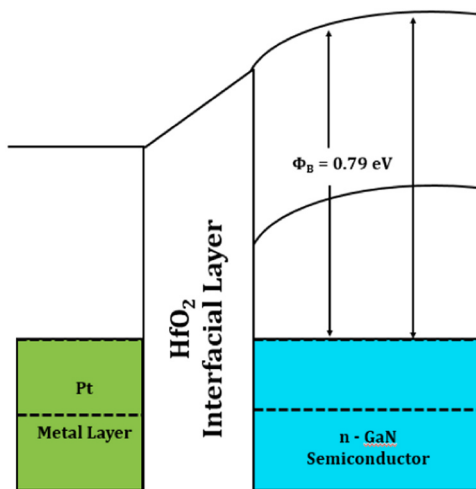


Fig. 28. Representation of the Pt/HfO₂/n-GaN diode barrier height [15].

3.5. Platinum (Pt)

Platinum is an important metal that is useful in many industries due to its unique properties and uses. Platinum, known for its catalytic ability, plays an important role in catalytic converters, reducing car emissions and considering their impact on the environment and it is incomparable to corrosion, oxidation, making it an important part of industrial usage processes. Looking to the future, platinum has great potential in technology, especially in fuel cells. Its efficiency as an energy source in converting hydrogen into electricity makes it an important element in the development of clean and sustainable solutions. As the world increases the use of environmentally friendly technologies, platinum is used not only for chemical reactions but also for revolutionary changes, providing a strong and powerful transition into the future.

As shown in Fig. 28. From this linear fit of the plot, they evaluated the values of richardson constant A^* to be $1.56 \times 10^{-6} \text{ A cm}^{-2} \text{ K}^{-2}$ and the barrier height Φ_B to be 0.3 eV. The value of richardson constant is found to be much lower than the theoretically expected value of $26.4 \text{ Acm}^{-2} \text{ K}^{-2}$ for GaN. The value of Φ_B of 0.3 eV is also found to be much lower than what we would expect for a Pt-GaN contact. This discrepancy in the values could be due to the presence of surface inhomogeneities at the Schottky contact interface. Due to the presence of these surface inhomogeneities, the value of the SBDs is not uniform over the entire metal contact area [15].

3.6. Palladium (Pd)

Palladium is a pure white precious metal that occupies a special position in many industries due to its unique properties and many uses. Widely known for its excellent catalytic properties, palladium is an important element in catalytic converters and plays an important role in reducing vehicle emissions. In addition to its role in controlling emissions, palladium continues to be used in electronics, dentistry and jewellery for its ductility and resistance to tarnish. Looking ahead, palladium is gaining traction in new technologies, particularly in hydrogen fuel production. Palladium's ability to catalyse important reactions in fossil fuels makes it an important element in the development of clean solutions. As the world looks to create sustainable changes, palladium's performance and catalytic abilities can play an important role in shaping environmental and technological change. The suitability of metals for optoelectronic applications depends on the specific requirements of the application. Different metals have different properties that make them suitable for different applications. Here is a brief summary of the impact of each metal in optoelectronics: Cu (Copper):

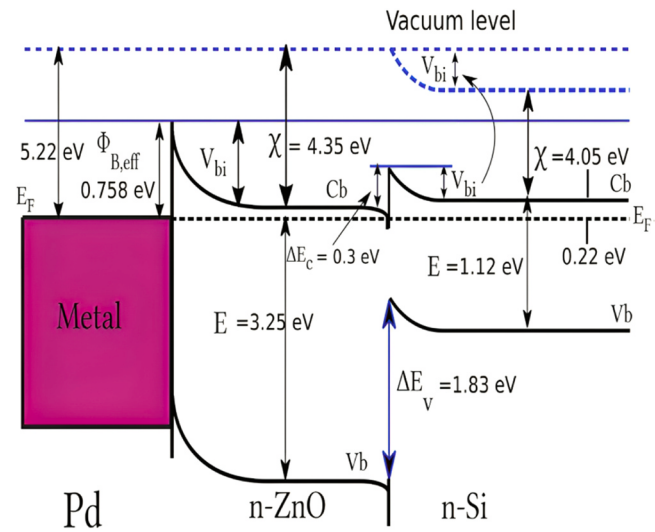


Fig. 29. Represents the change in the energy barrier height will affect the charge transport mechanism through the Schottky diode devices [75].

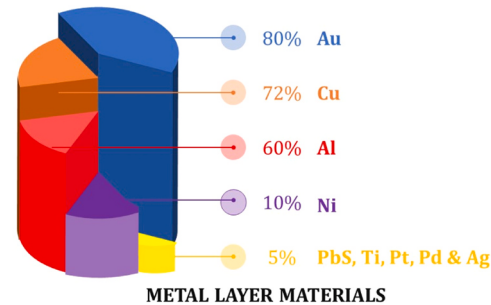


Fig. 30. Shows the Metal Layers Pie average pie chart. It represents the which type of metal layer material was used in the MIS diode structure.

Copper is frequently used in connections and electronics due to its very good conductivity. However, it is susceptible to oxidation, which can limit its use in some optoelectronic applications. Al (Aluminium): Aluminium is light and has good electrical properties. It is frequently used in reflective coatings in mirrors and some optoelectronic devices.

Energy gap of ZnO nanorods and bulk Si are respectively. The band gap of undoped ZnO nanorods and co-doped with Ce and Sm at 0.0, 0.2, 0.4, 0.6 and 0.8 Wt% were obtained from Tauc's plots (not shown here) and found to be 3.25, 3.27, 3.24, 3.25 and 3.27 eV, respectively. By using the electron affinity of ZnO (4.35 eV) and Si (4.05) the value of ΔE_c calculated is 0.3 eV which is the energy barrier height seeing by the majority electrons carriers to overcome from Si to n-ZnO. As shown in Fig. 29. in the presence of interface states or defects within the semiconductor band gap, which is unavoidable in the method used to fabricate the diode devices (i.e. chemical bath deposition) the fermi energy is no longer within the conduction band and is rather pinned by interface states. This pinning of the fermi energy level will make the energy Φ_B to be independent of the semiconductor work function. The pinning of the fermi energy level is about 1/3 of the band gap. Therefore, the change in the energy barrier height will affect the charge transport mechanism through the SDs devices [75].

Fig. 30. Shows the metal layers average chart representation. It represents the which type of metal layer material was used in the MIS diode structure.

4. Insulating layer materials of MIS diodes

The development of MIS diodes over time is closely related to the

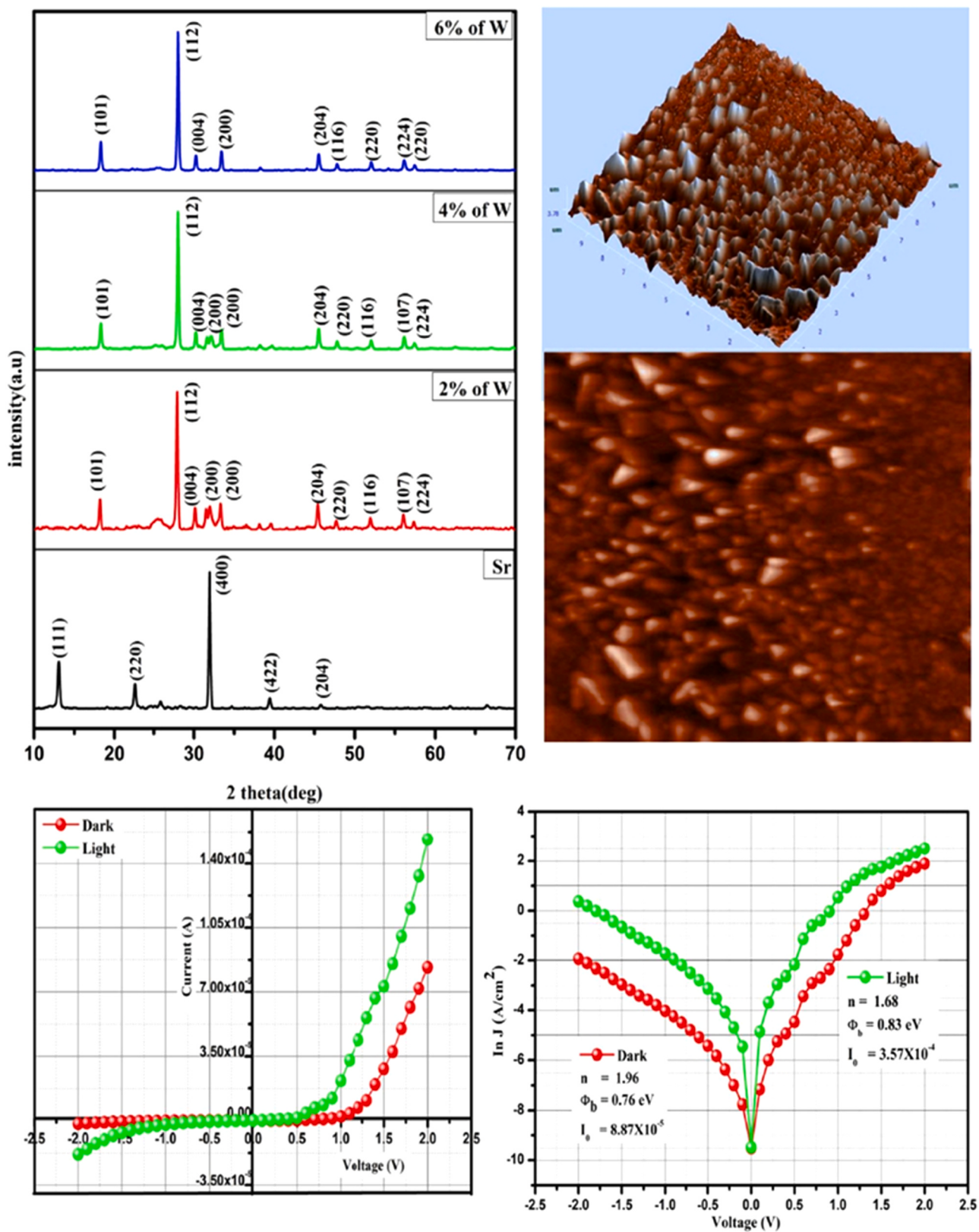


Fig. 31. The XRD results, AFM of 6 wt% Sr and I-V graphs [31].

special properties of chemical products from different groups and some of these are discussed below. Alkaline earth metals are the main components as gate materials of MIS diodes, which use their special ability to form a good insulating layer and also capability will help adjust the quality of electronic components to create a stable MIS structures when

precise control enabled by these metals increases the suitability of MIS diodes for many electrical applications. Transition metals play an important role in MIS diodes due to their different functions, careful selection of the transition metal leads to determination of electrical properties, allowing integration into a variety of electronic devices. The

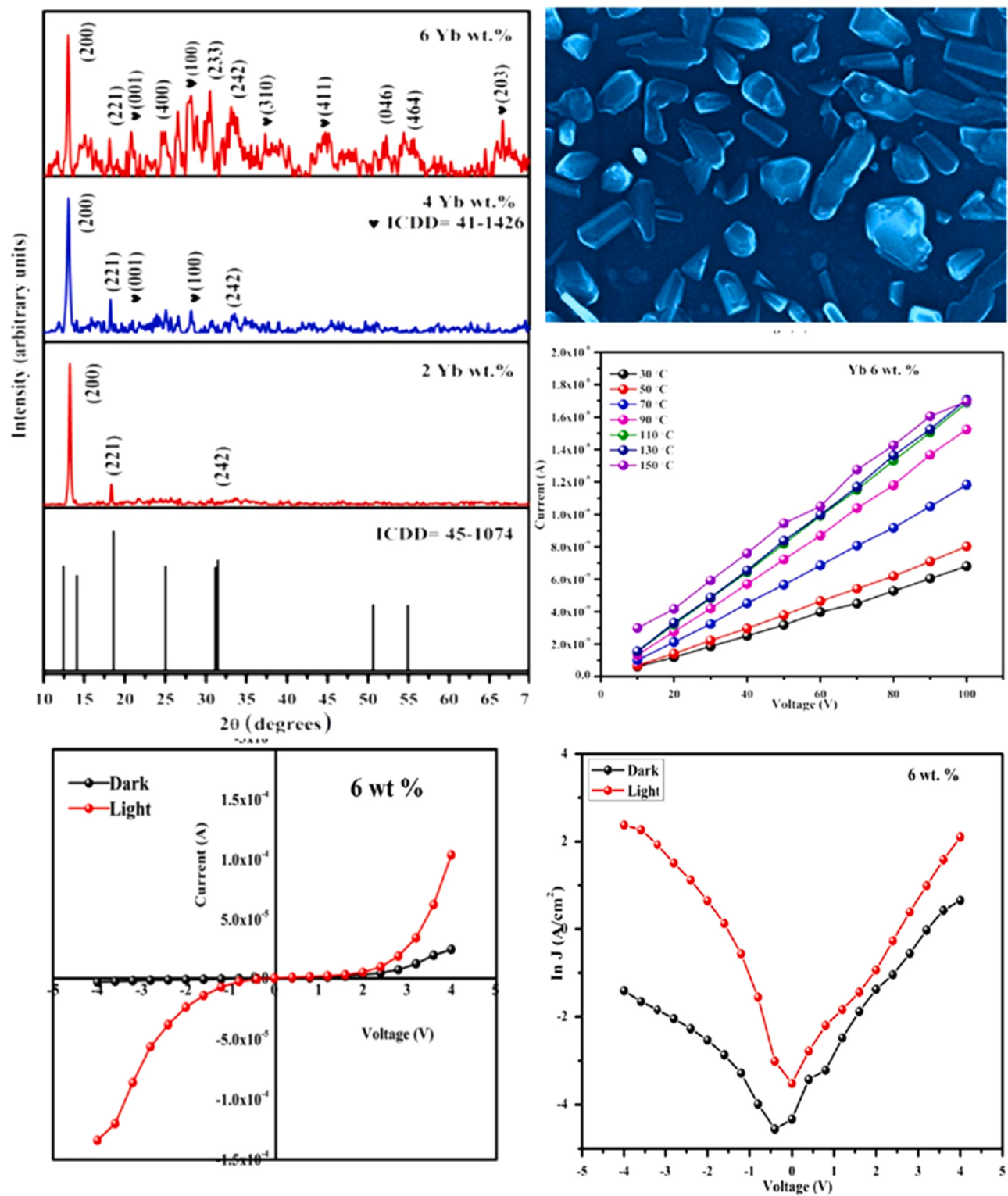


Fig. 32. XRD results, AFM image, I-V graphs of Cu/Yb@V₂O₅/n-Si Structured Yb content by 6 wt% [43].

versatility of MIS diodes is increased by their ability to form a stable oxide layer that acts as an insulator, which is important to prevent water leakage and ensure proper operation. Lanthanides are also characterized by providing special functionality helping to form good insulating layers and this performance allows for customization in electronics, expanding the applications of MIS diodes to areas such as transistors, sensors and storage devices. Metals play an important role in MIS process diodes, determining the energy barrier at the metal-semiconductor interface.

Silicon is versatile and stands out for its association with insulating materials and its role in creating a stable silicon dioxide layer. Control of carrier behaviour by metalloids greatly increases the stability and reliability of MIS diodes. Late transition metals exhibit different functions and are compatible with a variety of semiconductors and it makes a significant contribution to MIS diodes and it plays an important role in electronic modification and formation of stable insulating layers. Reactive non-metals disrupt the semiconductor material by forming an

insulating layer, thus giving MIS diodes a distinctive appearance and their functions play an important role in the design of electronic components of MIS diodes, highlighting their importance in achieving desired functions in electronic applications such as the combination of transistors.

From the various aspects we have figured out the best works among them in each materials like, alkali earth metals, transition metals, lanthanides, metalloids, post transition metals and reactive non-metals. In the following it is discussed detailly.

4.1. Alkali earth metals

Rare earth metals, especially strontium (Sr), barium (Ba) and calcium (Ca) had played an important role in the development of MIS-structured diodes due to their unique electronic properties and these alkaline earth metals are commonly used as gate materials in MIS diodes, which are responsible for modulating the electrical properties of semiconductors, then the choice of strontium, barium or calcium affects the ability to form a high-quality insulating layer, usually an oxide film, on top of the semiconductor. Thin insulator layer acts as a barrier between the metal electrode, the semiconductor, controlling the flow of charge carriers and affecting the performance of the entire devices.

Due to similar use Strontium, barium and calcium oxides exhibit excellent insulating properties that enable the creation of stable and reliable MIS structures. The specific choice of these metals depends on factors such as their work function, interface properties and compatibility with semiconductor materials. This ability of alkaline earth metals to form well-defined interfaces with semiconductors helps to control the electrical properties of MIS diodes makes them suitable for a variety of electronic applications, including transistors and capacitors. In summary, strontium, barium and calcium are effective gate materials, playing an important role in the development of MIS structured diodes. Its unique properties contribute to the formation of high-quality insulator layers that allow precise control of the electrical behaviour of semiconductor devices and improve their performance in electronic circuits.

From the Sr-W as an insulating layer V. Balasubramani et.al., achieved the best results in the alkali earth metals. Fig. 31. The XRD results show enhanced crystallinity in the film, indicating a high-quality preparation. 6 Wt%, AFM the film shows densely packed needles and rod-like features observed by AFM, the smooth top structure and intact Sr-W layer on n-Si improve the rectification capability of SBDs and MIS structure. I-V graph shows the Cu/Sr-W/n-Si diode under different conditions of bias and illumination. Thermal emission allows charge carriers to escape from a solid, when the thermal energy exceeds the binding potential. AFM images confirm smooth surface and growth of Sr-W layer on n-Si surface.

This work concluded that the lowest bandgap energy of 3.61 eV was obtained at higher doping concentrations compared to other films. In I-V curve for the Cu/Sr-W/n-Si SBDs, showing that doping W decreases n and increases the barrier height. The calculated value of n is greater than unity, indicating the avoidance of emission-dominant thermal behaviour in the diode. This shows the effect of W dopant concentration on Φ_B and valence band structure. I-V characteristics of Cu/SrW/n-Si type diode shows high rectification activity with minimum n value of 1.68 the results show that devices using light-conditioned films, MIS-structured diodes are not compatible with photodiodes associated with other devices [31].

4.2. Transition metals

Transition metals, including owing to similar use of vanadium (V), cobalt (Co), zinc (Zn), yttrium (Y), zirconium (Zr), molybdenum (Mo), tungsten (W), hafnium (Hf), titanium (Ti), iron (Fe), tantalum (Ta) and copper (Cu) have been extensively employed in the context of MIS structured diodes. Then the specific choice of transition metals is driven

by their unique electronic properties, work functions and compatibility with semiconductor materials. The work function of a metal is a critical parameter in MIS diodes, as it determines the energy barrier at the MIS, influencing a flow of charge carriers. For example, metals with higher work functions, such as tungsten and tantalum, tend to create a larger energy barrier, making them suitable for applications where precise control of the carrier concentration is crucial. On the other hand, metals with lower work functions, such as titanium and aluminium, are often preferred for their ability to inject carriers into the semiconductor more readily.

Vanadium, cobalt and zinc are transition metals with work functions that fall within a moderate range, making them versatile choices for MIS diodes. Yttrium and zirconium known for their stability and compatibility with oxide insulators, contribute to the formation of reliable insulating layers in MIS structures. Similar use of molybdenum, tungsten and hafnium are often selected for their high melting points and good adhesion properties, ensuring the durability and stability of MIS diodes under varying operating conditions. Titanium and iron, being commonly used transition metals, offer a balance between work function and cost-effectiveness. Tantalum is preferred for its ability to form stable oxides, making it suitable for high-performance MIS devices. As per the previous papers copper with its low resistivity and good conductivity, has found applications in advanced MIS structures, particularly in the context of emerging technologies. In summary, the selection of transition metals for MIS structured diodes is guided by a careful consideration of their work functions, compatibility with semiconductor materials and the desired electronic properties for specific applications. This diversity in transition metal choices allows for the tailoring of MIS diodes to meet the requirements of a wide range of electronic devices and circuits.

From the Yb@V₂O₅ as an insulating layer author bring the good results XRD analysis revealed the disordered structure of the ytterbium-doped V₂O₅ film; this led to a decrease in lattice parameters and crystalline phases. The 2 wt% Yb@V₂O₅ film exhibits improved crystallinity and increased defects, leading to increased photosensitivity of the diode. FE-SEM images show that the V₂O₅ morphology changes after Yb doping and forms a rod-like array with increasing pressure. The change in surface morphology corresponds to the increase in grain size and improvement in electrical properties in the V₂O₅ film, supporting the use of 2 wt% Yb as an interface layer in optoelectronic devices fabrication.

Fig. 32. In addition, electrical studies show that current increases the value of the Yb@V₂O₅ film linearly as a function of temperature and voltage, indicating good energy transfer. Morphological studies showed that nanorods and nanoplate-like structures were observed. Changes in Yb dopant concentration and I-V diagram of Cu/Yb@V₂O₅/n-Si diode show the process current based on the TE theory. Also, J-V of pure and Yb@V₂O₅ MIS-treated SBDs exhibit good properties under illumination conditions and show significant photovoltaic effects with calculated Φ_B values ranging from 0.66 to 0.79 eV. This behaviour indicates that the trapped charges do not have sufficient energy to escape when illuminated, resulting in the high photocurrent observed in the fabricated MIS structured SBDs. This work concluded that SBDs diodes were successfully prepared using the spinning process using Cu/Yb@V₂O₅/n-Si MIS structure and V₂O₅ was doped with 2, 4 and 6 Yb content by wt% [43]. The detection range of the coated film varied between 3.23 and 3.31 eV. The electrical properties of Cu/Yb@V₂O₅/n-Si SBDs showed that the performance of the photodiode in light was better than in the dark, this shows that fabricated diodes perform similar to photodiodes. Importantly, a high photosensitivity of 5545.70% was achieved for a 2 wt% diode. Yb@V₂O₅ diodes are ideal for fabricating photodiodes for optoelectronic applications.

4.3. Lanthanides

Lanthanides such as, lanthanum (La), cerium (Ce), neodium (Nd), ytterbium (Yb), samarium (Sm) and praseodymium (Pr) have shown utility in MIS structured diodes, advanced electronics contribute to the

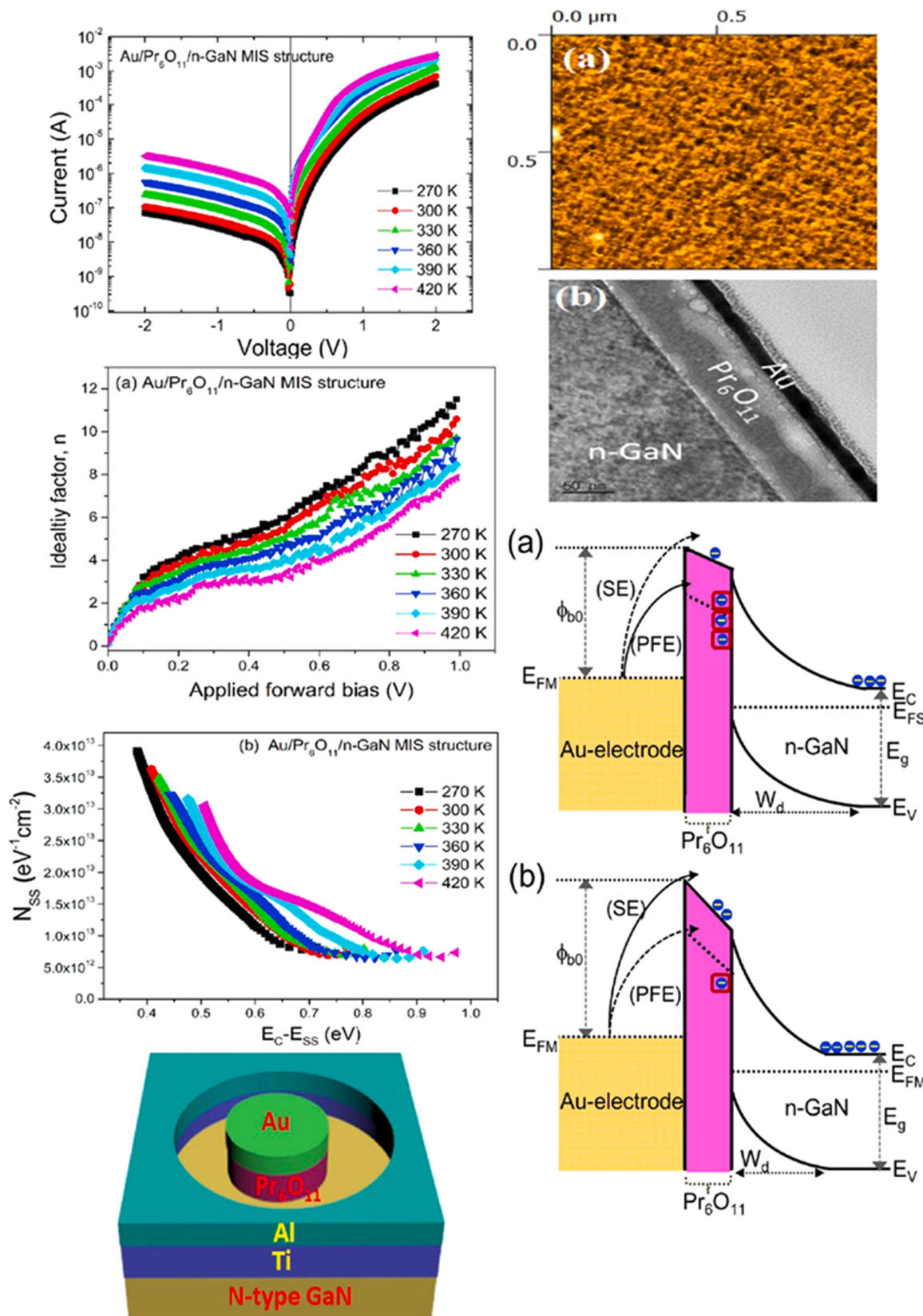


Fig. 33. AFM image, device structure, barrier height images of the device [37].

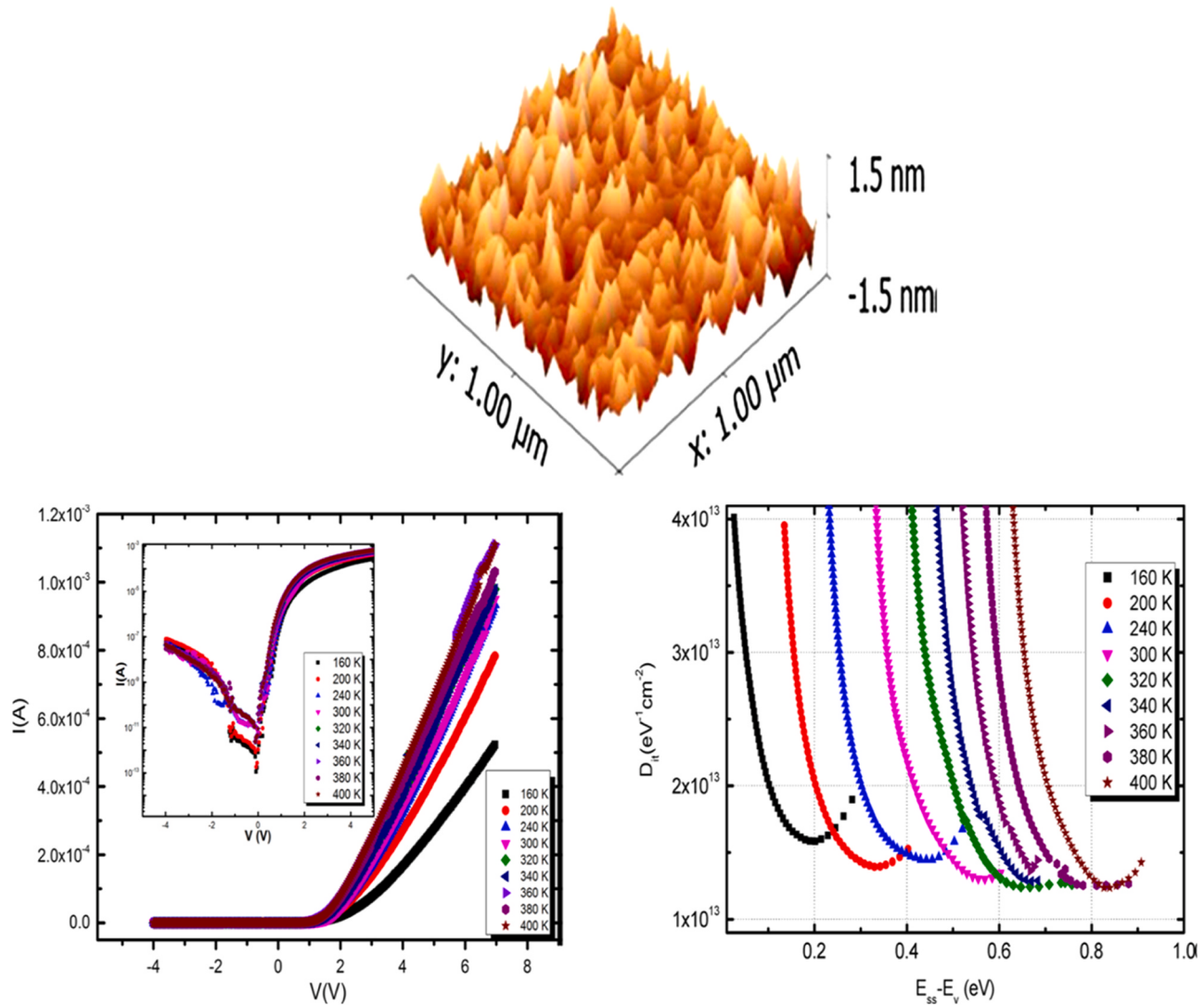


Fig. 34. Represents the AFM image and I-V graphs of the device. [76].

development of equipment. The unique properties of lanthanides, including work functions, make them valuable candidates for specific applications, work function, which is an important parameter in MIS diodes, affects the energy barrier at the MIS, charge carrier injection and modulation. Lanthanides show several functions that can be useful for tuning the electronic properties of MIS diodes. For example, ytterbium (Yb) and samarium (Sm) are known for their low work functions, making them suitable for efficient electron injection into n-type semiconductors. On the other hand, cerium (Ce) and neodymium (Nd), which have a high work function, can be used together with p-type semiconductors. In addition to their functional properties, lanthanides are often used to form insulator layers in MIS diodes. Lanthanide oxides, such as lanthanide oxide (La_2O_3) and cerium oxide (CeO_2) have good dielectric properties that allow the formation of stable, thin insulating layers on top of semiconductors and the insulator layer is necessary to prevent leakage current provide proper isolation between the metal and the semiconductor, contributing to the reliability and performance of the MIS diode.

The ability of lanthanides to form high-quality interfaces with semiconductors further enhances their suitability for MIS diodes and it as its compatibility with different semiconductor materials allows electronic devices to be tailored to specific requirements. This flexibility makes lanthanides valuable in the development of MIS diodes for applications, such as transistors, sensors and memory devices. In summary,

lanthanides play an important role in MIS structured diodes due to their functional properties, which allow specific modulation of charge carriers and formation of stable insulator layers, ensuring reliable device operations. Then the choice of a particular lanthanides depends on the desired electronic properties and the semiconductor material used in the MIS diode applications.

Schematic diagram showing the fabricated Au/ Pr_6O_{11} /n-GaN MIS Schottky structure, AFM image shows a smooth Pr_6O_{11} surface with a rms value of approximately 2.23 nm. A typical TEM image shows a homogeneous interface between Pr_6O_{11} , GaN substrate and Au. Then the Au/ Pr_6O_{11} /n-GaN MIS structure shows a higher barrier height (0.93 eV at 420 K) rectification properties at all temperatures compared to the Pt/ HfO_2 /n-GaN MIS diode. The leakage current increases with temperature, from 2.6×10^{-8} A (270 K) to 1.2×10^{-6} A (420 K), at a reverse voltage of 1 V and also ideal voltage factor, indicates progress, shows the effect of the country's interface density on current transport. The Au/ Pr_6O_{11} /n-GaN MIS structure exhibits an ideality factor greater than one in the linear region with high current distortion due to the interfacial density of states, Φ_B and the ideality factor are regulated by NSS, which play an important role in the MS interface. Schematic energy band diagram showing temperature-dependent mechanisms (PFE and SE) in the Au/ Pr_6O_{11} /n-GaN MIS structure.

This work found from the Fig. 33. that the interfacial density of states (NSS), obtained from I-V data, increases with decreasing temperature,

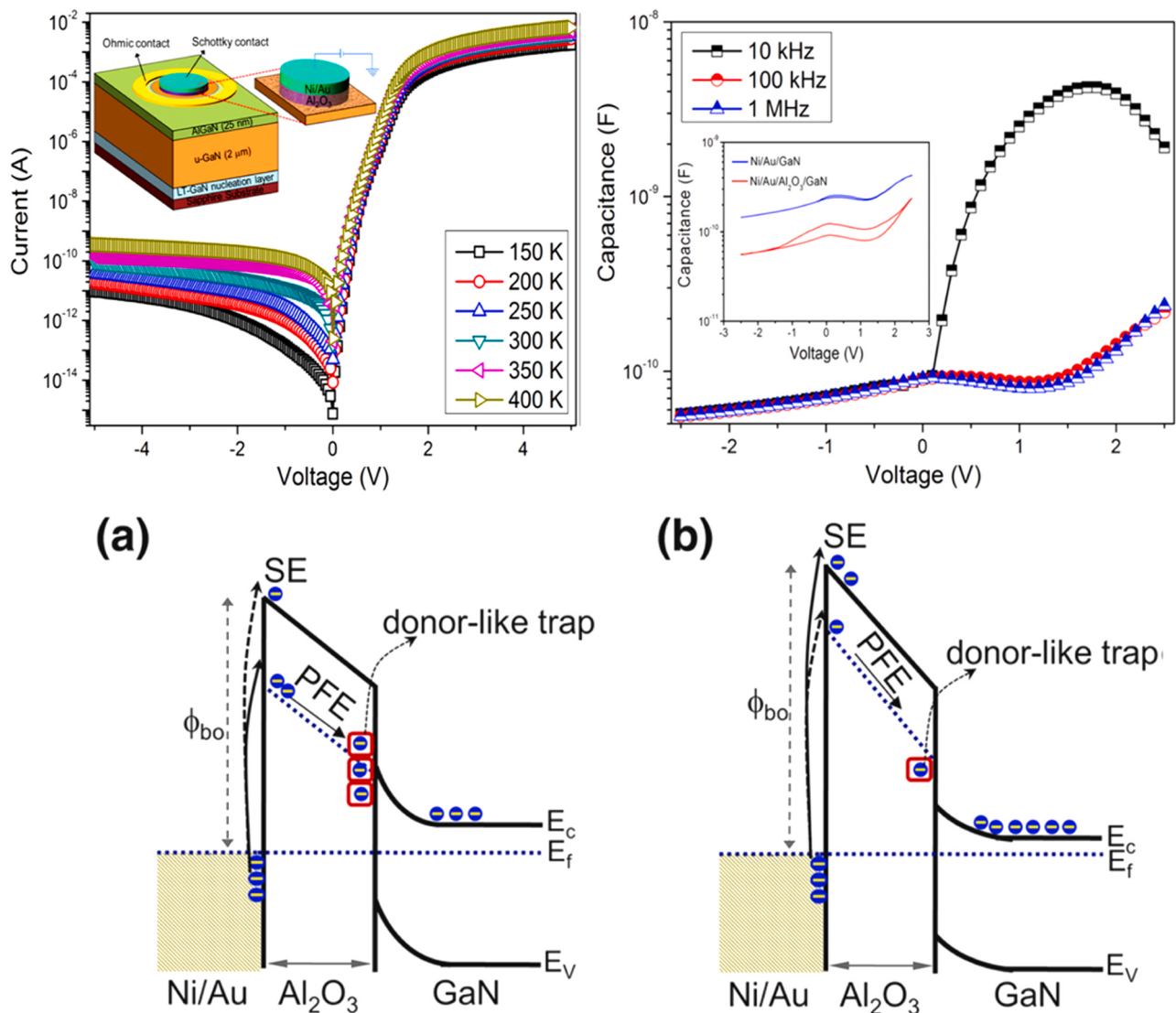


Fig. 35. Representation of the device structure, I-V and C-V graphs, barrier height of the Ni/Au/GaN and Ni/Au/Al₂O₃/GaN MIS diodes [80].

which can be attributed to the thermal modification and interfacial arrangement of Pr₆O₁₁/n-GaN. Results show that the current conduction mechanism was dominated by PFM in the temperature range from 270 K to 330 K, while Schottky emission is dominant above 330 K and these predicted results have potential for the fabrication of MIS devices high performances [37].

4.4. Metalloids

Silicon a metalloid, has played a pivotal role in the development and success of MIS structured diodes. Silicon is particularly noteworthy for its abundance, semiconductor properties and compatibility with various insulating materials in and it is often used as the semiconductor material, forming the foundation for the MIS device. The work function of silicon is a crucial parameter in MIS diodes, influencing the energy barrier at the MS interface. Silicon typically has a work function around 4.2 eV and this value is significant in determining the alignment of energy bands and the efficiency of carrier injection or extraction at the interface. One of the key advantages of using silicon in MIS diodes is its native oxide, silicon dioxide (SiO₂), which serves as the insulating layer. Silicon dioxide is known for its excellent insulating properties, high dielectric strength and stability. This oxide layer is typically formed through processes like thermal oxidation, ensuring a well-defined and

reliable insulator in MIS structures. The SiO₂ layer effectively separates the metal electrode from the silicon semiconductor, controlling the flow of charge carriers and preventing leakage currents.

Moreover, silicon is compatible with various metal gate materials, allowing for flexibility in designing MIS diodes for specific applications. By carefully selecting metals with appropriate work functions, the energy barrier at the MS interface can be optimized for desired electronic properties. This versatility has made silicon a fundamental material in the fabrication of integrated circuits and a wide range of semiconductor devices, including transistors and capacitors, based on MIS structures. In summary, the metalloid silicon is crucial for MIS structured diodes, serving as the semiconductor material with a well-matched work function and compatibility with various insulating and metal materials. The unique properties of silicon, combined with its ability to form stable oxide layers, make it a cornerstone in the field of semiconductor technology and integrated circuit design.

Fig. 34. shows the surface of Si₃N₄ film exhibits smooth and uniform features with a mean square roughness of 0.288 nm. The MIS diode structure is obtained by thermally evaporated dot-patterned Au rectifier contacts on the Si₃N₄ film layer. The resulting MIS model exhibits SBDs behaviour as the current increases with temperature. The rectification ratio is defined as the ratio of forward current to the reverse current of the voltage and is calculated to approximately three orders of

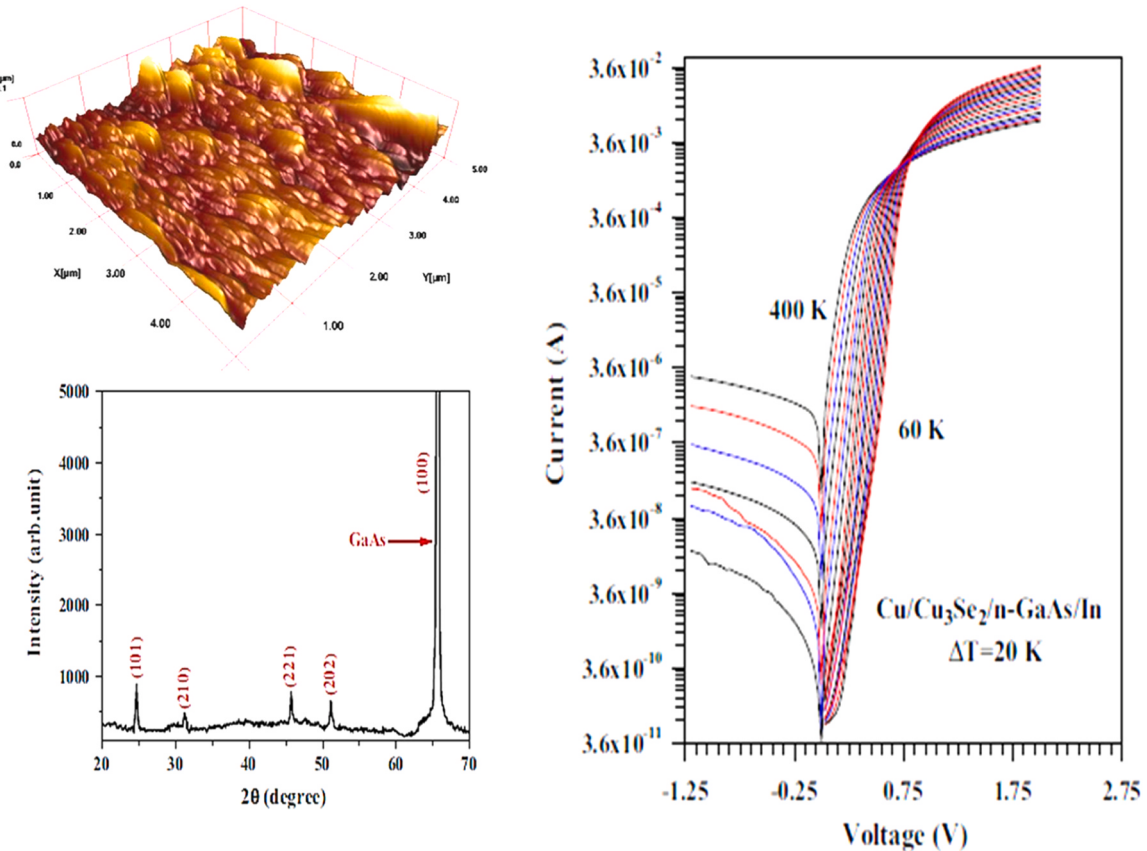


Fig. 36. Representation of the XRD patterns of copper selenide films, AFM image and I-V graphs of the Cu₃Se₂ film. [71].

magnitude. Ideally, pure TE should be the main current transport mechanism and this is not achieved by diode I-V measurement according to theory. The figure shows the decrease in the experimental values of the interfacial density with temperature, indicating that the interfacial process is rearranged and realigned in the temperature direction.

From that work [76], it concludes that the results are justified by the fact that they can be repeated and redetermined. Interface orders based on thermal effects. The effect of the insulating layer capacitance is measured by the Hill-Coleman method and did is calculated from the changes in f and T.

4.5. Post transition metals

Post transition metals, including polonium (Po), gallium (Ga), indium (In) and tin (Sn) been found to be useful in MIS systems. Electric and the work function of these late transition metals plays an important role in determining the energy barrier at the MS interface and thus affects the behaviour of the charge in the MIS diodes. Polonium, as an electronic material, is used only in applications due to safety concerns in MIS diodes. For this reason, it is not used very often in electronic products. However, gallium, indium and tin are widely used in MIS diodes, especially due to their different functions and compatibility with various semiconductor materials. Gallium and indium, in particular, are known for their low work activity, making them suitable for injecting electrons into n-type semiconductors. Tin, on the other hand, has a higher conductivity, making it suitable for p-type semiconductors.

Additionally, gallium, indium and tin can form stable and thin oxide layers that act as insulators. This insulating layer, usually made of gallium oxide (Ga₂O₃), indium oxide (In₂O₃) or tin oxide (SnO₂), provides good electrical insulation between the gate metal and the semiconductor. Creating a reliable insulator is important to prevent unnecessary leakage current and ensure the quality of the MIS diode. In

summary, late transition metals (except radioactive polonium) play an important role in MIS model diodes. They have a wide range of functions, are compatible with a variety of semiconductor materials and their ability to form a stable insulating layer facilitates their application as gate materials for MIS diodes and facilitates the fabrication of electronic devices.

From the Fig. 35. Current-voltage curves observed for TMAH-treated Ni/Au/Al₂O₃/GaN MIS diodes at different temperatures, the schematic configuration of the diode is shown in the Fig. 35. The capacitance voltage (C-V) characteristics of the diodes at various frequencies were tested at room temperature, C-V measurements showed that both Ni/Au/GaN and Ni/Au/Al₂O₃/GaN MIS diodes had small hysteresis loops and the large hysteresis loop observed for the Ni/Au/Al₂O₃/GaN MIS diode indicates a decrease in the MIS conductivity pattern and the corresponding density of states of the oxide-semiconductor junction as it enters an insulating layer (Al₂O₃). Schematic band diagram showing the control of donor-like trapping at the interface below room temperature leads to the PFE mechanism, while at room temperature and above heat trapping decreases due to the carrier absorbing thermal energy.

Using that Al₂O₃ as the insulating layer author that device achieved best results from the Post transition metals. This study on the thermal properties and transport of TMAH-treated Al₂O₃/GaN MIS diodes concluded that the Φ_B increases and the target value decreases with increasing temperature. Additionally, with temperature, the series resistance (RS) and interface state rate (NSS) decrease from 150 K to 400 K. It was discovered that the transport process exhibited different processes at different voltages and temperatures, especially those treated with TMAH. Al₂O₃/GaN MIS diodes exhibit PFE at temperatures between 150 K and 250 K, while Schottky emission dominates carrier transport at ≥300 K. This difference can be attributed to different loadings, such as SE occurring at the dielectric interface and PFE occurring from traps in the dielectric materials [80].

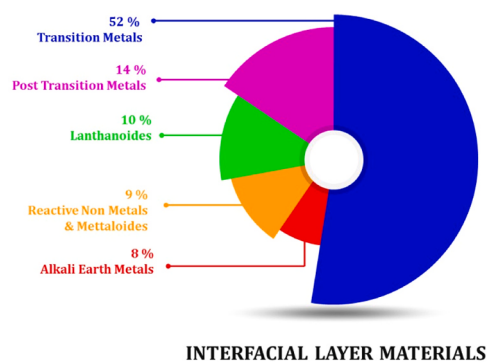


Fig. 37. Represents the average drawing of the materials that have used for the interfacial layer. From the graph it shows that transition metals were used in the most of the papers like 51.40%.

4.6. Reactive non – metals

Reactive non-metals such as oxygen (O), sulphur (S), nitrogen (N) and selenium (Se) are crucial components in the MIS structured diodes, particularly when considering the insulator layer. These non-metals are commonly utilized to form insulating materials, often oxides or nitrides, which play a vital role in controlling the electrical properties of the diode. The work function of oxygen in this context is indirectly important, as it influences the properties of the silicon dioxide layer and its effectiveness in providing electrical insulation between the metal electrode and the silicon semiconductor. Sulphur, in combination with other elements, can be involved in the formation of metal sulphides or other compounds used as insulating layers in MIS diodes and this compound can offer unique electrical properties, stability under specific conditions. The work function of sulphur in these compounds may affect the energy barrier at the metal-insulator interface and subsequently impact the overall performance of the MIS diode. Their involvement in the formation of oxides, nitrides or other compounds influences the dielectric properties and stability of the insulator layer, which in turn affects the overall performance of the MIS diode.

Nitrogen is often involved in the formation of nitrides, such as silicon nitride (Si_3N_4), which is another important insulating material in MIS diodes and it can provide an alternative to oxides, offering different dielectric properties and chemical stability. The work function of nitrogen influences the properties of the nitride insulator, affecting the overall performance of the MIS diode. Selenium, although less commonly used than the others, may be incorporated into insulating layers in MIS diodes, then the work function of selenium in these compounds plays a role in determining the energy barrier at the metal-semiconductor interface and can impact the device's electrical characteristics. The specific work functions of these non-metals in the insulating materials contribute to the precise control of charge carriers and the modulation of electrical properties in semiconductor devices.

From the Fig. 36, the XRD patterns of copper selenide films show that they have a polycrystalline structure. AFM studies have shown distinct particles with an average height of $0.6 \mu\text{m}$ and width of $0.056 \mu\text{m}$, resulting in a surface roughness of $0.05 \mu\text{m}$ for Cu_3Se_2 film comfort when the uniformity and low roughness of the sample surface helps prevent defects caused by circuit manufacturing materials and impurities in the Cu_3Se_2 film. The I-V diagram is constructed using temperature measurements of charge carriers to lattice interference and junctions in the saturation current region to series resistance. At high temperatures, reduced lattice distortion allows carrier mobility, which reduces the resistance associated with thick semiconductor materials.

In this work Author uses the SILAR method to deposit a copper selenide film on a GaAs substrate to study its structure and determine its morphological properties using XRD, SEM and AFM methods. It was formed in the $\text{Cu}/\text{Cu}_3\text{Se}_2/\text{n-GaAs}$ structure and its I-V properties were

analysed in the temperature range of $60\text{--}400 \text{ K}$, when the calculated SDs parameters, including the optimum Φ_B , show temperature dependence. The increase in the ideal and the decrease in the Φ_B potential with temperature are due to the inequality of the interface, especially between the MS interface. $\text{Cu}/\text{Cu}_3\text{Se}_2/\text{n-GaAs}/\text{Electrical}$ measurements on the sample indicate the temperature, which can be explained by TE with the GD of the high barrier. The dominance of hot electron FE is associated with the lateral distribution of the barrier height and this indicates that the increased conduction may be due to a local increase in the electric field causing a local decrease in Φ_B . [71].

Fig. 37 Represents the Average drawing of the Materials that have used for the interfacial layer. From the graph it shows that Transition metals were used in the most of the papers like 51.40%.

5. Semiconductor materials of MIS diodes

Semiconductors belong to a class of materials characterized by their unique electrical properties, which lie between those of conductors and insulators, then the conductors such as metals, which readily allow the flow of electric current. Semiconductor devices operate by harnessing light through components like photodiodes, phototransistors, photosensors, photodetectors and solar cells. These elements play a crucial role in the extensive applications in optoelectronic. [22]. They possess adjustable features rooted in swift optical responses, ultra-high speed, minimal current leakage, stability and an extended lifespan. This has captivated the scientific community, steering the research toward photonics-oriented devices. Specifically, SDs responsive to varying light intensities hold significant potential for performance enhancement through adjustable parameters [5]. Because of an integral role in semiconductor devices, such as radio-frequency generators, optical communication systems and smoke detectors [25]. Due to imperfections on the surface of the semiconductor, such as unpaired connections, deficiencies in oxygen atoms, the introduction of donor or acceptor atoms, irregularities within the semiconductor's structure, and the presence of various organic contaminants resulting from laboratory cleaning and preparation protocols [139]. The crystal structure of semiconductors is a critical factor influencing their electrical properties. Many semiconductors, including silicon and germanium, possess a crystalline lattice structure where atoms are arranged in a highly organized pattern. The semiconducting MIS structured diode offers several advantages, including quick response, higher efficiency at low operating power, making it an ideal electronic device for rectifier, switch and voltage stabilizer functions in various electronic circuits. Researchers have explored various interlayer transition metals, such as TiO_2 , WO_3 , MoO_3 , SnO_2 , In_2O_3 , CdO and ZrO_2 , aiming to enhance the electrical conduction properties of the MIS diode. This ongoing research seeks to optimize the performance of the MIS diode, making it a versatile component for diverse applications in electronic systems [32,140,141]. Comprehensive bandgap semiconductor oxides like TiO_2 , WO_3 , MoO_3 , V_2O_5 and RhO_3 demonstrate promising optical, electrical and gas sensing properties, making them pivotal in diverse research areas. Their versatile applications have been extensively studied, highlighting their potential in various scientific and technological domains [142,143]. Semiconductor materials play a crucial role in modern electronics due to their unique electrical properties. Silicon (Si) is the most widely used semiconductor in the industry, known for its stability and reliability, Gallium arsenide (GaAs) is valued for its high electron mobility, making it suitable for high-frequency applications, other semiconductor materials like gallium nitride (GaN) and indium phosphide (InP) offer advantages in optoelectronics. Emerging materials such as organic semiconductors, perovskite materials show promise for flexible electronics and next-generation solar cells. Then the constant exploration and development of new semiconductor materials contribute to the advancement of electronic devices across various applications. Silicon stands out as the predominant material in the semiconductor industry. Its abundance, stability, well-established fabrication processes make it ideal for

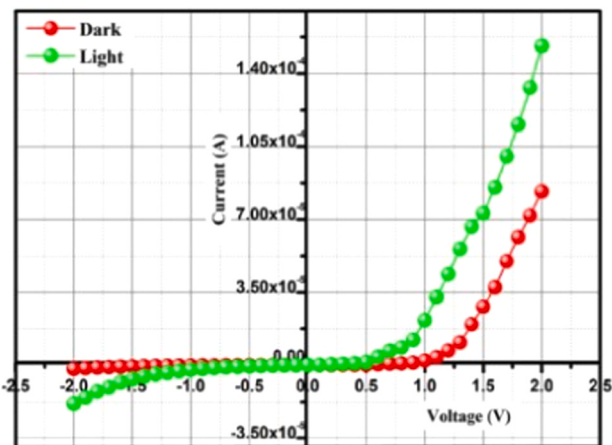
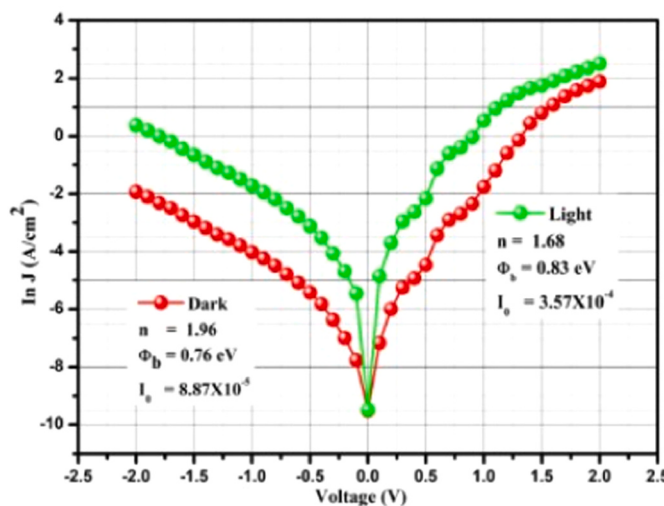


Fig. 38. Representation of I-V characteristics of the Cu/Sr-W/n-Si MIS diode were assessed through forward and reverse bias measurements [31].

integrated circuits and a wide range of electronic devices. n-type Si serves as electrical properties, such as electron mobility and conductivity, make it suitable for various electronic applications, p-type silicon (Si) with a low work function serves as an ideal rectifying MIS contact, demonstrating superior adhesion to the thin oxide layer [24]. Barium oxide (BaO) is an II-VI semiconductor with a sizable 4.4 eV direct band gap, offering robust mechanical strength and high thermal stability. Its atomic-level film thickness control makes it a valuable candidate for device miniaturization in semiconductor applications [33]. Numerous researchers have dedicated efforts to investigate the electrical characteristics of p-Si SBDs through various metallization schemes and these studies explore the potential applications of p-Si, SBDs in sensing and optoelectronics [38]. Gallium arsenide (GaAs) stands as a critical material for low-power, high-speed devices and also comprehensive understanding of the electrical characteristics of GaAs-based SDs is indispensable for its effective application in various technologies [50]. Indium phosphide (InP) is a desirable semiconductor for optoelectronic and high-speed electronic devices due to its direct band gap transition and high electron mobility [60]. Gallium Nitride (GaN)-based optoelectronic and microelectronic devices have experienced rapid development, driven by their potential applications in the next generation of technology [80].

5.1. Types of semiconductors

Semiconductors can be broadly classified into various types based on their properties and composition. Elemental semiconductors, such as silicon (Si), germanium (Ge), consist of a single element and form the foundation of semiconductor technology. Compound semiconductors, like gallium arsenide (GaAs) and indium phosphide (InP), are formed by combining elements from different groups in the periodic table and organic semiconductors, composed of carbon-based materials, find applications in flexible electronics LED. Inorganic semiconductors encompass both elemental, compound materials, with silicon playing a dominant role in integrated circuits and microelectronics. Then the semiconductors, like (GaAs, InP) involve elements from groups III and V, while II-VI semiconductors, such as (CdS, ZnSe), combine elements from groups II and VI.

5.2. Silicon as a Semiconductor

Silicon is a crystalline solid with a diamond cubic crystal structure. As the second-most abundant element on Earth, silicon forms the basis for integrated circuits and microelectronics. Its crystalline structure,

semiconducting properties make it an ideal material for manufacturing transistors, diodes and other semiconductor devices. In its pure form, silicon is a poor conductor of electricity at room temperature, when certain impurities are intentionally introduced through a process called doping, silicon becomes a more efficient conductor and the doping process involves adding specific atoms, such as phosphorus or boron, to the silicon crystal lattice, creating n-type (negative) or p-type (positive) semiconductors.

5.3. n-type silicon

n-type silicon is valued for its distinct electrical characteristics, including high electron mobility and conductivity, rendering it well-suited for a diverse range of electronic and photodetector applications [144,145]. Then the higher electron mobility of n-type silicon, compared to p-type silicon, is advantageous in high-frequency devices and certain types of transistors, enhancing the overall performance of electronic components T. Akila. et.al. [146]. Additionally, combining a metal with an n-type semiconductor forms a Schottky or MS diode junction, characterized by unique electronic properties, making it valuable for diverse electronic applications. The authors opted for the utilization of n-type silicon semiconductor in their research papers, leveraging its specific electrical properties for their study and their fabricated MIS diodes.

From all the papers we have referred and finalized that the work shows that the n-type is best for the diode fabrication. I-V characteristics of the Cu/Sr-W/n-Si MIS diode were assessed through forward and reverse bias measurements, I-V plot was recorded in the voltage range of -2 to +2 V under both dark and light conditions. A semi-logarithmic $\ln(J)$ -V curve was plotted for the Cu/Sr-W/n-Si SDs, it shows that the good Ideal parameters and diode parameters, as shown in Fig. 38. $n=1.68$, $\Phi_B=0.83\text{eV}$ and I-V nature of this MIS diode indicates higher rectifying activity with minimum n values. The results consummated that the device, MIS-structured diode with light condition films signify inconsistent photodiode performance associated with other devices. V. Balasubramani. et.al., [31].

5.4. p-type silicon

p-type silicon is created by doping silicon with atoms such as boron, introducing holes or vacancies in the crystal lattice. Holes become the majority charge carriers, leading to a positively charged material. p-type silicon is essential for forming MIS Selecting suitable transparent conducting oxides (e.g., Mo, Cu, Au) or thinner metals (< 100 nm) for the

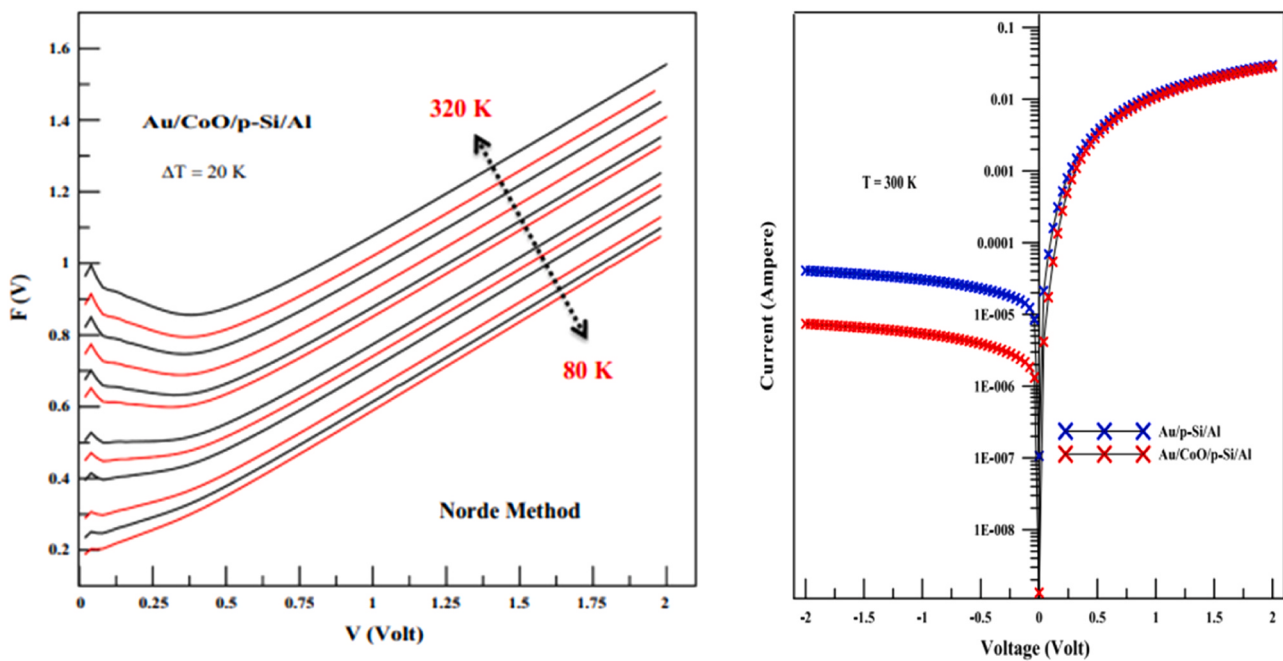


Fig. 39. $F(V)$ – V graphs of $\text{Au}/\text{CoO}/\text{p-Si}/\text{Al}$ diode in the 80 K–320 K temperature range and the I-V plots of the diode $\text{Au}/\text{CoO}/\text{p-Si}/\text{Al}$. [78].

top electrode in a MIS device can enhance responsivity and this improves light penetration from the metal electrode to the semiconductor (p-Si) surface. Metals with higher work functions further reduce tunnelling effects between the metal and p-Si , potentially boosting overall device performance [147].

We are referred to the specific MIS p-type Si in their research papers, capitalizing on its distinct electrical properties for their investigation and the fabrication of MIS diodes. After examining various research papers, it is evident that the research conducted by *AliRiza Deniz et al.*, the preference for diode fabrication is towards the p-type. I-V measurements of reference $\text{Au}/\text{p-Si}/\text{Al}$ and $\text{Au}/\text{CoO}/\text{p-Si}/\text{Al}$ diodes produced under the same conditions were analysed. As shown in Fig. 39. I-V measurements for $\text{Au}/\text{CoO}/\text{p-Si}/\text{Al}$ diode showed temperature-dependent variations in n , Φ_B and with increasing temperature, $n=1.19$ decreased, while $\Phi_B=0.82\text{eV}$ increased. C-V measurements at varying frequencies for the $\text{Au}/\text{CoO}/\text{p-Si}/\text{Al}$ diode showed a decline in N_a , V_d and Φ_B values with increasing frequency. This suggests the introduction of CoO as an interface material influences the diode's electrical properties, evident in the altered values of n , Φ_B , N_a and V_d . The results of this device to analyse the utilization of a material with diverse electrical and magnetic properties in diode applications [78].

5.5. Silicon carbide (SiC)

It is a compound semiconductor that has gained significant attention for its exceptional properties, making it a versatile material with applications in various industries. Comprising silicon (Si) and carbon (C) atoms, SiC . Silicon carbide (SiC) is a well-known material due to its extraordinary mechanical, physical properties, such as hardness, abrasive wear resistance, chemical inert and high thermal conductivity [55]. Then the crystalline structure of SiC can exist in various polytypes, with hexagonal and cubic being the most common.

5.6. n-type silicon carbide ($n\text{-SiC}$)

n-type silicon carbide (SiC) is a semiconductor material intentionally doped with impurities to introduce additional electrons as the majority charge carriers, then the doping process typically involves elements like nitrogen or phosphorus this results in enhanced electrical

conductivity, making n-type SiC a crucial component in high-performance electronic devices, particularly in power electronics. Its excellent electron mobility, thermal stability and high breakdown voltage make n-type SiC well-suited for applications such as power diodes, transistors and other devices that demand efficiency, high-power capabilities and reliable performance in challenging environments.

5.7. Germanium (Ge)

Germanium was one of the first materials used in semiconductor devices, it has similar properties to silicon but is less commonly used today due to its sensitivity to temperature changes and germanium diodes and transistors were crucial in the early development of electronic components.

5.8. Gallium arsenide (GaAs)

Gallium arsenide is a compound semiconductor composed of gallium, arsenic. It has higher electron mobility than silicon, making it suitable for high frequency applications such as microwave devices and high-speed transistors. GaAs is popular as a basic component of electronic devices in use of high-speed electronics, optoelectronics devices, detectors and lasers [148]. Using thermal oxidation for gate oxide on GaAs substrates is problematic due to the inferior quality of the native GaAs oxide, which lacks the desired properties for effective gate insulation. Additionally, depositing silicon dioxide onto GaAs leads to a lofty interface state density, introducing undesirable electronic states at the semiconductor-oxide interface, adversely impacting device performance [52].

5.9. n-type gallium arsenide ($n\text{-GaAs}$)

n-type gallium arsenide ($n\text{-GaAs}$) is a semiconductor material that has been intentionally doped with impurities to increase the concentration of free electrons as the majority carrier charges. Gallium arsenide is a compound semiconductor composed of gallium (Ga) and arsenic (As) atoms. In its intrinsic form, gallium arsenide (GaAs) has a crystalline structure, its electrical conductivity is relatively low and n-type GaAs is characterized by a surplus of negative charge carriers (electrons)

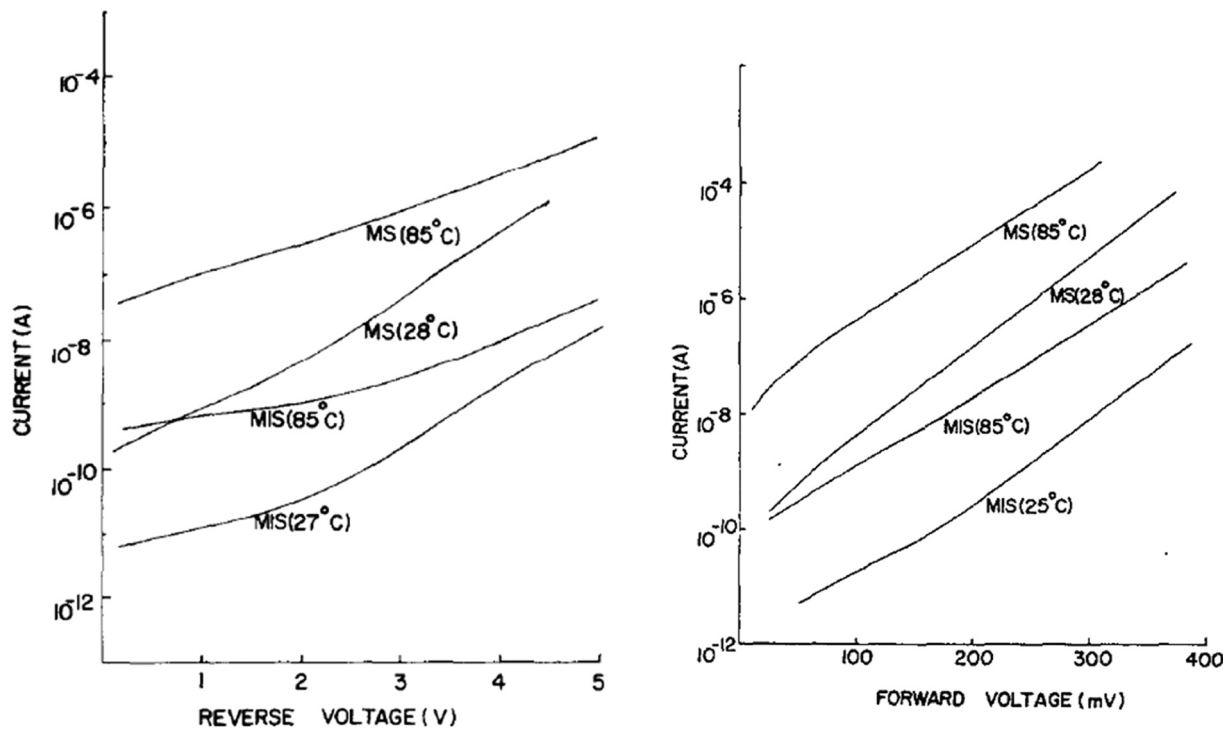


Fig. 40. Representation of Reverse I-V characteristics of MIS and MS diodes, forward I-V characteristics of MIS and MS diodes. [81].

that are free to move when an external electric field is applied. This high electron mobility makes n-type GaAs suitable for applications where fast and efficient electronic transport is crucial. The authors selected n-type gallium arsenide semiconductor for their research papers, harnessing its unique electrical properties to conduct their study and fabricate MIS diodes.

Among the whole n-type GaAs papers, work emphasizes that this semiconductor is good for diode fabrication. Then the forward I-V characteristics of the MIS diode suggest classical thermionic or TFE across the temperature range considered in the measurements. The reverse current in MIS diodes arises from generation in the space charge layer at low voltages, at higher bias levels, it is influenced by electric field modulation of the barrier by the interfacial layer and interface states. As shown in Fig. 40, the density of interface states, as inferred

from reverse current data, aligns closely with independent evaluations derived from C-V data. The reverse current is comparable to the extrapolated value obtained from the low-voltage, excess current region of the forward logarithmic I-V curve. I-V characteristics demonstrate favourable ideal parameters and diode characteristics $n=1.10$ and $\Phi_B=0.91$ eV and these output results are good at the electrical devices Ashok. et.al., [81].

5.10. p-type gallium arsenide (p-GaAs)

GaAs (gallium arsenide) stands out as a highly promising alternative channel material owing to its superior electron mobility, low power consumption, high breakdown field and direct bandgap, these attributes make GaAs a compelling choice for various semiconductor applications,

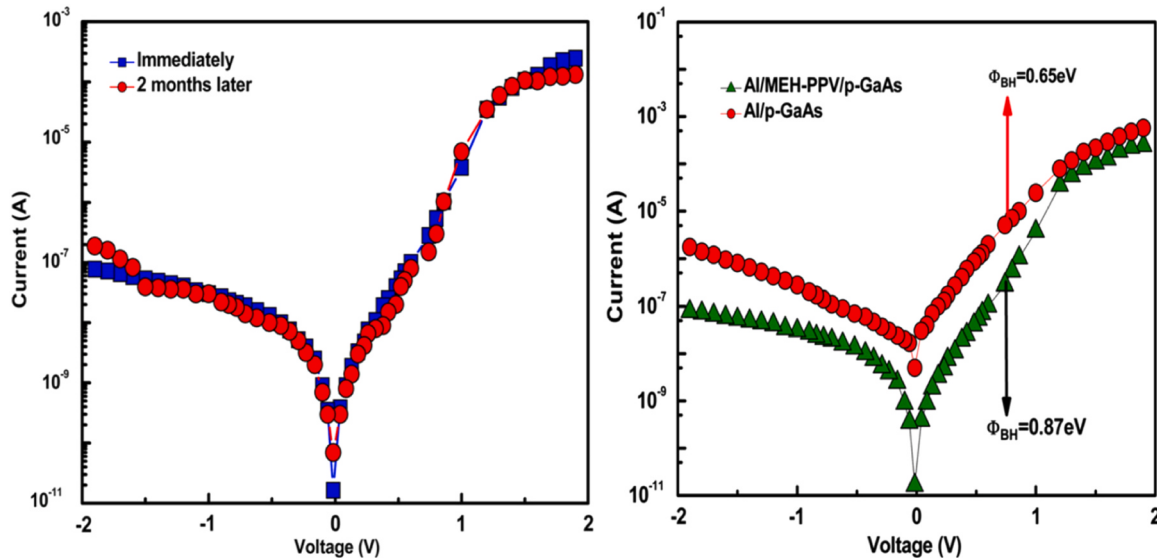


Fig. 41. Representation of the I-V characteristics exhibit alignment with those reported for inorganic/organic hybrid Schottky devices [74].

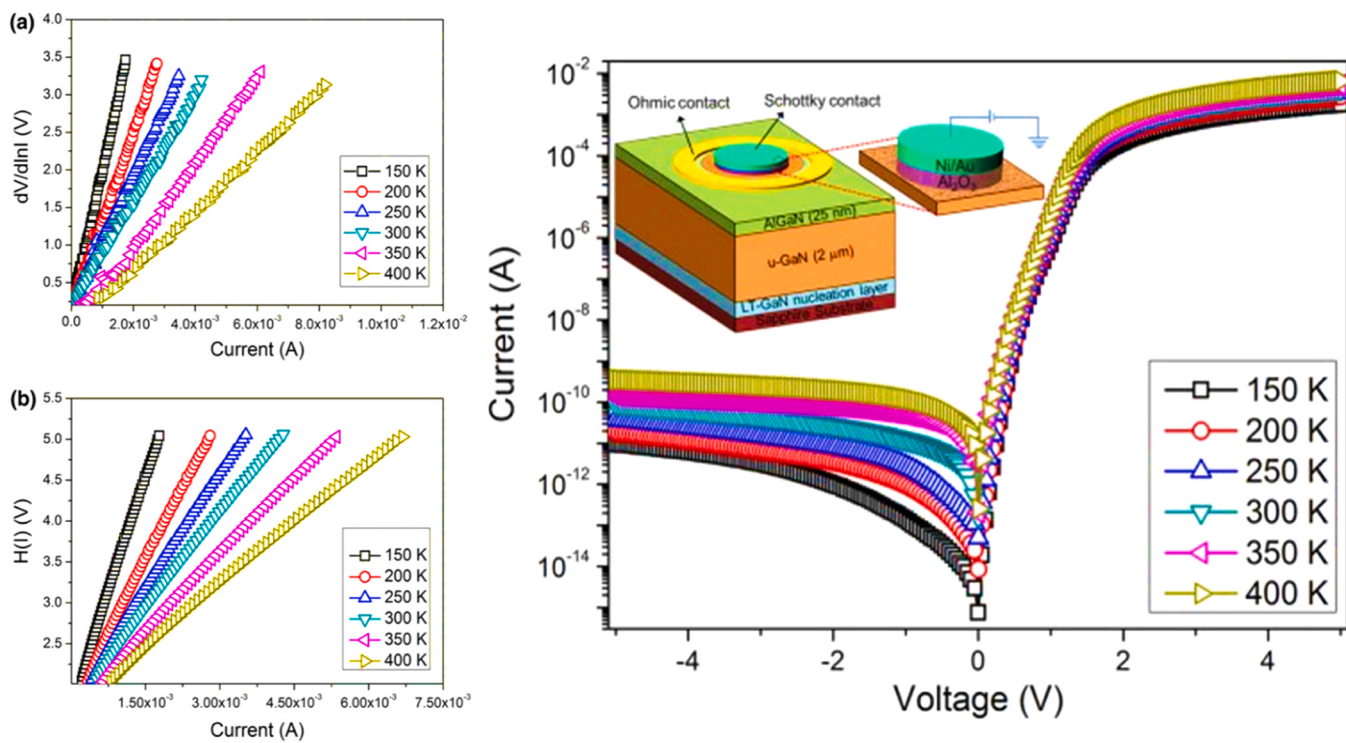


Fig. 42. Cheung plots of (a) $dV/d(\ln I)$ versus I and (b) $H(I)$ versus I for TMAH-treated $\text{Ni}/\text{Au}/\text{Al}_2\text{O}_3/\text{GaN}$ MIS diode as function of temperature and current–voltage curves of TMAH-treated $\text{Ni}/\text{Au}/\text{Al}_2\text{O}_3/\text{GaN}$ MIS diode as function of temperature [80].

particularly in electronic and optoelectronic devices where high-speed performance, efficiency are critical [74]. P-type gallium arsenide (p-GaAs) is a crucial semiconductor material known for its intentional doping to create a surplus of positive charge carriers or "holes," within its crystalline structure. Gallium arsenide, composed of gallium (Ga) and arsenic (As) atoms, serves as the foundation for various electronic and optoelectronic devices when modified into its p-type form. Then this process of p-type doping involves introducing specific, p-type GaAs exhibits notable characteristics that make it suitable for various applications.

Moreover, p-type GaAs is employed in optoelectronic applications such as LEDs and semiconductor lasers, then the combination of p-type and n-type GaAs enables efficient light emission through the recombination of electrons and holes, making it integral to the advancement of photonics.

Overall, we are concentrated their research on MIS diode, p-type GaAs, utilizing its distinctive electrical properties for their investigation and the construction MIS diodes. Upon thorough examination of multiple papers, it becomes apparent that said that the optimal choice for diode fabrication involves the use of p-type materials. As shown in Fig. 41, the I-V characteristics exhibit alignment with the reported for inorganic or organic hybrid Schottky devices. Notably, at a voltage of 0.5 V, the measured leakage current stands at 1.1×10^{-6} and 5.30×10^{-8} A, underscoring the consistency with prior research findings. The barrier height and ideality factor in the MIS device, these values were 0.87 eV and 1.17, respectively. Consequently, due to MEH-PPV, the barrier height increased by 0.22 eV. MEH-PPV is recognized as a stable material, facilitating the attainment of a high-quality organic inorganic interface. It emerges as promising organic material for the development of electronic and photovoltaic devices. Souvik Kundu et.al., [74].

5.11. Gallium nitride (GaN)

Gallium nitride is also a compound semiconductor with wide-bandgap properties it is used in power electronics, high-frequency

devices and optoelectronics. GaN-based transistors are employed in applications like power amplifiers and RF devices. GaN LED are known for their efficiency in lighting applications. Remarkably, the GaN (MIS) diode serves as a cornerstone in power electronics technology, playing a pivotal role in high-power, high-frequency and high-temperature applications [149].

After thoroughly referred various papers, as shown in Fig. 42, have concluded that gallium nitride materials are the preferred choice for diode fabrication. Additionally, the TMAH-treated $\text{Ni}/\text{Au}/\text{Al}_2\text{O}_3/\text{GaN}$ diodes show temperature-dependent variations in ideality factor and barrier height. At elevated temperatures, the $n=1.09$ decreases and $\Phi_B=0.96$ eV increases and it is favourable for electrical behaviour Siva Pratap Reddy et.al., [80].

5.12. n-type gallium nitride (n-GaN)

It is a semiconductor material intentionally doped to introduce an excess of free electrons as the predominant charge carriers. This characteristic makes n-type gallium nitride suitable for various electronic devices, including high-power and high-frequency applications. When the semiconductor materials, particularly gallium nitride (GaN) have garnered significant attention in the fabrication of high-power, high-frequency and high-temperature devices [58].

Some of them to preferred the n-type gallium nitride is good for diode fabrication. After a comprehensive preferred some papers, M. Uma et al. have determined that diode fabrication is best achieved using n-type materials. The characteristic temperature (T_0) value is determined through Cheung's functions and the T_0 value obtained from the $dV/d(\ln I)$ -I plot aligns well with the value obtained from the $H(I)$ -I plot. As shown in Fig. 43. Experimental results indicate a thermal coefficient (K_J) of -2.1 mV/K. The interface state density (N_{SS}) extracted from I-V data shows an increase with decreasing temperature, suggesting a correlation with the thermally-driven restructuring and reordering of the $\text{Pr}_6\text{O}_1/\text{n-GaN}$ interface. As temperature rises, $\Phi_B=0.93$ eV increase, while $n=1.42$ decrease, these consistent findings hold promise for the production of

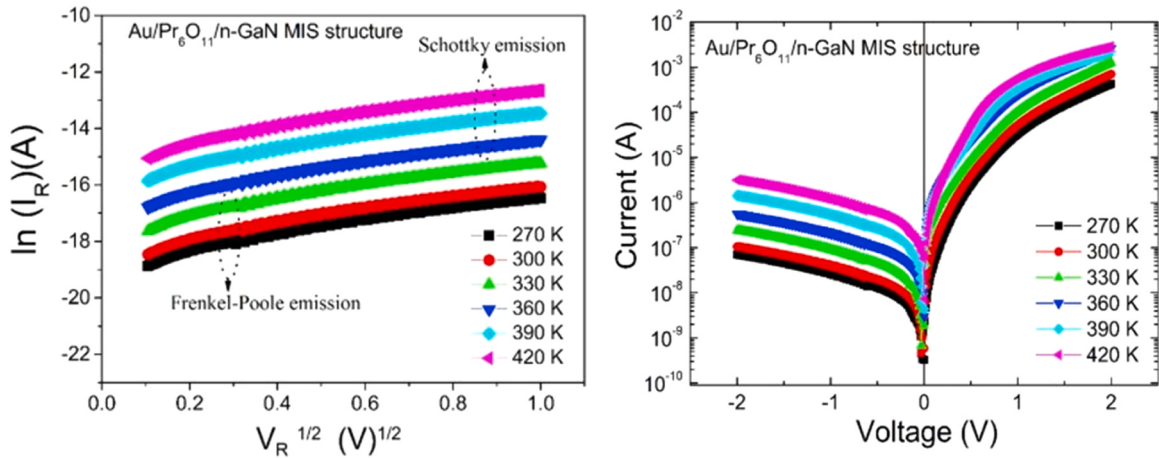


Fig. 43. I-V data shows an increase with decreasing temperature, suggesting a correlation with the thermally-driven restructuring and reordering of the Pr₆O₁₁/n-GaN interface. [37].

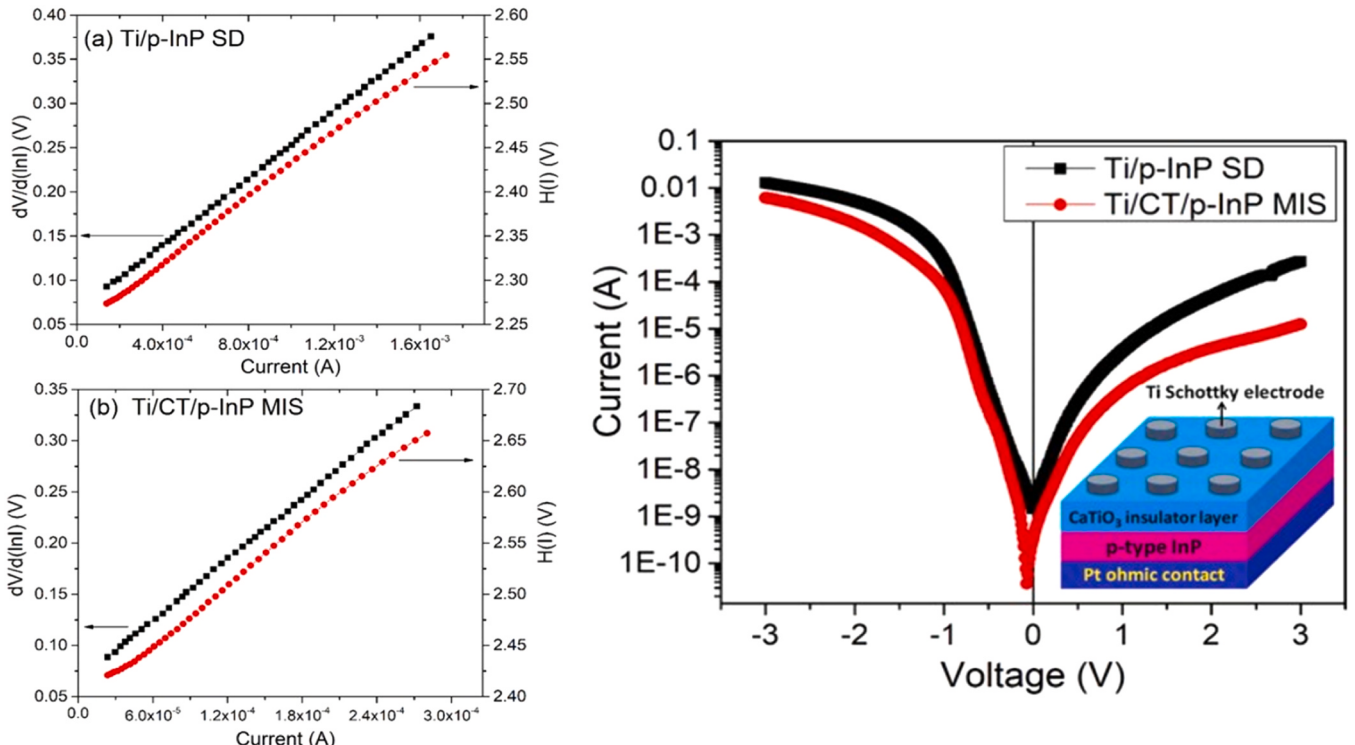


Fig. 44. Representation plot of $dV/d(\ln I)$ versus I and $H(I)$ versus I of the (a) Ti/p-InP SDs and (b) Ti/CT/p-InP MIS diode. forward and reverse bias current-voltage (I-V) features of Ti/p-InP SD and Ti/CT/p-InP MIS diode. [60].

high-performance MIS devices [37].

5.13. Indium phosphide (InP)

Indium phosphide is used in the fabrication of high-speed electronic and optoelectronic devices it has applications in telecommunications, where it is utilized for making photonic devices such as lasers and photodetectors indium phosphide (InP) is an explicitly found extensive semiconductor for the construction of HEMTs, high-speed MISFET, laser diodes, photo-detectors, microwave devices and solar cells [150].

5.14. p-type indium phosphide (p-InP)

It is a semiconductor material intentionally doped to create an excess

of positive charge carriers or "holes", p-InP exhibits a surplus of mobile holes, contributing to enhanced electrical conductivity.

Following an extensive of various papers have concluded that the optimal choice for diode fabrication involves p-type InP materials. As shown in Fig. 44. the I-V characteristics below demonstrate favourable ideal parameters and diode characteristics $n=1.22$ and $\Phi=0.84\text{eV}$. The analysis suggests that the CT layer holds significant potential as a material for producing high-performance MIS devices based on InP. Sai Krupa et.al., [60].

5.15. n-type indium phosphide (n-InP)

It is a semiconductor material deliberately doped to increase the concentration of free electrons as its majority charge carriers and this

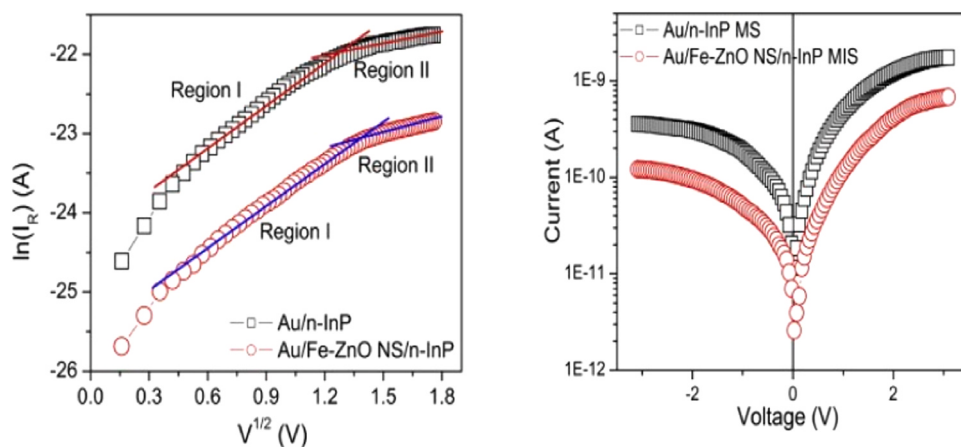


Fig. 45. Plot of $\ln(I_R)$ versus $V^{1/2}$ for the Au/n-InP MS and Au/Fe-ZnO NS/n-InP MIS Schottky structures at room temperature. The semi-logarithmic current-voltage (I-V) characteristics of Au/n-InP MS and Au/Fe-ZnO NS/n-InP MIS Schottky structures at room temperature [65].

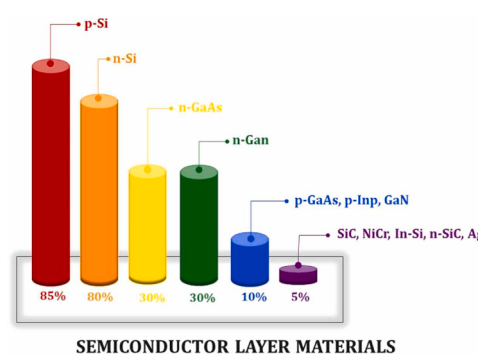


Fig. 46. Representation of the materials that used for the semiconductor layer of the MIS structured diodes.

surplus of mobile electrons enhances electrical conductivity, making n-InP valuable for high-speed electronic and optoelectronic devices. Its properties contribute to the construction of transistors, integrated circuits and semiconductor lasers, playing a crucial role in the advancement of telecommunications and photonics technologies.

After referred the papers, it is established that work emphasizes the superiority of n-type In-P materials for diode fabrication, in the specific case of Au/Fe₂-ZnO NS/n-InP as shown in Fig. 45. MIS Schottky structures, the obtained Φ_B and n values are 0.90 eV and 1.90, respectively. It is good choice for application as a Schottky rectifier in electronic devices. R. Padma et.al., [65].

Fig. 46 it shows the representation of the materials that used for the semiconductor layer of the MIS structured diodes.

6. Concluding remarks and future perspective

We concluded, exploration of the focus on transition metals as the cornerstone of future MIS devices and applications. This strategic choice arises from a meticulous analysis of the interplay between material properties and device performance, unveiling transition metals as the most promising candidates for achieving enhanced functionality and efficiency. MIS SBDs suffer from poor electrical performance owing to strong fermi level confinement and metal-to-metal gap states present at the interface. The in-depth study presented in this review underscores the critical role played between the metals and semiconductors of MIS devices, thereby elevating their overall performance to unprecedented levels.

The intricate details of MIS-based diode fabrication are further elucidated, providing a comprehensive understanding of the nuances

involved in the preparation of metal, insulator-specific details, and semiconductor layers. It is through this detailed examination that the path to optimal MIS device fabrication becomes clearer, guiding researchers and engineers towards more precise and effective methodologies. The acknowledgment of transition metals as key players in this fabrication reinforces the notion that innovation in materials science is at the heart of technological progress. As we draw insights from the historical significance of MIS SDs, it becomes evident that their foundational role in electronic devices is undeniably crucial.

Finally, we extensively consulted last 50 year's research papers on maximum MIS SBDs, deciphering that copper stands out as the optimal metal layer within the transition metal group. Copper (Cu) boasts significant benefits, such as outstanding electrical and thermal conductivity, rendering it an ideal substance for wires and devices. The interfacial layer, belonging to the transition metal group, proves to be augmented. Silicon Semiconductor emerges as an applaudable choice, particularly the n-type silicon material. This amalgamation of elements proves apt for fabricating the MIS structure of SBDs, widely employed in the future applications of Optoelectronic devices and Photodetector.

Declaration of Competing Interest

The authors declare that they have no known competing financial interests or personal relationships that could have appeared to influence the work reported in this paper.

Data Availability

Data will be made available on request.

Acknowledgements

Authors would thank to the Saveetha School of Engineering, Saveetha Institute of Medical and Technical Sciences, Saveetha University for providing lab facilities. And also, author Dr. V. Balasubramani would like to express heartfelt thanks to Dr. J. Chandrasekaran, whose determined assistance and guidance have significantly contributed to the completion of this work.

References

- [1] S. Riazimehr, S. Kataria, R. Bornemann, P. Haring Bolívar, F.J.G. Ruiz, O. Engström, M.C. Lemme, High photocurrent in gated graphene–silicon hybrid photodiodes, *ACS Photonics* 4 (2017) 1506–1514.
- [2] M. Casalino, U. Sassi, I. Goykhman, A. Eiden, E. Lidorikis, S. Milana, A.C. Ferrari, vertically illuminated, resonant cavity enhanced, graphene–silicon Schottky photodetectors, *ACS Nano* 11 (2017) 10955–10963.

- [3] L. Qian, Y. Sun, M. Wu, D. Xie, L. Ding, G. Shi, A solution-processed high-performance phototransistor based on a perovskite composite with chemically modified graphenes, *Adv. Mater.* 29 (2017) 1606175.
- [4] N. Terasaki, N. Yamamoto, M. Hattori, N. Tanigaki, T. Hiraga, K. Ito, K. Nakazato, Photosensor based on an FET utilizing a biocomponent of photosystem I for use in imaging devices, *Langmuir* 25 (2009) 11969–11974.
- [5] H. Kanbur, S. Altindal, T. Mammadov, Y. Şafak, Effects of illumination on I-V, C-V and G/w-V characteristics of Au/n-CdTe Schottky barrier diodes, *J. Optoelectron Adv. Mater.* 13 (2011) 713–718.
- [6] S. Sil, A. Dey, J. Datta, M. Das, R. Jana, S. Halder, P.P. Ray, Analysis of interfaces in bornite (Cu_5FeS_4) fabricated Schottky diode using impedance spectroscopy method and its photosensitive behaviour, *Mater. Res. Bull.* 106 (2018) 337–345.
- [7] S.O. Tan, H. Tecimer, O. Cicek, Comparative investigation on the effects of organic and inorganic interlayers in Au/n-GaAs Schottky diodes, *IEEE Trans. Electron Devices* 64 (2017) 984–990.
- [8] P.W.M. Blom, Molecular and polymer semiconductors, transport properties of, *Encyclopaedia of Materials: Science and Technology* (Second Edition) (2001): 5758–5765.
- [9] A. Turut, Dilber Esra Yıldız, Abdülkerim Karabulut, İkram Orak, Electrical characteristics of atomic layer deposited Au/Ti/HfO₂/n-GaAs MIS diodes in the wide temperature range, *J. Mater. Sci.: Mater. Electron.* 31 (2020) 7839–7849.
- [10] K. Ravikumar, S. Agilan, M. Raja, R. Marnadu, Thamraa Alshahrani, Mohd Shkir, M. Balaji, R. Ganesh, Investigation on microstructural and opto-electrical properties of Zr-doped SnO₂ thin films for Al/Zr: SnO₂/p-Si Schottky barrier diode application, *Phys. B: Condens. Matter* 599 (2020) 412452.
- [11] M. Chandra Sekhar, N. Nanda Kumar Reddy, B. Purusottam Reddy, B. Poorna Prakash, Harish Sharma Akkera, S. Uthanna, Si-Hyun Park, Influence of substrate bias voltage on crystallographic structure, optical and electronic properties of Al/(Ta₂O₅)_{0.85}(TiO₂)_{0.15}/p-Si MIS Schottky barrier diodes fabricated by dc magnetron sputtering, *Mater. Sci. Semicond. Process.* 76 (2018) 80–86.
- [12] R. Ertugrul-Uyar, A. Buyukbas-Uluscan, A.D.E.M. Tataroglu, Ionizing radiation effects on Au/TiO₂/n-Si metal-insulator-semiconductor (MIS) structure, *J. Mater. Sci.: Mater. Electron.* 31 (2020) 19846–19851.
- [13] A. Buyukbas-Uluscan, A.D.E.M. Tataroglu, Electrical characterization of silicon nitride interlayer-based MIS diode, *J. Mater. Sci.: Mater. Electron.* 31 (2020) 9888–9893.
- [14] A. Tataroglu, H. Tanrikulu, E. E. Tanrikulu, and A. Büyükbaba Uluşan. "Electrical characterization of MIS diode prepared by magnetron sputtering." *Indian Journal of Pure & Applied Physics (IJPAP)* 56, (2018): 142-148.
- [15] Arjun Shetty, Basanta Roul, Shruti Mukundan, Lokesh Mohan, Greeshma Chandan, K.J. Vinoy, S.B. Krupanidhi, Temperature dependent electrical characterisation of Pt/HfO₂/n-GaN metal-insulator-semiconductor (MIS) Schottky diodes, *AIP Adv.* 5 (2015).
- [16] B. Prasanna Lakshmi, V. Rajagopal Reddy, V. Janardhanam, M. Siva Pratap Reddy, Jung-Hee Lee, Effect of annealing temperature on the electrical properties of Au/Ta₂O₅/n-GaN metal-insulator-semiconductor (MIS) structure, *Appl. Phys. A* 113 (2013) 713–722.
- [17] T. Lazar, P. Gowrisankar, E. Selva Esakkki, V. Balaprakash, R. Seeniammal, Fabrication and photosensitivity analysis of MIS Schottky barrier diodes with different molar concentrations of MoO₃ thin films, *Solid State Commun.* 369 (2023) 115194.
- [18] T. Alshahrani, M. Shkir, A. Khan, A.M. El-Toni, A.A. Ansari, M.A. Shar, H. Ghaithan, S. AlFaify, T. Dai Nguyen, V.R.M. Reddy, A remarkable effect of substrate temperature on novel Al/Y₂O₃/n-Si heterojunction diodes performance fabricated by facile jet nebulizer spray pyrolysis for optoelectronic applications, *Chin. J. Phys.* 75 (2022) 14–27.
- [19] A. Narmada, P. Kathirvel, Lakshmi Mohan, S. Saravanan Kumar, R. Marnadu, J. Chandrasekaran, Jet nebuliser spray pyrolysed indium oxide and nickel doped indium oxide thin films for photodiode application, *Optik* 202 (2020) 163701.
- [20] V. Jagadeesan, R. Sakthivel, S. Shanmuga Priya, Improved design and development of an automated jet nebulizer spray pyrolysis system for Ag/Zn: Cu/O/Si structured diode application, *Mater. Today.: Proc.* (2023).
- [21] J. Thangabalu, S. Selvi, J.H. Chang, K. Mohanraj, Impact of substrate temperature on the properties of yttrium oxide thin films prepared by nebulizer spray pyrolysis technique, *Mater. Today.: Proc.* 48 (2022) 229–233.
- [22] R. Marnadu, J. Chandrasekaran, S. Maruthamuthu, V. Balasubramani, P. Vivek, R. Suresh, Ultra-high photo response with superiorly sensitive metal-insulator-semiconductor (MIS) structured diodes for UV photodetector application, *Appl. Surf. Sci.* 480 (2019) 308–322.
- [23] R. Marnadu, J. Chandrasekaran, S. Maruthamuthu, P. Vivek, V. Balasubramani, P. Balraju, Jet nebulizer sprayed WO₃-Nanoplate arrays for high-photosensitivity based metal-Insulator-Semiconductor structured Schottky barrier diodes, *J. Inorg. Organomet. Polym. Mater.* 30 (2020) 731–748.
- [24] R. Marnadu, J. Chandrasekaran, P. Vivek, V. Balasubramani, S. Maruthamuthu, Impact of phase transformation in WO₃ thin films at higher temperature and its compelling interfacial role in Cu/WO₃/p-Si structured Schottky barrier diodes, *Z. Phys. Chem.* 234 (2020) 355–379.
- [25] R. Marnadu, J. Chandrasekaran Joseph, Maruthamuthu Subramanian, P. Vivek Perumalsamy, Vijayakumar Elayappan, Superior photo response MIS Schottky barrier diodes with nano porous: Sn-WO₃ films for ultraviolet photodetector application, *N. J. Chem.* 44 (2020) 7708–7718.
- [26] R. Marnadu, J. Chandrasekaran, M. Raja, M. Balaji, V. Balasubramani, Impact of Zr content on multiphase zirconium-tungsten oxide (Zr-WO_x) films and its MIS structure of Cu/Zr-WO_x/p-Si Schottky barrier diodes, *J. Mater. Sci.: Mater. Electron.* 29 (2018) 2618–2627.
- [27] P. Harish Senthil, J. Chandrasekaran, R. Marnadu, Mohd Shkir, Enhancing of Al/Sn-HfO₂/n-Si (MIS) Schottky barrier diode performance through the incorporation of Sn ions on high dielectric HfO₂ thin films formed by spray pyrolysis, *J. Inorg. Organomet. Polym. Mater.* 31 (2021) 3686–3699.
- [28] P. Harishsenthil, J. Chandrasekaran, R. Marnadu, P. Balraju, C. Mahendran, Influence of high dielectric HfO₂ thin films on the electrical properties of Al/HfO₂/n-Si (MIS) structured Schottky barrier diodes, *Phys. B: Condens. Matter* 594 (2020) 412336.
- [29] P. Harishsenthil, J. Chandrasekaran, R. Marnadu, V. Balasubramani, Incorporation of Zn ions on high dielectric HfO₂ thin films by spray pyrolysis and fabrication of Al/Zn@HfO₂/n-Si Schottky barrier diodes, *Sens. Actuators A: Phys.* 331 (2021) 112725.
- [30] P. Harishsenthil, J. Chandrasekaran, D. Thangaraju, V. Balasubramani, Fabrication of strontium included hafnium oxide thin film-based Al/Sr:HfO₂/n-Si MIS-Schottky barrier diodes for tuned electrical behavior, *New J. Chem.* 45 (2021) 19476–19486.
- [31] V. Balasubramani, R. Marnadu, R. Priya, S. Thanikaikaran, A. Sivakumar, Mohd Shkir, F. Maiz, Woo Kyung Kim, Vasudeva Reddy Minnam Reddy, Analysis of opto-electrical properties of Cu/Sr-W/n-Si (MIS) Schottky barrier diode for optoelectronic applications, *J. Mater. Sci.: Mater. Electron.* 34 (2023) 560.
- [32] P. Vivek, J. Chandrasekaran, R. Marnadu, S. Maruthamuthu, V. Balasubramani, P. Balraju, Zirconia modified nanostructured MoO₃ thin films deposited by spray pyrolysis technique for Cu/MoO₃-ZrO₂/p-Si structured Schottky barrier diode application, *Optik* 199 (2019) 163351.
- [33] P. Vivek, J. Chandrasekaran, R. Marnadu, S. Maruthamuthu, V. Balasubramani, Incorporation of Ba²⁺ ions on the properties of MoO₃ thin films and fabrication of positive photo-response Cu/Ba-MoO₃/p-Si structured diodes, *Superlattices Microstruct.* 133 (2019) 106197.
- [34] P. Vivek, J. Chandrasekaran, R. Marnadu, S. Maruthamuthu, Fabrication of illumination-dependent Cu/p-Si Schottky barrier diodes by sandwiching MoO₃ nanoplates as an interfacial layer via JNSP technique, *J. Electron. Mater.* 49 (2020) 4249–4264.
- [35] P. Vivek, J. Chandrasekaran, V. Balasubramani, Fabrication of Cu/Y-MoO₃/p-Si type Schottky barrier diodes by facile spray pyrolysis technique for photodetection application, *Sens. Actuators A: Phys.* 335 (2022) 113361.
- [36] P. Vivek, J. Chandrasekaran, V. Balasubramani, A. Manimekalai, Insertion of Ga-MoO₃ thin film at Cu/p-Si interface for the fabrication of MIS structure Schottky barrier diodes, *Surf. Interfaces* 37 (2023) 102689.
- [37] M. Uma, M. Siva Pratap Reddy, K. Ravindranatha Reddy, V. Rajagopal Reddy, Electrical and carrier transport properties of Au/Pr₆O₁₁/n-GaN MIS structure with a high-k rare-earth oxide interlayer at high temperature range, *Vacuum* 174 (2020) 109201.
- [38] K.S. Mohan, A. Panneerselvam, J. Chandrasekaran, R. Marnadu, Mohd Shkir, An in-depth examination of opto-electrical properties of In-Yb₂O₃ thin films and fabricated Al/In-Yb₂O₃/p-Si (MIS) hetero junction diodes, *Appl. Nanosci.* 11 (2021) 1617–1635.
- [39] K.S. Mohan, A. Panneerselvam, R. Marnadu, J. Chandrasekaran, Mohd Shkir, Adem Tataroglu, A systematic influence of Cu doping on structural and opto-electrical properties of fabricated Yb₂O₃ thin films for Al/Cu-Yb₂O₃/p-Si Schottky diode applications, *Inorg. Chem. Commun.* 129 (2021) 108646.
- [40] V. Balasubramani, Phuong V. Pham, A. Ibrahim, Jabir Hakami, Mohd Zahid Ansari, Top Khac Le, Enhanced photosensitive of Schottky diodes using SrO interfaced layer in MIS structure for optoelectronic applications, *Opt. Mater.* 129 (2022) 112449.
- [41] V. Balasubramani, J. Chandrasekaran, Tien Dai Nguyen, S. Maruthamuthu, R. Marnadu, P. Vivek, S. Sugarthi, Colossal photosensitive boost in Schottky diode behaviour with Ce-V₂O₅ interfaced layer of MIS structure, *Sens. Actuators A: Phys.* 315 (2020) 112333.
- [42] V. Balasubramani, J. Chandrasekaran, V. Manikandan, Top Khac Le, R. Marnadu, P. Vivek, Improved photodetector performance of high-k dielectric material (La) doped V₂O₅ thin films as an interfacial layer in Schottky barrier diodes, *Surf. Interfaces* 25 (2021) 101297.
- [43] V. Balasubramani, J. Chandrasekaran, V. Manikandan, Top Khac Le, R. Marnadu, P. Vivek, Upgraded photosensitivity under the influence of Yb doped on V₂O₅ thin films as an interfacial layer in MIS type Schottky barrier diode as photodiode application, *J. Solid-State Chem.* 301 (2021) 122289.
- [44] V. Balasubramani, J. Chandrasekaran, V. Manikandan, R. Marnadu, P. Vivek, P. Balraju, Influence of rare earth doping concentrations on the properties of spin coated V₂O₅ thin films and Cu/Nd-V₂O₅/n-Si Schottky barrier diodes, *Inorg. Chem. Commun.* 119 (2020) 108072.
- [45] V. Balasubramani, J. Chandrasekaran, R. Marnadu, P. Vivek, S. Maruthamuthu, S. Rajesh, Impact of annealing temperature on spin coated V₂O₅ thin films as interfacial layer in Cu/V₂O₅/n-Si structured Schottky barrier diodes, *J. Inorg. Organomet. Polym. Mater.* 29 (2019) 1533–1547.
- [46] K. Sasikumar, R. Bharathi Kannan, J. Chandrasekaran, M.J.Jo.I. Raja, Effect of organic additives on the characteristics of Al/organic additive: ZrO₂/p-Si metal-insulator-semiconductor (MIS) type schottky barrier diodes, *J. Inorg. Organomet. Polym. Mater.* 30 (2020) 564–572.
- [47] K. Sasikumar, R. Bharathi Kannan, M. Raja, B. Mohanbabu, Fabrication and characterization of rare earth (Ce, Gd, and Y) doped ZrO₂ based metal-insulator-semiconductor (MIS) type Schottky barrier diodes, *Superlattices Microstruct.* 139 (2020) 106424.
- [48] K. Sasikumar, R. Bharathi Kannan, M. Raja, Effect of Annealing Temperature on Structural and Electrical Properties of Al/ZrO₂/p-Si MIS Schottky Diodes, *Silicon* 11 (2019) 137–143.

- [49] R. Priya, R. Mariappan, J. Chandrasekaran, V. Balasubramani, Characterization and fabrication of indium doped LaPO_4 as an interfacial layer of $\text{Cu}/\text{In}-\text{LaPO}_4/\text{n-Si}$ and developed for Schottky barrier diode, *J. Mater. Sci.: Mater. Electron.* 34 (2023) 423.
- [50] Yıldız, Dilber Esra, Abdülkerim Karabulut, I. Orak, A. Turut, Effect of atomic-layer-deposited HfO_2 thin-film interfacial layer on the electrical properties of $\text{Au}/\text{Ti}/\text{n-GaAs}$ Schottky diode, *J. Mater. Sci.: Mater. Electron.* 32 (2021) 10209–10223.
- [51] Kaymak, Nuriye, Esra Efil, Elanur Seven, A.D.E.M. Tataroglu, Sema Bilge Ocak, and Elif Oz Orhan, "Atomic Layer Deposition Grown Zinc-Oxide Based MIS-Type Schottky Barrier Diode," (2018).
- [52] Abdulkerim, İkram Orak, Mujdat Caglar, Abdulmecit Turut, The current–voltage characteristics over the measurement temperature of 60–400 K in the $\text{Au}/\text{Ti}/\text{n-GaAs}$ contacts with high dielectric HfO_2 interfacial layer, *Surf. Rev. Lett.* 26 (2019) 1950045.
- [53] Abdulmecit Turut, A. Karabulut, K. Ejderha, Necmi Biyikli, Capacitance–conductance–current–voltage characteristics of atomic layer deposited $\text{Au}/\text{Ti}/\text{Al}_2\text{O}_3/\text{n-GaAs}$ MIS structures, *Mater. Sci. Semicond. Process.* 39 (2015) 400–407.
- [54] C.S.A. Guclu, F. Ozdemir, D.A. Aldemir, S. Altindal, The reverse bias current–voltage–temperature (I–V–T) characteristics of the ($\text{Au}/\text{Ti}/\text{Al}_2\text{O}_3/\text{n-GaAs}$) Schottky barrier diodes (SBDs) in temperature range of 80–380 K, *J. Mater. Sci.: Mater. Electron.* 32 (2021) 5624–5634.
- [55] Sahar Alialy, S. Altindal, E.E. Tanrikulu, Dilber Esra Yıldız, Analysis of temperature dependent current-conduction mechanisms in $\text{Au}/\text{TiO}_2/\text{n-4H-SiC}$ (metal/insulator/semiconductor) type Schottky barrier diodes, *J. Appl. Phys.* 116 (2014).
- [56] A. Turut, A. Karabulut, K. Ejderha, Necmi Biyikli, Capacitance–conductance characteristics of $\text{Au}/\text{Ti}/\text{Al}_2\text{O}_3/\text{n-GaAs}$ structures with very thin Al_2O_3 interfacial layer, *Mater. Res. Express* 2 (2015) 046301.
- [57] Esra Balci, Barış Kinaci, Caglar Cetinkaya, Erman Çokduygular, Tugce Ataşer, Nihan Akın Sonmez, Semran Saglam, Suleyman Ozcelik, Structural and morphological analysis of rf sputtered nano ZnSe coatings as a function of thickness: investigation of the effect of metal contact on MIS structure with ZnSe interfacial layer, *J. Mater. Sci.: Mater. Electron.* 34 (2023) 1290.
- [58] V. Rajagopal Reddy, C. Venkata Prasad, Surface chemical states, electrical and carrier transport properties of $\text{Au}/\text{ZrO}_2/\text{n-GaN}$ MIS junction with a high-k ZrO_2 as an insulating layer, *Mater. Sci. Eng.: B* 231 (2018) 74–80.
- [59] C. Venkata Prasad, V.Rajagopal Reddy, Chel-Jong Choi, Electrical and carrier transport properties of the $\text{Au}/\text{Y}_2\text{O}_3/\text{n-GaN}$ metal-insulator-semiconductor (MIS) diode with rare-earth oxide interlayer, *Appl. Phys. A* 123 (2017) 1–10.
- [60] S. Sai Krupa, V. Rajagopal Reddy, Chel-Jong Choi, Chemical states and electrical features of Ti/CaTiO_3 (CT)/ p-InP MIS-type Schottky diode with a high-k CT interlayer, *Mater. Sci. Semicond. Process.* 169 (2024) 107876.
- [61] M. Uma, N. Balaram, P.R. Sekhar Reddy, V. Janardhanam, V. Rajagopal Reddy, Hyung-Joong Yun, Sung-Nam Lee, Chel-Jong Choi, "Structural, chemical and electrical properties of $\text{Au}/\text{La}_2\text{O}_3/\text{n-GaN}$ MIS junction with a high-k lanthanum oxide insulating layer", *J. Electron. Mater.* 48 (2019) 4217–4225.
- [62] Ramadan Rehab, Raúl J. Martín-Palma, Electrical characterization of MIS Schottky barrier diodes based on nanostructured porous silicon and silver nanoparticles with applications in solar cells, *Energies* 13 (2020) 2165.
- [63] Mahato Somnath, Cristobal Voz, Debaleen Biswas, Satyaban Bhunia, Joaquim Puigdollers, Defect states assisted charge conduction in $\text{Au}/\text{MoO}_{3-x}/\text{n-Si}$ Schottky barrier diode, *Mater. Res. Express* 6 (2018) 036303.
- [64] V. Manjunath, V. Rajagopal Reddy, P.R. Sekhar Reddy, V. Janardhanam, Chel-Jong Choi, Electrical and frequency-dependent properties of $\text{Au}/\text{Sm}_2\text{O}_3/\text{n-GaN}$ MIS junction with a high-k rare-earth Sm_2O_3 as interlayer, *Curr. Appl. Phys.* 17 (2017) 980–988.
- [65] R. Padma, N. Balaram, I. Neelakanta Reddy, V. Rajagopal Reddy, Influence of nanostructure Fe-doped ZnO interlayer on the electrical properties of $\text{Au}/\text{n-type InP}$ Schottky structure, *Mater. Chem. Phys.* 177 (2016) 92–98.
- [66] Necati Basman, Songul Fiat Varol, High temperature characterization of a MIS Schottky diode based on diamond-like carbon nanocomposite film, *J. Electron. Mater.* 48 (2019) 7874–7881.
- [67] V. Balasubramani, G. Alan Sibu, Shine Kadaikunnan, Jamal M. Khaled, Proliferation in the photo-response characteristics of MDC thin films for optoelectronic applications through NSP technique, *Sens. Actuators A: Phys.* (2024) 115008.
- [68] M. Uma, V. Rajagopal Reddy, V. Janardhanam, Chel-Jong Choi, Effect of rare-earth Pr_6O_{11} insulating layer on the electrical properties of $\text{Au}/\text{n-GaN}$ Schottky electrode and its chemical and structural characterization, *J. Mater. Sci.: Mater. Electron.* 30 (2019) 18710–18719.
- [69] M. Uma, M. Siva Pratap Reddy, V. Rajagopal Reddy, Statistical distribution of barrier heights, current conduction mechanism and voltage-dependent capacitance–frequency characteristics of $\text{Au}/\text{Fe}_3\text{O}_4/\text{n-GaN}$ heterojunction, *SN Appl. Sci.* 1 (2019) 1–9.
- [70] R. Marnadu, J. Chandrasekaran, M. Raja, M. Balaji, S. Maruthamuthu, P. Balraju, Influence of metal work function and incorporation of Sr atom on WO_3 thin films for MIS and MIM structured SBDs, *Superlattices Microstruct.* 119 (2018) 134–149.
- [71] Betul Guzeldir, Mustafa Saglam, A. Ateş, A.B.D.U.L.M.E.C. İ.T. Turut, Determination of some electronic parameters of nanostructure copper selenide and $\text{Cu}/\text{Cu}_3\text{Se}_2/\text{n-GaAs}/\text{In}$ structure, *J. Alloy. Compd.* 627 (2015) 200–205.
- [72] Ömer Gullu, A. Türüt, Electronic properties of $\text{Al}/\text{DNA}/\text{p-Si}$ MIS diode: Application as temperature sensor, *J. Alloy. Compd.* 509 (2011) 571–577.
- [73] Engin Arslan, Serkan Butun, Yasemin Şafak, Habibe Uslu, İlke Taşçıoğlu, S. Altindal, Ekrem Özbay, Electrical characterization of MS and MIS structures on $\text{AlGaN}/\text{AlN}/\text{GaN}$ heterostructures, *Microelectron. Reliab.* 51 (2011) 370–375.
- [74] Souvik Kundu, S.Banerjee Ajit Kumar, P. Banerji, Electrical properties and barrier modification of GaAs MIS Schottky device based on MEH-PPV organic interfacial layer, *Mater. Sci. Semicond. Process.* 15 (2012) 386–392.
- [75] Mustafa A. Ahmed, Liza Coetsee, Walter E. Meyer, Jackie M. Nel, Influence (Ce and Sm) co-doping ZnO nanorods on the structural, optical and electrical properties of the fabricated Schottky diode using chemical bath deposition, *J. Alloy. Compd.* 810 (2019) 151929.
- [76] F. Yigitler, Hasan H.üseyin Gülli, Özge Bayraklı, Dilber Esra Yıldız, Temperature-dependent electrical characteristics of $\text{Au}/\text{Si}_3\text{N}_4/4\text{H n-SiC}$ MIS diode, *J. Electron. Mater.* 47 (2018) 2979–2987.
- [77] Sedat Zeyrek, S. Altindal, H.üsметtin Yüzer, Mehmet Mahir Bülbül, "Current transport mechanism in $\text{Al}/\text{Si}_3\text{N}_4/\text{p-Si}$ (MIS) Schottky barrier diodes at low temperatures, *Appl. Surf. Sci.* 252 (2006) 2999–3010.
- [78] Ali Rıza Deniz, Analysis of temperature dependent current-voltage and frequency dependent capacitance-voltage characteristics of $\text{Au}/\text{CoO}/\text{p-Si}/\text{Al}$ MIS diode, *Microelectron. Reliab.* 147 (2023) 115114.
- [79] Mustafa Okutan, Fahrettin Yakuphanoglu, Analysis of interface states and series resistance of $\text{Ag}/\text{SiO}_2/\text{n-Si}$ MIS Schottky diode using current–voltage and impedance spectroscopy methods, *Microelectron. Eng.* 85 (2008) 646–653.
- [80] M. Siva Pratap Reddy, Peddathimula Puneetha, V. Rajagopal Reddy, Jung-Hee Lee, Seong-Hoon Jeong, Chinho Park, Temperature-dependent electrical properties and carrier transport mechanisms of TMAH-treated Ni/ $\text{Au}/\text{Al}_2\text{O}_3/\text{GaN}$ MIS diode, *J. Electron. Mater.* 45 (2016) 5655–5662.
- [81] S. Ashok, J.M. Borrego, R.J. Gutmann, Electrical characteristics of GaAs MIS Schottky diodes, *Solid-State Electron.* 22 (1979) 621–631.
- [82] Surucu Ozge, Dilber Esra Yıldız, Murat Yıldırım, A study on the dark and illuminated operation of $\text{Al}/\text{Si}_3\text{N}_4/\text{p-Si}$ Schottky photodiodes: optoelectronic insights, *Appl. Phys. A* 130 (2024) 103.
- [83] Y.İldiz, Dilber Esra, Adem Kocayigit, Murat Yıldırım, Investigation of $\text{Ag}/\text{ZnO}/\text{p-Si}$ heterostructure for diode and photodiode applications in visible spectrum, *Phys. Scr.* 99 (2023) 015913.
- [84] D.Esra Yıldız, Adem Kocayigit, Murat Yıldırım, Comparison of $\text{Al}/\text{TiO}_2/\text{p-Si}$ and $\text{Al}/\text{ZnO}/\text{p-Si}$ photodetectors, *Opt. Mater.* 145 (2023) 114371.
- [85] Dilber Esra Yıldız, Abdulkérkim Karabulut, Murat Yıldırım, The influence of light and temperature stimuli on the characteristics of $\text{Au}/\text{ZnO}/\text{n-Si}$ Schottky-type device, *J. Mater. Sci.: Mater. Electron.* 34 (2023) 2272.
- [86] N. Sethupathi, P. Thirunavukkarasu, V.S. Vidhya, R. Thangamuthu, G.V. M. Kiruthika, K. Perumal, Hari C. Bajaj, M. Jayachandran, Deposition and optoelectronic properties of $\text{ITO}/(\text{In}_2\text{O}_3:\text{Sn})$ thin films by jet nebulizer spray (JNS) pyrolysis technique, *J. Mater. Sci.: Mater. Electron.* 23 (2012) 1087–1093.
- [87] R. Suresh, V. PonnuSwamy, J. Chandrasekaran, D. Manoharan, R. Mariappan, The effect of annealing temperature and the characteristics of p–n junction diodes based on sprayed polyaniline/ZnO thin films, *J. Semicond.* 34 (2013) 083001.
- [88] P. Vidhya, K. Shanmugasundaram, P. Thirunavukkarasu, T. Govindaraj, V. Balasubramani, B. Yugeswari, M. Karuppusamy, Enhancement of optoelectronic properties of PbS thin films grown by jet nebulizer spray pyrolysis technique for photodetector applications: an impact of substrate temperature, *J. Mater. Sci.: Mater. Electron.* 34 (2023) 1023.
- [89] K. Kukli, M. Ritala, T. Sajavaara, J. Keinonen, M. Leskelä, Comparison of hafnium oxide films grown by atomic layer deposition from iodide and chloride precursors, *Thin Solid Films* 416 (2002) 72–79.
- [90] N. Biyikli, A. Karabulut, H. Efeolu, B. Guzeldir, A. Turut, Electrical characteristics of $\text{Au}/\text{Ti}/\text{n-GaAs}$ contacts over a wide measurement temperature range, *Phys. Scr.* 89 (2014) 095804.
- [91] D.A. Aldemir, A. Kökce, A.F. Özdemir, Temperature effects on the electrical characteristics of $\text{Al}/\text{PTh-SiO}_2/\text{p-Si}/\text{Al}/\text{PTh-SiO}_2/\text{p-Si}$ structure, *Bull. Mater. Sci.* 40 (2017) 1435–1439.
- [92] K.K. Mentel, A.V. Emelianov, A. Philip, A. Johansson, M. Karppinen, Mikael Pettersson, Area-Selective Atomic Layer Deposition on Functionalized Graphene Prepared by Reversible Laser Oxidation, *Adv. Mater. Interfaces* 9 (2022) 2201110.
- [93] Y.S. Hsieh, C.Y. Lin, Chang-Min Lin, Na-Fu Wang, Jian V. Li, Mau-Phon Houn, Investigation of metal-insulator-semiconductor diode with alpha- Ga_2O_3 insulating layer by liquid phase deposition, *Thin Solid Films* 685 (2019) 414–419.
- [94] N. Bathaei, B. Weng, H. Sigmarsson, Crystallization of GeTe phase change thin films grown by pulsed electron-beam deposition, *Mater. Sci. Semicond. Process.* 148 (2022) 106781.
- [95] M. Nistor, N.B. Mandache, J. Perrière, Pulsed electron beam deposition of oxide thin films, *J. Phys. D: Appl. Phys.* 41 (2008) 165205.
- [96] V. Dansoh, F. Gertz, J. Gump, A. Johnson, J.I. Jung, M. Klingensmith, Y. Liu, et al., Cerium oxide thin films via ion assisted electron beam deposition, *Adv. Ceram. Coat. Interfaces III: Ceram. Eng. Sci. Proc.* 46 (2009) 87.
- [97] G. Zhang, X. Fu, S. Song, K. Guo, J. Zhang, Influences of oxygen ion beam on the properties of magnesium fluoride thin film deposited using electron beam evaporation deposition, *Coatings* 9 (2019) 834.
- [98] M. Ito, N. Tajima, H. Murotani, T. Matsudaira, Super hydrophilic low refractive index SiO_2 optical thin films deposited by using a combination coating method, *e-J. Surf. Sci. Nanotechnol.* 22 (2023) 53–57.
- [99] R.M. Florea, Sustainable anti-corrosive protection technologies for metal products by electrodeposition of HEA layers." In IOP Conference Series, in: Materials Science and Engineering 591, IOP Publishing, 2019, p. 012014.

- [100] T. Zhang, J. Lin, A. Patran, D. Wong, S.M. Hassan, S. Mahmood, T. White, et al., Optimization of a plasma focus device as an electron beam source for thin film deposition, *Plasma Sources Sci. Technol.* 16 (2007) 250.
- [101] A. Augustin, K. Rajendra Udupa, K. Udaya Bhat, Effect of Pre-Zinc Coating on the Properties and Structure of DC magnetron sputtered copper thin film on aluminium, *Am. J. Mater. Sci.* 5 (2015) 58–61.
- [102] E. Endarko, Siti Rabi'atul Adawiyah, Experimental study of TiO₂ nanoparticles fabrication by sol-gel and Co-precipitation methods for TiO₂/SnO₂ composite thin film as photoanode, *J. ILMU DASAR* 20 (2019) 61–66.
- [103] V.H. Choudapur, S.B. Kapatkar, A.B. Raju, Structural and optoelectronic properties of zinc sulfide thin films synthesized by Co-precipitation method, *Acta Chem. Iasi* 27 (2019) 287–302.
- [104] V. Manikandan, Xiaogan Li, R.S. Mane, J. Chandrasekaran, Room temperature gas sensing properties of Sn-substituted nickel ferrite (NiFe₂O₄) thin film sensors prepared by chemical co-precipitation method, *J. Electron. Mater.* 47 (2018) 3403–3408.
- [105] S. Fallahzadeh, M. Gholami, M.R. Rahimi, A. Esrafili, M. Farzadkia, M. Kermani, Enhanced photocatalytic degradation of amoxicillin using a spinning disc photocatalytic reactor (SDPR) with a novel Fe₃O₄@ void@ CuO/ZnO yolk-shell thin film nanostructure, *Sci. Rep.* 13 (2023) 16185.
- [106] V.S. Kamble, R.K. Zemase, R.H. Gupta, B.D. Aghav, S.A. Shaikh, J.M. Pawara, S. K. Patil, S.T. Salunkhe, Improved toxic NO₂ gas sensing response of Cu-doped ZnO thin-film sensors derived by simple co-precipitation route, *Opt. Mater.* 131 (2022) 112706.
- [107] G.A. Kadhim, M.H. Suhaib, Polyaniline thin film as a gas sensor Prepared by electrochemical polymerization method, *Iraqi J. Sci., Part A, PP* (2016) 74–81.
- [108] S. Saxena, R. Guda, (Digital Presentation) Fabrication of Monolayer-Protected Gold Cluster Thin Films: Electrochemical and Optical Properties, *Electrochem. Soc. Meet. Abstr.* 241 (2022), 1103-1103.
- [109] R.äupke andré, Alex Palma-Cando, Eugen Shkura, Peter Teckhausen andreas Polywka, Patrick Görn, Ullrich Scherf, Thomas Riedl, Highly sensitive gas-phase explosive detection by luminescent microporous polymer networks, *Sci. Rep.* 6 (2016) 29118.
- [110] R. Miyashita, Kazuki Yanagida, Hiromasa Goto, (Digital presentation) electrochemical polymerization of thiophene in cholesteric liquid crystal with vitamins, *Electrochem. Soc. Meet. Abstr.* 241 (2022), 2483-2483.
- [111] F. Saouti, S. Belaaouad, A. Cherqaoui, Y. Naimi, Polyaniline thin film prepared by electrochemical polymerization method, *Biointerface Res Appl. Chem.* 12 (2021) 5523–5533.
- [112] K. Komaba, R. Kumai, H. Goto, (Digital Presentation) Synthesis of Conjugated Polymer Alloy Prepared by Electrochemical Polymerization in Chiral Liquid Crystal, *Electrochem. Soc. Meet. Abstr.* 241 (2022), 2473-2473.
- [113] G. Yergaliuly, B. Soltabayev, S. Kalybekkyzy, Z. Bakenov, A. Mentbayeva, Effect of thickness and reaction media on properties of ZnO thin films by SILAR, *Sci. Rep.* 12 (2022) 851.
- [114] B.C. Ghos, S.F. Uddin Farhad, Md Abdul Majed Patwary, S. Majumder, Md. A. Hossain, N.I. Tanvir, M.A. Rahman, T. Tanaka, Q. Guo, Influence of the substrate, process conditions and postannealing temperature on the properties of ZnO thin films grown by the successive ionic layer adsorption and reaction method, *ACS Omega* 6 (2021) 2665–2674.
- [115] H.S. Min, D. Saha, J.M. Kalita, M.P. Sarma, Ayan Mukherjee, Benjamin Ezekoye, Veronica A. Ezekoye, et al., Nanostructure thin films: synthesis and different applications, *Funct. Nanomater. I: Fabr.* 20 (2020) 71.
- [116] E. Jose, M.C. Santhosh Kumar, Room temperature deposition of highly crystalline Cu-Zn-S thin films for solar cell applications using SILAR method, *J. Alloy. Compd.* 712 (2017) 649–656.
- [117] A.A. Yatem, M.S. Rammoor, Nanostructured silver thin film: using successive ionic layer adsorption and reduction method, *Sci. J. Univ. Zakho* 11 (2023) 73–77.
- [118] E. Jose, M.C. Santhosh Kumar, Room-temperature wide-range luminescence and structural, optical and electrical properties of SILAR deposited Cu-Zn-S nano-structured thin films, *Nanostruct. Thin Films IX vol. 9929* (2016) 222–228.
- [119] D. Shikha, V. Mehta, S.C. Sood, J. Sharma, Structural and optical properties of ZnO thin films deposited by sol-gel method: effect of stabilizer concentration, *J. Mater. Sci.: Mater. Electron.* 26 (2015) 4902–4907.
- [120] G. Ehrhart, B. Capoen, O. Robbe, Ph Boy, S. Turrell, M. Bouazaoui, Structural and optical properties of n-propoxide sol-gel derived ZrO₂ thin films, *Thin Solid Films* 496 (2006) 227–233.
- [121] Zi-Neng Ng, K.Y. Chan, T. Tohsophon, "Effects of annealing temperature on ZnO and AZO films prepared by sol-gel technique", *Appl. Surf. Sci.* 258 (2012) 9604–9609.
- [122] O. Shekoofa, J. Wang, D. Li, Fabrication of N-type nanocrystalline silicon thin-film by magnetron sputtering and antimony induced crystallization, *Arch. Adv. Eng. Science* 16 (2023) 1–11.
- [123] J. Dybala, M. Mazur, Electrical and optical properties of the WO_x thin films, prepared by magnetron sputtering and analysis of their highest value, *Biul. WAT* 71 (2022) 15–25.
- [124] Y. Yang, Y. Zhang, M. Yan, A review on the preparation of thin-film YSZ electrolyte of SOFCs by magnetron sputtering technology, *Sep. Purif. Technol.* (2022) 121627.
- [125] Y. Xi, L. Liu, J. Zhao, X. Qin, J. Zhang, C. Zhang, W. Liu, Effects of oxygen flow during fabrication by magnetron sputtering on structure and performance of Zr-doped HfO₂ thin films, *Materials* 16 (2023) 5559.
- [126] T. Shen, Y. Chen, Y. Zhu, G. Gan, J. Yi, Progress in preparation of Cu₂ZnSnS₄ thin film by magnetron sputtering, *Cailiao Daobao/Mater. Rev.* 30 (2016) 14–20.
- [127] Z.Y. Li, S.M. Song, W. Wang, M.J. Dai, S.S. Lin, T.Y. Chen, H. Sun, Amorphous N-doped InSnZnO thin films deposited by RF sputtering for thin-film transistor application, *Mater. Adv.* 4 (2023) 6535–6541.
- [128] K.R. Babu, R. Singh, Effect of RF power on structural, magnetic and optical properties of CoFe₂O₄ thin films, *J. Supercond. Nov. Magn.* 31 (2018) 4029–4037.
- [129] S. Satapathy, P.K. Siwach, H.K. Singh, R.P. Pant, K.K. Maurya, Structural and magnetic properties of YIG thin films deposited by pulsed laser deposition and RF magnetron sputtering technique, *Phys. Scr.* 98 (2023) 105508.
- [130] S. Alghamdi, T. Moorsom, F. Al Ma'Mari, A. Walton, Z. Aslam, M. Ali, B.J. Hickey, O. Cespedes, Tuning the magnetic properties of Fe thin films with RF-sputtered amorphous carbon, *J. Magn. Magn. Mater.* 557 (2022) 169461.
- [131] B. Noikaew, L. Wangmooklang, S. Niyomsoan, S. Larpiattaworn, Preparation of transparent alumina thin films deposited by RF magnetron sputtering, *J. Met., Mater. Miner.* 31 (2021) 96–103.
- [132] E.N. Irawan, F. Aslami, M. Matthew Janotama, A.M. Putra, M.S. Muntini, S. Thaowankaew, W. Namhongsa, A. Vora-Ud, K. Singsoog, T. Seetawan, Fabrication of p-type (MCCO) thin film using DC magnetron sputtering as a preparator for thermoelectric module, *J. Phys.: Theor. Appl.* 7 (2023) 36–44.
- [133] Soumik Kumar Kundu, Samit Karmakar, Gouranga Sundar Taki, Crystallinity Study of Cu Thin Film Deposited by Indigenously Developed DC Magnetron Sputtering Setup, *In, Macromol. Symp.* vol. 407 (2023) 2100356.
- [134] Bassam Abdallah, M. Kakhia, W. Alsadat, Deposition of TiN and TiAlVN thin films by DC magnetron sputtering: composition, corrosion and mechanical study, *Int. J. Struct. Integr.* 11 (2020) 819–831.
- [135] Nirun WITIT-ANUN, Adisorn BURANAWONG, High-temperature oxidation resistance of CrAlN thin films prepared by DC reactive magnetron sputtering, *J. Met., Mater. Miner.* 33 (2023), 1600–1600.
- [136] Wei-Chieh Chen, Zhao-Ying Wang, Chiao-Yi Yu, Bo-Huei Liao, Ming-Tzer Lin, A study of the phase transformation of low temperature deposited tantalum thin films using high power impulse magnetron sputtering and pulsed DC magnetron sputtering, *Surf. Coat. Technol.* 436 (2022) 128288.
- [137] G. Vijaya, M.S. Krupashankara, B.K. Sridhara and T.N. Shridhar, "Studies on Nanostructure Aluminium Thin Film Coatings Deposited using DC magnetron Sputtering Process," In IOP Conference Series: Materials Science and Engineering, vol. 149, p. 012071.
- [138] M. Bellardita, A. Di Paola, S. Yurdakal, and L. Palmisano. "Preparation of catalysts and photocatalysts used for similar processes." In Heterogeneous Photocatalysis, (2019): 25–56.
- [139] Barkhordari Ali, Hamid Reza Mashayekhi, Pari Amiri, S. Altindal, Yashar Azizian-Kalandaragh, Optoelectric response of Schottky photodiode with a PVP: ZnTiO₃ nanocomposite as an interfacial layer, *Opt. Mater.* 148 (2024) 114787.
- [140] Neha Desai, Sawanta Mali, Vijay Kondalkar, Rahul Mane, Chang Hong, Popatrao Bhosale, Chemically grown MoO₃ nanorods for antibacterial activity study, *J. Nanomed. Nanotechnol.* 6 (2015) 1.
- [141] E.M. McCarron III, D.M. Thomas, J.C. Calabrese, Hexagonal molybdates: crystal structure of (Na·2H₂O) Mo₅, 33 [H₄] 0.67 O18, *Inorg. Chem.* 26 (1987) 370–373.
- [142] N. Miyata, T. Suzuki, and R. Ohyama, "Physical properties of evaporated molybdenum oxide films." *Thin Solid Films* cc.
- [143] A. Manimekalai, R. Parimaladevi, M. Umadevi, Enhanced photovoltaic and photocatalytic activity of flower-like Fe₂WO₆/WO₃ contact layers, *J. Inorg. Organomet. Polym. Mater.* 30 (2020) 3487–3492.
- [144] Hasan Elamen, Yosef Badali, Murat Ulusoy, Yashar Azizian-Kalandaragh, S. Altindal, Muhammet Tahir Güneşer, The photoresponse behavior of a Schottky structure with a transition metal oxide-doped organic polymer (RuO₂: PVC) interface, *Polym. Bull.* 81 (1) (2024) 403–422.
- [145] Selçuk Demirezen, Murat Ulusoy, Haziret Durmuş, Halit Cavusoglu, Kurtuluş Yılmaz, S. Altindal, Electrical and photodetector characteristics of schottky structures interlaid with P (EHA) and P (EHA-co-AA) functional polymers by the iCVD method, *ACS Omega* 8 (49) (2023) 46499–46512.
- [146] T. Akila, P. Gayathri, G. Alan Sibu, V. Balasubramani, Hamad Al-Lohedan, and Dhaifallah M. Al-Dhayani, "Augmented photovoltaic performance of Cu/Ce-(Sn: Cd)/n-Si Schottky barrier diode utilizing dual-doped Ce-(Sn: Cd) thin films, *Opt. Mater.* 149 (2024) 115133.
- [147] Mine Kurkbinar, Erhan İbrahimoglu, Ahmet Demir, Fatih Çalışkan, S. Altindal, Improvement of electric and photoelectric properties of the Al/n-ZnO/p-Si/Al photodiodes by green synthesis method using chamomile flower extract, *J. Mater. Sci.: Mater. Electron.* 34 (3) (2023) 242.
- [148] H. Gullu, H.D.E. Yıldız, M. Yıldırım, I. Demir, I. Altuntas, Electrical characteristics of Al/AlGaAs/GaAs diode with high-Al concentration at the interface, *J. Mater. Sci.: Mater. Electron.* 35 (2024) 189.
- [149] M. Čapajna, J. Kuzmík, A comprehensive analytical model for threshold voltage calculation in GaN based metal-oxide-semiconductor high-electron-mobility transistors, *Appl. Phys. Lett.* 100 (2012).
- [150] Gang Niu, Giovanni Capellini, Fariba Hatami, Antonio Di Bartolomeo, Tore Niermann, Emad Hameed Hussein, Markus Andreas Schubert, et al., Selective epitaxy of InP on Si and rectification in graphene/InP/Si hybrid structure, *ACS Appl. Mater. Interfaces* 8 (2016) 26948–26955.



Dr. G. Alan Sibu is currently working as a Researcher in Department of Physics at Saveetha School of Engineering, Chennai, India. Previously, he earned BS degree from Bharathidasan University, Trichy, and he earned MS degree from Kamarajar University, Madurai, India. He is currently working in thin film, Schottky barrier diode and low cost for optoelectronic applications.



Dr. R. Marnadu is currently working as a Assistant Professor at Government Arts College for Women, Dindigul, TN, India. He has received his B.Sc. degree in Physics from Madurai Kamaraj University, Madurai (India) and M.Sc. in Physics from Bharathiar University, Coimbatore (India). He has received his Ph. D. degree in Physics from Bharathiar university (India) with specialization in Material Science. His research interest focuses on the development of low-cost UV photo-detector, Diodes, Supercapacitors etc., for optoelectronic applications.



Dr. P. Gayathri is currently working as a Researcher in Department of Physics at Saveetha School of Engineering, Chennai, India. Previously, she earned BS degree and MS degree from Mother Teresa Women's University, Kodaikanal, Dindigul, India. She is currently working in thin film, Schottky barrier diode and optoelectronic applications.



Dr. V. Balasubramani is currently working as a Assistant Professor at Saveetha School of Engineering, Saveetha University, Chennai. He completed his Doctoral degree from Bharathiar University, Coimbatore, India. Previously he earned BS, MS and Master of Philisophy degree in Physics from Periyar university, Salem, India. His current research interests include thin film, MIS type Schottky diode, photodetectors, Solar Cell and fabrication of low-Cost Photovoltaic Devices.



Dr. T. Akila is currently working as a Researcher in Department of Physics at Saveetha School of Engineering, Chennai, India. Previously, she earned BS and MS degree from Periyar University, Selam, India. She is currently working in thin film, Schottky barrier diode and highly sensitive optoelectronic applications.